To the Graduate Council:

I am submitting herewith a thesis written by Michael C. Allison entitled "Trace Element Distribution in Pyrite and Pyrrhotite from the Ducktown Mining District, Tennessee." I have examined the final copy of this thesis for form and content and recommend that it be accepted in partial fulfillment of the requirements for the degree of Master of Science, with a major in Geology.

Kula C. Misra

Kula C. Misra, Major Professor

We have read this thesis and recommend its acceptance:

Otto C. Kopp

Harry G. McDowell

Accepted for the Council:

Lewis Nikel

The Graduate School

TRACE ELEMENT DISTRIBUTION IN PYRITE AND PYRRHOTITE, FROM THE DUCKTOWN MINING DISTRICT, TENNESSEE

A Thesis

Presented for the

Master of Science

Degree

The University of Tennessee, Knoxville

Michael C. Allison

June 1984

TO MARY AND DAVID

ACKNOWLEDGMENTS

I am indebted to my advisor, Dr. Kula Misra, and to my committee members, Dr. Otto Kopp and Dr. Hap McSween, for their contributions in an advisory capacity and for critical review of the thesis. I thank the Mining Department Staff at the Tennessee Chemical Company, Ducktown, Tennessee, for providing drill core samples from the study area. I would particularly like to thank Randy Slater and Charles Acker of the Tennessee Chemical Company, who contributed both their time and expertise on the geology of the Ducktown District. Dr. William Dennen, Director, Cabot Spectrographic Laboratory, University of Kentucky, Lexington, Kentucky, made available all facilities including the use of the laser microprobe. He was extremely helpful, willing and always available for discussions and solving problems that arose in connection with my work. I am also very grateful to Gary and Terri Runyon for all of the drafting necessary for my thesis, and especially to Gary for his friendship and helpful suggestions. Special thanks to Dr. Larry Taylor for interesting discussions on various aspects of this study. I would like to thank Dr. M. S. Bhatia, Austin Peay State University, Clarksville, Tennessee, for his helpful suggestions on the standards for laser microprobe analysis. Dr. Steve Driese and Kem Fronabarger provided assistance on statistical treatment of the data. I would like to thank the Gulf Oil Company for supplying assistance in making the photographic plates in my thesis. The study was also supported through money from The University of Tennessee, Knoxville, Geology Department Discretionary Funds. I must acknowledge many of my fellow students for their helpful

discussions concerning this project, especially, Steve Absher and Steve Knapp. I would also like to thank Radio Shack for manufacturing my computer, which greatly aided in the data reduction and word processing required for this study.

I thank my parents, Dr. and Mrs. Ronald Allison, for their financial and moral support during this endeavor.

Finally, to my wonderful wife, Mary, and our new son, David, for their never-ending support and companionship, and the greatest incentive one could have for completing a thesis.

ABSTRACT

Pyrite and pyrrhotite were analyzed for 7 trace elements in 59 samples by laser microprobe spectrographic analysis. The concentrations of Co, Ni, Mn, Pb, Ti, Sn and Ag in pyrite and pyrrhotite were determined. This is the first attempt to analyze pyrrhotite using a laser microprobe. Frequency distribution plots of all of the trace elements from both pyrite and pyrrhotite show that the trace elements approach a log-normal distribution rather than an arithmetic-normal distribution. The trace element distribution patterns in the sulfide minerals were examined with respect to effects of metamorphism and ore genesis.

The spatial distribution of trace elements in the sulfide phases from the country rocks (Ocoee Gorge) to the orebodies show definite patterns which can be explained by mobilization of trace elements along with other sulfide constituents during prograde metamorphism. The trace element contents of the sulfides in the Calloway and Cherokee orebodies are quite different. This may be explained by the presence of two distinct ore horizons related to the original syngenetic deposition of the ore. Variations in the trace elements in the sulfides from the hanging wall to the footwall indicate that the orebodies may be zoned. The patterns observed are in good agreement with bulk assay data and may be related to hydrothermal processes during the formation of the orebodies lying horizontally within a sedimentary pile. The reversal of some of the trends in the Cherokee orebody indicate that the Cherokee orebody is overturned. The trace elements in pyrite and pyrrhotite

showed several trends from the upper to the lower levels of the Calloway orebody. These patterns may represent lateral zoning in the original orebody subsequently modified by metamorphism. Pyrite from the Cherokee orebody and the country rocks show the highest and lowest Co contents and Co:Ni ratios, respectively. This data along with bulk Zn and Cu assays and stratigraphic relationships, indicate that the Cherokee orebody may have formed during an earlier and possibly higher temperature phase of ore deposition than the Calloway orebody. Co and Ni data for pyrite plot near the boundary between sedimentary/syngenetic and volcanogenic massive sulfide deposits, suggesting a mixed genetic environment.

The trace element data suggest that the Ducktown deposits had a complex history and cannot be explained by any single genetic model. Early deposition of syngenetic (premetamorphic) massive sulfide lenses occurred away from any volcanic center. Subsequent prograde metamorphism produced mobilization of sulfide constituents, including trace elements, from the country rocks into the orebodies. This process may have added significant amounts of sulfide material and produced one of the largest massive sulfide deposits in the world.

TABLE OF CONTENTS

CHAPTER		PAGE
I.	INTRODUCTION	1
II.	METHODS OF INVESTIGATION	12
	Sampling	12
	Ore Petrography	13
	Laser Microprobe Analysis	14
	Standards	16
	Photographic Plate Calibration	18
	Working Curves	18
	Precision and Accuracy	21
III.	ORE PETROGRAPHY	24
	Pyrrhotite	24
	Pyrite	25
	Chalcopyrite	31
	Sphalerite	34
IV.	TRACE ELEMENT DISTRIBUTION IN PYRITE AND PYRRHOTITE FROM THE DUCKTOWN MINING DISTRICT	36
	Variation in the Trace Element Contents of Pyrite and Pyrrhotite from the Ocoee Gorge Metasedimentary Rocks to the Orebodies	37
	Pyrite	40
	Pyrrhotite	40
	Variations of Trace Element Contents of Pyrite and Pyrrhotite between the Calloway and Cherokee Orebodies	40
	Pyrite	44
	Pyrrhotite	44
	Variations in the Trace Element Contents of Pyrite and Pyrrhotite from the Hanging Wall to the Footwall of the Calloway Orebody	45
	Pyrite	57
	Pyrrhotite	57
	Variations in Trace Element Contents of Pyrite and Pyrrhotite from the Hanging Wall to the Footwall of the Cherokee Orebody	57
	Pyrite	58
	Pyrrhotite	58

CHAPTER PAGE

Variations in the Trace Element Contents of Pyrite and Pyrrhotite from the Upper to the Lower Levels of the Calloway Orebody 58
Pyrite 64
Pyrrhotite 64
Cobalt, Nickel, and the Co:Ni Ratio in Pyrite and Pyrrhotite 65

V. INTERPRETATION AND DISCUSSION 67

Comparison of the Country Rocks and the Orebodies . . . 67
Comparison of the Calloway and the Cherokee Orebodies 68
Vertical Zoning from the Hanging Wall to the Footwall within the Calloway and Cherokee Orebodies 70
Lateral Zoning within the Calloway Orebody 74
Proposed Model for the Ducktown District 74

VI. SUMMARY 79

BIBLIOGRAPHY 81

APPENDICES 88

A. SAMPLE PREPARATION 89
B. STATISTICAL TERMS AND EQUATIONS 92
C. CHEMICAL ANALYSES OF INITIAL SET OF STANDARDS 95
D. INSTRUMENTATION, WORKING CURVE, PRECISION, AND ACCURACY DATA 97
E. OPAQUE MINERALOGY 102
F. TRACE ELEMENT REVIEW 105
G. GEOMETRIC MEAN DATA 115
H. ARITHMETIC MEAN DATA 124
I. REGRESSION LINE DATA 142
J. STUDENT'S t-TEST, CORRELATION COEFFICIENTS, AND COEXISTING PHASE DATA 145

VITA 150

LIST OF TABLES

TABLE		PAGE
1.	Summary of Trace Element Data for Various Sulfide Minerals, Obtained from the Literature for the Ducktown District	10
2.	Summary of Geometric Mean Data for Pyrite from the Ocoee Gorge Metasediments, and the Calloway and Cherokee Orebodies	43
3.	Summary of Geometric Mean Data for Pyrrhotite from the Ocoee Gorge Metasediments, and the Calloway and Cherokee Orebodies	43
4.	Summary of Arithmetic Mean Data for Pyrite from the Calloway and Cherokee Orebodies	46
5.	Summary of Arithmetic Mean Data for Pyrrhotite from the Calloway and Cherokee Orebodies	47
6.	Summary of the Geometric Mean Data for Pyrite from the Four Sets of Cores Sampled from the Calloway Orebody	61
7.	Summary of the Geometric Mean Data for Pyrrhotite from the Four Sets of Cores Sampled from the Calloway Orebody	61
8.	Comparison of Cobalt and Nickel Contents and the Co:Ni Ratios of Pyrite and Pyrrhotite from the Ocoee Gorge Metasediments, and the Calloway and Cherokee Orebodies	66
C-1.	Chemical Analyses of Samples Selected for the Initial Set of Standards Chosen for LMP Analysis	96
D-1.	Spectral Lines, Instrumentation, and Laser Microprobe Settings Used for Trace Element Determinations	98
D-2.	Best Fit Line Equations, Correlation Coefficients, and Confidence Limits for Working Curves	99
D-3.	Precision Data for a Typical Sample of Pyrite and Pyrrhotite	100
D-4.	Comparison of a Pyrite Standard Analyzed by the Laser Microprobe and Atomic Absorption	101

TABLE		PAGE
E-1.	Opaque Mineralogy of Samples Used in This Study, Ducktown Area, Tennessee	103
F-1.	Comparison of Cobalt and Nickel Contents and Co:Ni Ratios from Sedimentary (Syngenetic), Hydrothermal, and Volcanic-Exhalative (Massive Sulfide) Pyrite	112
G-1.	Geometric Mean Data for Pyrite from the Ocoee Gorge Metasediments	116
G-2.	Geometric Mean Data for Pyrite from the Calloway Orebody	117
G-3.	Geometric Mean Data for Pyrite from the Cherokee Orebody	119
G-4.	Geometric Mean Data for Pyrrhotite from the Ocoee Gorge Metasediments	120
G-5.	Geometric Mean Data for Pyrrhotite from the Calloway Orebody	121
G-6.	Geometric Mean Data for Pyrrhotite from the Cherokee Orebody	123
H-1.	Arithmetic Mean Data for Pyrite from the 628/629 Core in the Calloway Orebody	125
H-2.	Arithmetic Mean Data for Pyrite from the 300/301 Core in the Calloway Orebody	126
H-3.	Arithmetic Mean Data for Pyrite from the 469/470 Core in the Calloway Orebody	128
H-4.	Arithmetic Mean Data for Pyrite from the 965/966 Core in the Calloway Orebody	129
H-5.	Arithmetic Mean Data for Pyrite from the 857/858 Core in the Cherokee Orebody	131
H-6.	Arithmetic Mean Data for Pyrrhotite from the 628/629 Core in the Calloway Orebody	132
H-7.	Arithmetic Mean Data for Pyrrhotite from the 300/301 Core in the Callowy Orebody	134
H-8.	Arithmetic Mean Data for Pyrrhotite from the 469/470 Core in the Calloway Orebody	136

TABLE		PAGE
H-9.	Arithmetic Mean Data for Pyrrhotite from the 965/966 Core in the Calloway Orebody	138
H-10.	Arithmetic Mean Data for Pyrrhotite from the 857/858 Core in the Cherokee Orebody	140
I-1.	Regression Lines for Pyrite Trace Element Data	143
I-2.	Regression Lines for Pyrrhotite Trace Element Data . . .	144
J-1.	Student's t-Test Data	146
J-2.	Correlation Coefficients for Trace Elements in Pyrite . .	147
J-3.	Correlation Coefficients for Trace Elements in Pyrrhotite	148
J-4.	Arithmetic Mean Values of Trace Element Concentrations for Coexisting Pyrite and Pyrrhotite	149

LIST OF FIGURES

FIGURE		PAGE
1.	Location of Study Area in Relation to Major Tectonic Provinces of the Southern Appalachians	2
2.	Precambrian and Cambrian Stratigraphy of Southeastern Tennessee, Southwestern North Carolina, and Georgia . . .	3
3.	Schematic Diagram Showing Deformational and Metamorphic Events, and Suggested Times of Ore Emplacement	4
4.	Detailed Structural Map of the Ducktown Mining District Showing the Distribution of the Orebodies	6
5.	Map Displaying Local Stratigraphy, Structure, Metamorphic Isograds, Sample/Drill Hole Locations, and Ore Deposits of the Ducktown Mining District, Tennessee-North Carolina	7
6.	Schematic Diagram of the Laser Microprobe Spectrograph Source	15
7.	Calibration Curve for Plate Response	19
8.	Standard Working Curves for Co, Ni, Mn, Pb, Ti, Sn, Ag, and Cu in Pyrite and Pyrrhotite	22
9.	Photomicrographs of Sulfide Assemblages in the Great Smoky Group Metasedimentary Rocks and Ducktown Orebodies	26
10.	Photomicrographs of Sulfide Assemblages in the Great Smoky Group Metasediments and Ducktown Orebodies	28
11.	Photomicrographs of Sulfide Assemblages in the Ducktown Orebodies	32
12.	Frequency Histograms of Co and Ni in Pyrite from the Calloway Orebody	38
13.	Log Probability Plots for Nine Trace Elements in Pyrite from the Calloway Orebody	39
14.	Variation of Trace Elements in Pyrite from the Metasedimentary Rocks and Orebodies of the Ducktown Area as a Function of Increasing Grade of Metamorphism . .	41

FIGURE		PAGE
15.	Variation of Trace Elements in Pyrrhotite from the Metasedimentary Rocks and Orebodies of the Ducktown Area as a Function of Increasing Grade of Metamorphism . .	42
16.	Variation of Trace Elements in Pyrite from the Hanging Wall to the Footwall in Core 628/629 from the Calloway Orebody	48
17.	Variation of Trace Elements in Pyrite from the Hanging Wall to the Footwall in Core 300/301 from the Calloway Orebody	49
18.	Variation of Trace Elements in Pyrite from the Hanging Wall to the Footwall in Core 469/470 from the Calloway Orebody	50
19.	Variation of Trace Elements in Pyrite from the Hanging Wall to the Footwall in Core 965/966 from the Calloway Orebody	51
20.	Variation of Trace Elements in Pyrrhotite from the Hanging Wall to the Footwall in Core 628/629 from the Calloway Orebody	52
21.	Variation of Trace Elements in Pyrrhotite from the Hanging Wall to the Footwall in Core 300/301 from the Calloway Orebody	53
22.	Variations of Trace Elements in Pyrrhotite from the Hanging Wall to the Footwall in Core 469/470 from the Calloway Orebody	54
23.	Variations of Trace Elements in Pyrrhotite from the Hanging Wall to the Footwall in Core 965/966 from the Calloway Orebody	55
24.	Examples of Least Squares Regression Plots Used to Statistically Study the Trends Observed in Figures 17 to 25	56
25.	Variation of Trace Elements in Pyrite from the Hanging Wall to the Footwall in Core 857/858 from the Cherokee Orebody	59
26.	Variations of Trace Elements in Pyrrhotite from the Hanging Wall to the Footwall in Core 857/858 from the Cheorkee Orebody	60

FIGURE PAGE

27. Variations of Trace Elements in Pyrite from the Upper Levels to the Lower Levels in the Calloway Orebody 62

28. Variations of Trace Elements in Pyrrhotite from the Upper Levels to the Lower Levels in the Calloway Orebody 63

29. Zn:Cu Ratios from Bulk Assay Data for the Four Cores (628/629, 300/301, 469/470, and 965/966) from the Calloway Orebody Obtained from the Tennessee Chemical Company 71

30. Comparison of Cobalt and Nickel Contents of Syngenetic, Hydrothermal, and Volcanic-Exhalative (Massive Sulfide) Pyrite with Pyrite from the Metasedimentary Rocks and Orebodies in the Ducktown Area, Tennessee 77

LIST OF PLATES

PLATE

1. Generalized Geologic Cross Section of the Calloway Orebody . . . . . In Pocket

2. Generalized Geologic Cross Section of the Cherokee Orebody . . . . . In Pocket

CHAPTER I

INTRODUCTION

The Ducktown mining district is located in the southeastern corner of Tennessee, within the Blue Ridge belt of Tennessee and North Carolina. The Blue Ridge province is separated from the Inner Piedmont igneous and metamorphic complex by the Brevard Zone and from the Valley and Ridge Province by the Great Smoky fault zone (Figure 1).

The stratigraphy in the vicinity of Ducktown district has been studied by many authors (Hurst, 1955; Hurst and Schlee, 1962; Hernon, 1968; Magee, 1968; Holcombe, 1973; and Weiner and Merschat, 1978). In this area, the upper Precambrian metasedimentary rocks of the Ocoee Series and the upper Precambrian/Cambrian Murphy Marble Belt comprise the exposed stratigraphic section. Figure 2 is a summary of the Precambrian and Cambrian stratigraphy of the region compiled by Runyon (1983).

The structural and metamorphic history of the Ducktown area has been discussed by Carpenter (1970), Addy (1973), Holcombe (1973), and, most recently, by Addy and Ypma (1977). As illustrated in Figure 3, Addy and Ypma (1977) concluded that the Ducktown area experienced five episodes of deformation (F_1-F_5) and three phases of metamorphism (M_1-M_3): a syntectonic phase of prograde metamorphism (M_1) during the Taconic deformation (F_1), a posttectonic phase of prograde metamorphism (M_2) following the Acadian deformation (F_2), and a retrograde phase of metamorphism (M_3) during the Alleghenian brittle deformation events

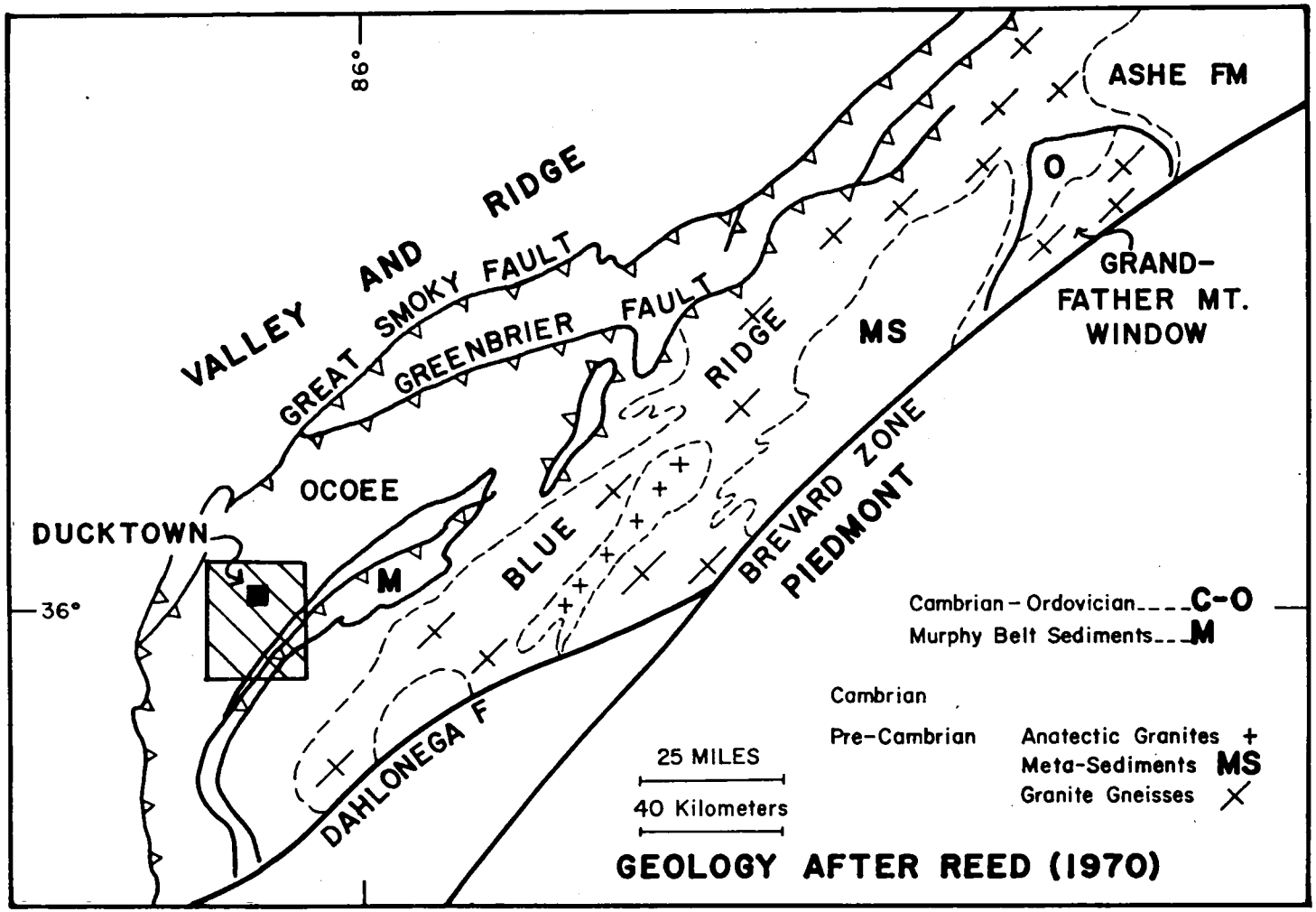


Figure 1. Location of study area in relation to major tectonic provinces of the southern Appalachians.

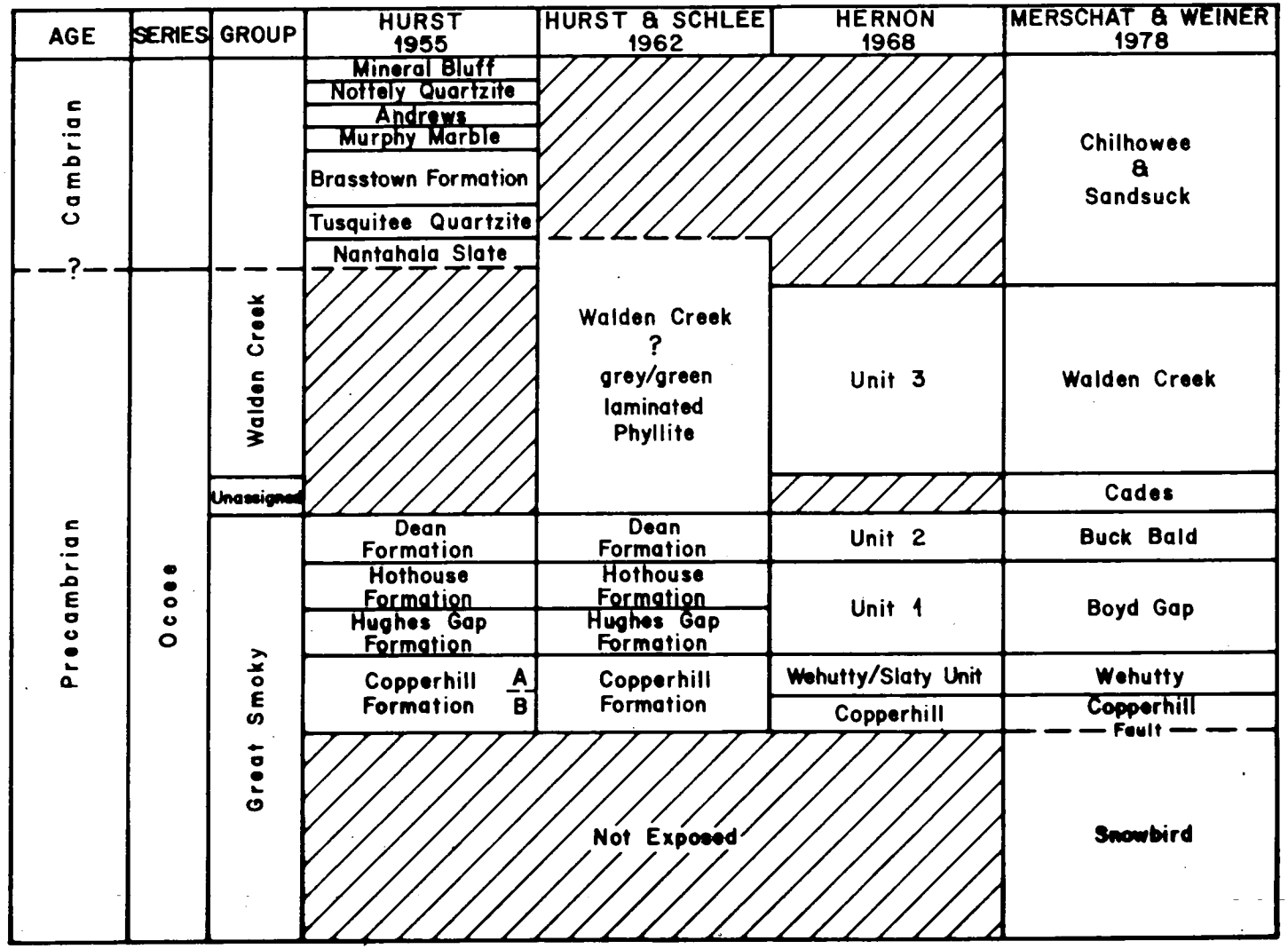


Figure 2. Precambrian and Cambrian stratigraphy of southeastern Tennessee, southwestern North Carolina, and Georgia (compiled by Runyon, 1983).

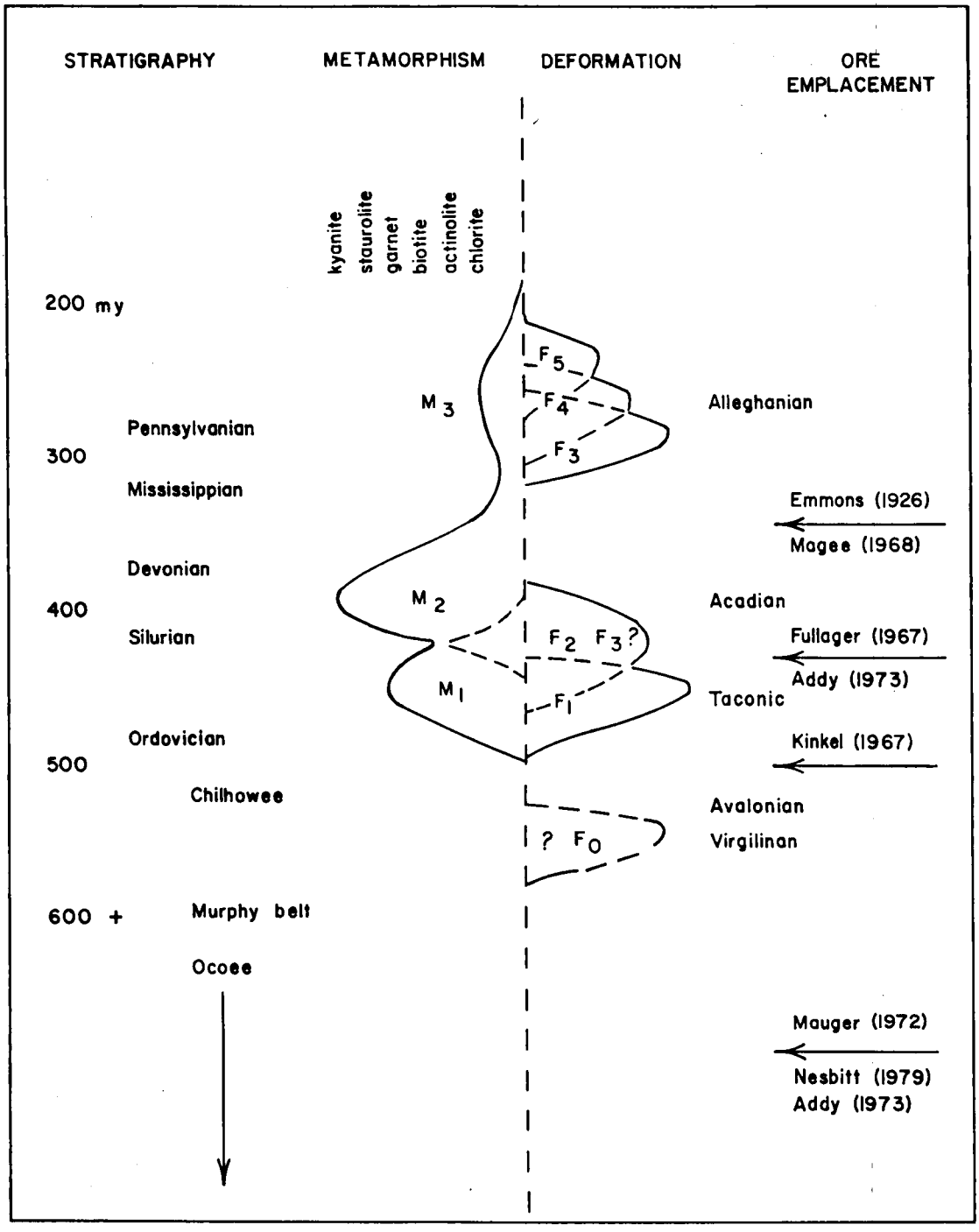


Figure 3. Schematic diagram showing deformational and metamorphic events, and suggested times of ore emplacement (after Butler, 1972; and Addy, 1973).

(F_3-F_5). According to this interpretation, the major fold structures of the Ducktown mining district, the Burra anticlinorium and the Coletown synclinorium, are related to F_2 deformation and the present isograds to M_2 metamorphism. However, most workers now believe that the main regional metamorphic episode in the Blue Ridge belt was Taconic (450-480 m.y. B.P.) and not Acadian (Butler, 1972, 1973; Dallmeyer, 1975; and Hatcher et al., 1980). Based on carbonate thermometry and silicate phase equilibria, Nesbitt and Essene (1982) have inferred a temperature of 540° ± 40°C and a pressure of 6 ± 1 kb for the metamorphic peak at Ducktown.

The known major ore deposits of the district include eight tabular orebodies which occur as relatively conformable lenses in the highly deformed Copper Hill Formation of the Precambrian Great Smoky Group. These deposits strike approximately N 35°E and dip about 50° to 80°SE (Figure 4). Rocks of the Copper Hill Formation consist of metagraywackes, mica schists, metaconglomerates, quartzite, chlorite garnet schists, and minor amphibolites (Magee, 1968). The sulfide mineralization is restricted to the staurolite-kyanite zones of regional metamorphism and commonly occurs along shear zones (Figure 5). The primary ore assemblage consists of pyrrhotite, pyrite, chalcopyrite, sphalerite, with subordinate amounts of galena and Fe-Ti oxides (Magee, 1968). The individual deposits range in size from 250,000 to more than 70 million tons, and have a total tonnage of more than 180 million tons. The ore has an average grade of approximately 1.04 percent copper, 0.89 percent zinc, 24.3 percent sulfur, and 35.4 percent iron (Slater, 1982). The

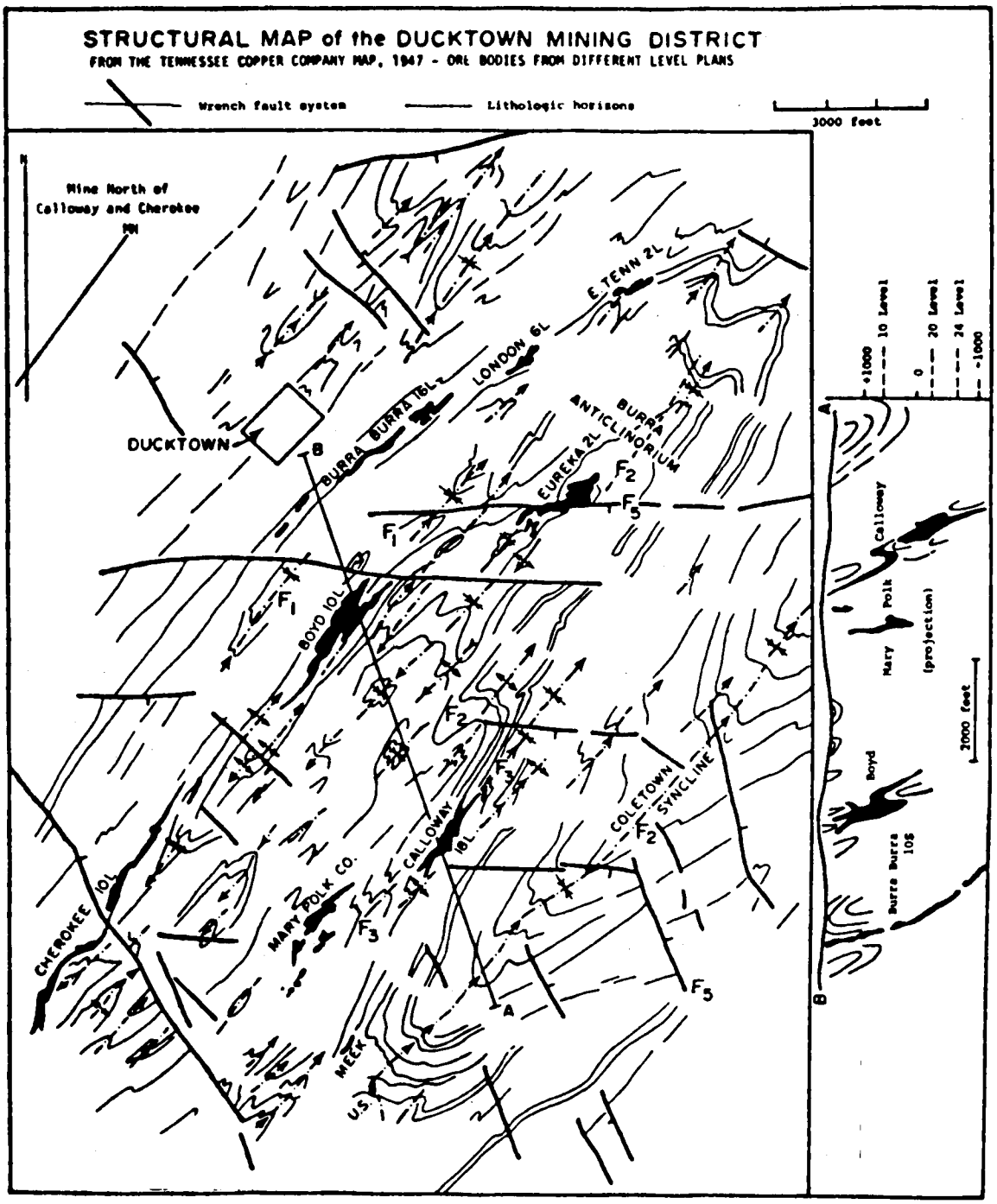


Figure 4. Detailed structural map of the Ducktown mining district showing the distribution of the orebodies. The section A-B shows the conformable nature of the orebodies (after Addy and Ypma, 1977).

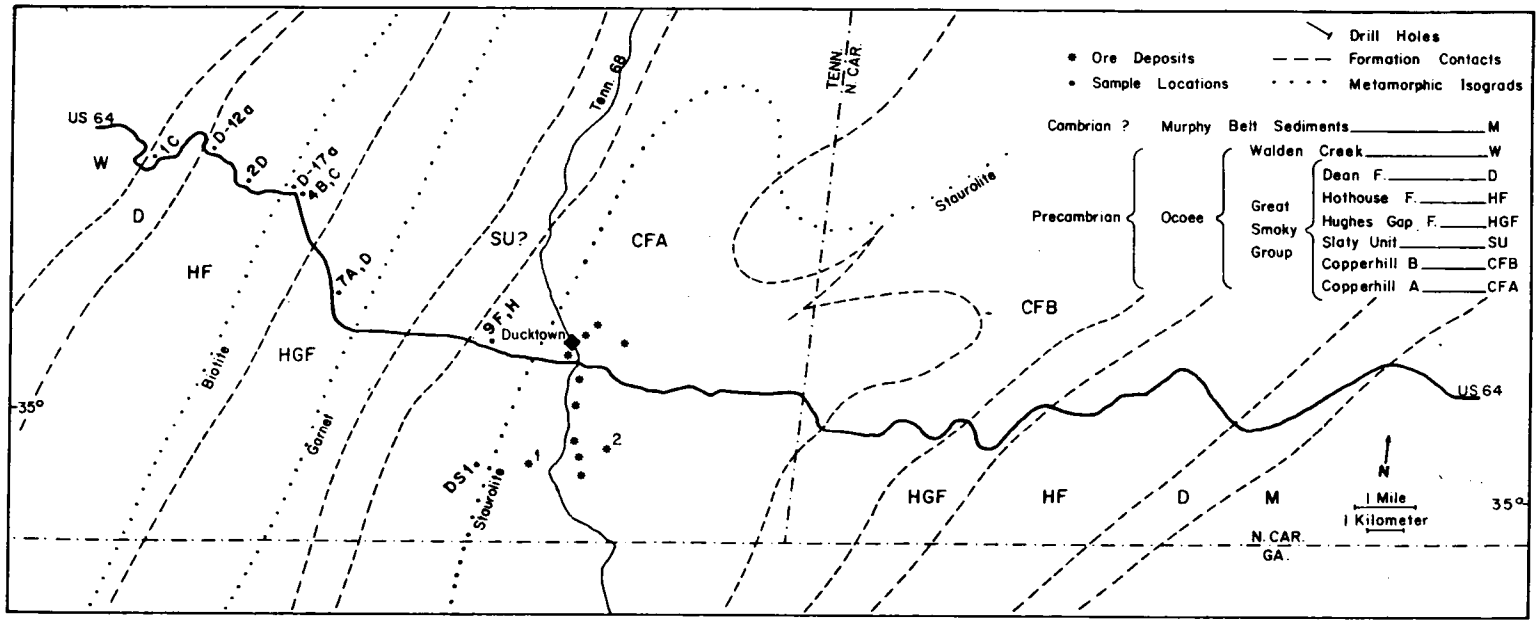


Figure 5. Map displaying local stratigraphy, structure, metamorphic isograds, sample/drill hole locations, and ore deposits of the Ducktown Mining District, Tennessee-North Carolina (compiled by Runyon, 1983).

ore is commonly surrounded by an alteration zone of sericite and/or chlorite schist up to 100 meters wide, but massive sulfides in direct contact with unmineralized metagraywackes are not uncommon (Slater, 1978).

A broad spectrum of hypotheses have been proposed for the origin of these deposits. Originally, they were thought to be postmetamorphic in origin, and produced by hydrothermal replacement of carbonate and other reactive units (Emmons and Laney, 1926; Ross, 1935; Brown, 1962; Hernon, 1968; and Magee, 1968). By the late 1960's and early 1970's, several authors began to seriously question the postmetamorphic origin (Fullagar, 1967; Kinkel, 1967; and Mauger, 1972). They favored a premetamorphic origin but recognized the possibility of some ore remobilization during metamorphism. Mauger (1972) favored a syngenetic origin similar to the Red Sea brine pools, where the sulfides were deposited with the sediments around hot submarine vents. Later the deposits were subjected to metamorphism. Brown (1976) suggested a submarine volcanic origin. Addy (1977) proposed a multistage origin, partly premetamorphic and syngenetic, and partly hydrothermal due to remobilization of disseminated sulfides and trace metals from the country rocks during later regional metamorphism. Slater (1982) noted some features common to volcanogenic massive sulfide deposits. These include: (1) occurrence of amphibolites (possibly of igneous origin); (2) thick chlorite and sericite alteration zones around the orebodies; and (3) copper enriched footwall mineralization and zinc enriched hanging wall mineralization (metal zoning). It must be noted that although there is

some evidence of igneous rocks in the district, generally, they are lacking. Studies by Brown (1962), Fullagar et al. (1967), Tung (1968), and Harvey (1975), suggested that the observed iron depletion in the alteration zone surrounding the sulfide orebodies might account for the iron in the ore sulfides. Recently, Runyon (1983) has suggested that appreciable migration of sulfide constituents from the country rocks could have occurred during prograde metamorphism.

The present study is an attempt to examine the distribution of selected trace elements in the sulfide phases of the Ducktown orebodies and country rocks with the objective of providing some additional constraints for ore genesis in the district.

All previously reported trace element data for the sulfides of the Ducktown district are summarized in Table 1. Data in these previous studies were reported as mean values without ranges or number of samples analyzed. These studies were generally regional in scope and dealt with the establishment of metallogenic provinces, comparisons of different types of deposits, and environments of deposition. The conclusions of these studies appear to have been based on a small number of samples from each district and utilized analytical methods which require mineral separation of high purity and have severe problems with trace element contamination. Therefore, it is the conclusion of this author that these earlier studies are subject to many errors and should be interpreted with caution.

An interesting story related by M. Fleischer (pers. comm., 1982) dealt directly with the Ducktown district and illustrates how conclusions based on few samples could lead to costly mistakes. During World

Table 1. Summary of Trace Element Data for Various Sulfide Minerals, Obtained from the Literature for the Ducktown District.

Sulfide Phase	Analytical Method	Source	Mean Concentrations (ppm)							
			Co	Ni	Mn	Pb	Sn	Ag	Au	As
Py conc.	E. Spec.	1	930	*	*	*	*	*	*	*
Py conc.	E. Spec.	1	510	*	*	*	*	*	*	*
Py conc.	E. Spec.	1	115	*	*	*	*	*	*	*
Py conc.	E. Spec.	1	1650	*	*	*	*	*	*	*
Po conc.	E. Spec.	2	0-70	tr	*	*	*	*	*	*
Py conc.	E. Spec.	2	4000	tr	*	*	*	*	*	*
Cp conc.	E. Spec.	2	tr	n.d.	*	*	*	*	*	*
Py conc.	E. Spec.	3	498	n.d.	*	18	300	*	*	347
Py conc.	AA	4	460	16	26	2050	820	*	10	*
Po conc.	AA	4	29	18	610	n.d.	820	*	*	*
Cp conc.	AA	4	27	21	625	62	1375	*	*	*
Sph conc.	AA	4	120	18	1860	1360	*	*	*	*
Py + Po conc.	AA	4	620	18	1050	560	*	*	*	*

E. Spec.--Emission Spectroscopy

AA--Atomic Absorption

1--Carr & Turekian, 1961; country rocks (phyllite)

2--Espenshade, 1963; Isabella Mine

3--Lenker, 1962; location not known

4--Tilden, 1971; Burra Burra Mine

Py conc.--Pyrite concentrate

Po conc.--Pyrrhotite concentrate

Cp conc.--Chalcopyrite concentrate

Sph conc.--Sphalerite concentrate

tr--trace

*--no data

War II, the U.S. Government was searching for domestic sources of strategic elements, in this case cobalt. Spectrographic analysis on several samples from the Isabella Mine in the Ducktown district showed that the pyrite contained 4000 ppm cobalt (Table 1). Based on the known reserves of sulfide ores in the Ducktown district, it was determined that this could be a major source of cobalt for the United States. There are several problems with this conclusion: (1) the ore consists of only about 30 percent pyrite which is very erratic in its distribution; (2) the number of samples analyzed was very small and represented only one of eight orebodies; and (3) the analytical technique used, emission spectrography, requires a great amount of mineral separation to produce high purity samples. The following data will show that the trace element contents vary not only from orebody to orebody but also from sample to sample in a given orebody. Fortunately, the Ducktown smelter was not converted for producing cobalt.

This is the first systematic study of the trace element distribution in the sulfides in the Ducktown district. The research presented here includes: (a) developing a suitable technique for the determination of trace elements in sulfides; (b) examination of the variation of selected trace elements (Co, Ni, Mn, Pb, Ti, Sn, Ag) in sulfide phases (pyrite, pyrrhotite) of ore assemblages; (c) comparison of the trace element distribution in sulfides from the country rocks to the orebodies, between orebodies, and within orebodies; and (d) interpretation of the trace element distribution patterns, with an attempt to relate them to ore genesis.

CHAPTER II

METHODS OF INVESTIGATION

Sampling

Samples for this study were collected from two of the orebodies and from sulfide-bearing country rocks. Samples of the country rocks were obtained from the departmental collection (collected by G. Runyon and by Dr. K. C. Misra). These samples were collected along Highway 64 in southeastern Tennessee (Figure 5). Samples from the ore bodies were collected from eight cores drilled at four levels in the Calloway Mine and two cores drilled at a single level in the Cherokee Mine (Plates 1 and 2). The core samples were obtained from the Tennessee Chemical Company. A representative sample was selected for every five or ten feet of core for petrographic study. It may be noted that in the earlier stages of exploration and development, the cores were not drilled much farther than the massive ore; therefore, samples far out into the country rocks (alteration zone) were generally not available. Samples to be analyzed for trace elements were selected on the basis of the presence of sulfides, size of individual sulfide grains, relationships to the orebody, and textural variety. Due to the size of the crater produced by the laser beam (100-200 microns) and imperfect beam alignment, the sulfide grains had to be on the order of a couple of millimeters in diameter to prevent any possible trace element contamination from gangue minerals. Wherever possible, samples were chosen which represented the hanging wall rocks, the massive orebody, and the

footwall rocks, in order to examine the trace element distribution laterally across the orebody. Texturally, these ores are quite complicated. In selecting samples for chemical analysis, particular attention was paid to the presence of tiny inclusions in the sulfide phases of interest, a potential source of contamination, and to different textural varieties of pyrite which might represent different generations of sulfide mineralization.

Ore Petrography

Polished sections (1 inch diameter) were prepared for representative samples from each core and studied using reflected light. The ore petrography served two main purposes: (1) identification of the opaque phases and their textural varieties in each sample; and (2) selection of suitable samples for trace element analysis. Samples which contained the sulfide phases of interest as small grains or with tiny inclusions that might contaminate the trace element data were eliminated. Each selected grain was photographed to ensure that the trace element analysis was done on the selected grains. The sulfide phases chosen for analysis were pyrite and pyrrhotite. These are the major sulfides present in the district (>90 percent of the ore), they are composed of large enough grains to analyze, and most of the literature on trace elements in sulfides related to ore genesis has been devoted to these phases. Other phases, such as chalcopyrite and sphalerite, are minor and generally occur as inclusions in pyrite and pyrrhotite.

Laser Microprobe Analysis

One of the major problems in the trace element analysis of a sulfide phase (or any other single phase) is contamination. Techniques such as Atomic Absorption, Emission Spectrography, and XRF, which have been used for trace element analysis of sulfides, require ultra-pure mineral concentrates. Due to impurities present in these concentrates (generally, 1-2 percent), one must use caution when interpreting such trace element data. This problem has been pointed out by several authors including Both (1973) and Bhatia (1976).

A major emphasis of this study has been directed toward eliminating this problem of contamination, as much as possible, by utilizing a Laser Microprobe (LMP) for analysis of trace elements. This instrument allows in situ microanalysis. Although not commonly used for trace element analysis in sulfides, it is very well adapted for this purpose. The laser microprobe is a laser generating unit combined with an emission spectrograph (Figure 6). A small area (100 to 200 microns in diameter) is vaporized by a laser burst focused on the sample. The rising vapor is further excited when a discharge is triggered between two carbon electrodes positioned 2 millimeters above the sample surface. The spectrum is subsequently recorded on a photographic plate in the camera attached to the emission spectrograph. By examination of the spectrum using a densitometer, one can relatively quickly identify the major, minor, and trace elements in the microsample and their concentrations. Details of the construction, applicability and limitations of the laser microprobe have been discussed by Harding-Barlow et al. (1973), and Keil

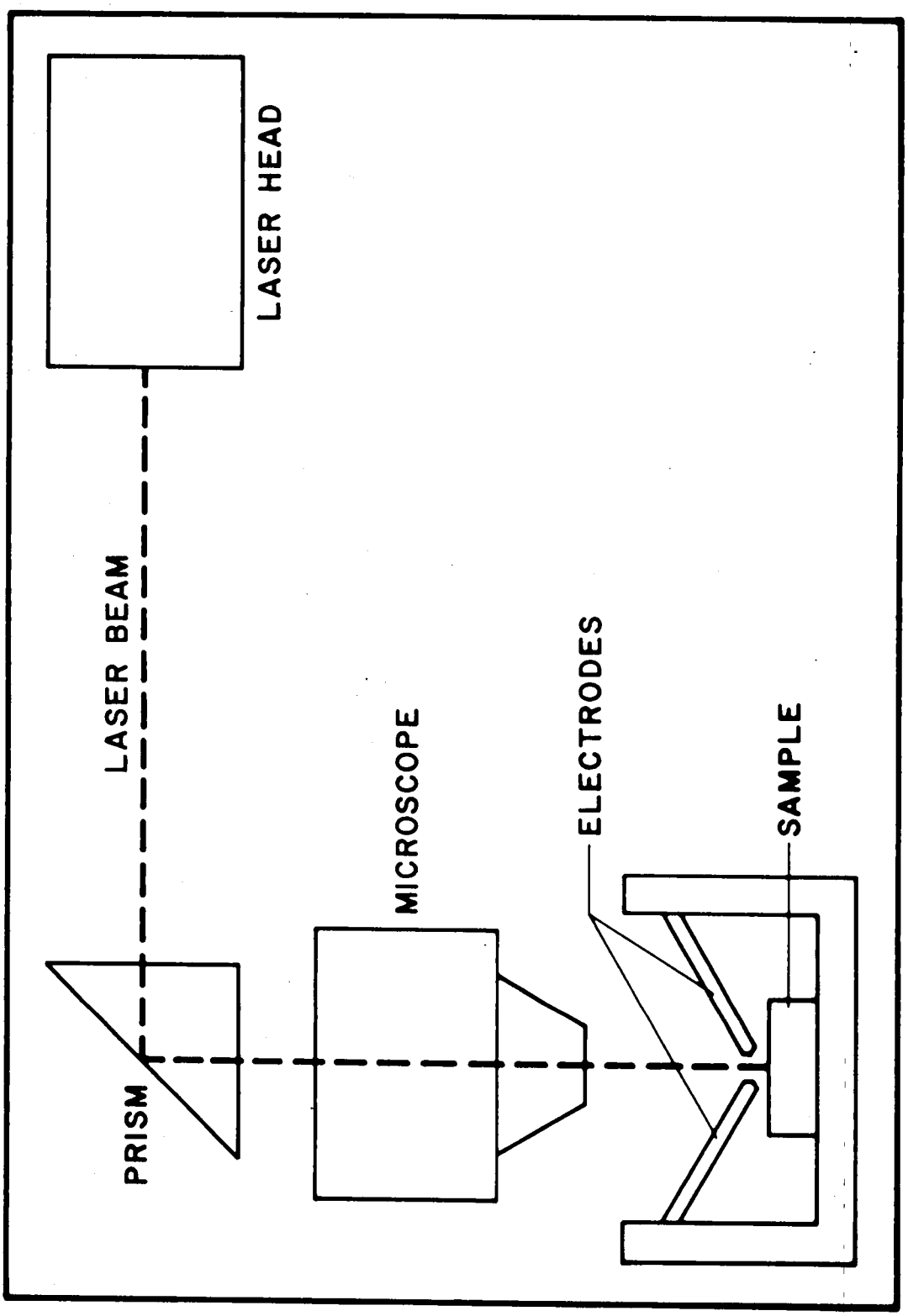


Figure 6. Schematic diagram of the laser microprobe spectrograph source.

and Snetsinger (1973). For the most part, this instrument has been used to perform qualitative analysis on various materials. The studies by Snetsinger and Keil (1967), Estes (1972), Blackburn (1968, 1969, 1977), Eremin (1975), Tsui et al. (1975), and Bhatia (1976, 1981) are among the only published reports which utilized the LMP for quantitative analysis on geological materials.

The LMP analyses were performed at the Cabot Spectrographic Laboratory located at the University of Kentucky, Lexington, with assistance from Professors William H. Dennen and William H. Blackburn.

Standards. The problems of selecting and preparing standards for the laser microprobe are similar in many respects to those encountered in electron microprobe analysis. Normally, one employs standards which are homogeneous and have a similar matrix to the substance being analyzed. Fortunately, the matrix problems that exist for the electron microprobe are not as crucial when using emission spectrographic analysis (Adler, 1966). In contrast to the longer-lasting arc or spark excitation used in standard arc-source emission spectrography, the laser microprobe utilizes a short laser pulse which produces only minimal matrix effects (Keil and Snetsinger, 1973).

Several types of standards have been employed in laser microprobe analysis. Blackburn (1968, 1977) used chemically analyzed samples of silicate minerals that were powdered, homogenized, and fused to glass in aluminia boats at 1400°C in a combustion furnace. Tsui et al. (1975) prepared liquid standards by placing holes in pure silica plates filled with the standard solutions. He used these standards to determine the

chemical composition of fluid inclusions in minerals. Bhatia (1976) prepared synthetic standards for the analysis of various sulfide minerals. He used "unfused" standards that were synthesized from "spec-pure" elements of at least 99.9999 percent reported purity. He used a method in which the element that made up the bulk of the standard was used as an internal standard. For example, lead was used for galena standards, iron for pyrite standards, etc. Each internal standard was then diluted by the appropriate trace elements in varying amounts, resulting in standards with 5, 10, 50, 100, 500, and 1,000 ppm concentrates of the element. The standards were thoroughly homogenized and then compressed into discs with a lithium tetraborate backing.

The initial set of standards tried for the present study comprised aliquots of Fe-, Zn-, and Cu-concentrates obtained from the mill of the Tennessee Chemical Company. These were chosen for three reasons: (1) similar matrix material; (2) similar trace elements present as in unknowns; and (3) similar range of trace element concentrations as unknowns. The ore concentrates were analyzed for 21 elements by X-ray Assay Laboratories Limited, Don Mills, Ontario. They were subsequently ground to various size ranges and homogenized as thoroughly as possible. These "unfused" standards (powders) were then pressed into discs with a boric acid backing and analyzed. The results of the analysis were extremely erratic, presumably due to inherent inhomogeneity of the samples, and were considered unacceptable for this study (Appendix C, Table C-1).

It was then decided to use spectrographic standards marketed by Chemplex Industries, Inc. Each of their standards were formulated from

selective high-purity inorganic compounds and contained 53 different analytes at concentration levels of 50 ppm, 100 ppm, 500 ppm, and 1,000 ppm, respectively. The matrix material that made up each standard was lithium carbonate which was thoroughly homogenized and ground to -325 mesh (Chemplex Set Cat No. 6400). As with the previous standards discussed, these standards were further homogenized and then compressed into discs with a boric acid backing (for procedures see Appendix A).

Photographic Plate Calibration. After the spectrum of the vaporized sample was recorded on a photographic plate, the response had to be corrected using a plate calibration curve. Each photographic emulsion has its own characteristic response which varies with incident wavelength and intensity; therefore, it is necessary to correct all obtained densities for photographic plate response (for details on the procedure see Sawyer, 1951, Estes, 1972, and Bhatia, 1976). The calibration curve for the present analytical set-up is shown in Figure 7. One determines the percent transmission of a particular spectral line using a densitometer and obtains a corresponding relative intensity value from the calibration curve.

Working Curves. Each of the standards was "shot" 17 times. Since there were four standards (50, 100, 500, and 1,000 ppm), a total of 68 shots were fired. The transmission data were reduced to intensity data by using the plate calibration curve (Figure 7). The data were further reduced by taking the log of the ratio of the intensity of the trace element of interest to the intensity of the internal standard, i.e., log

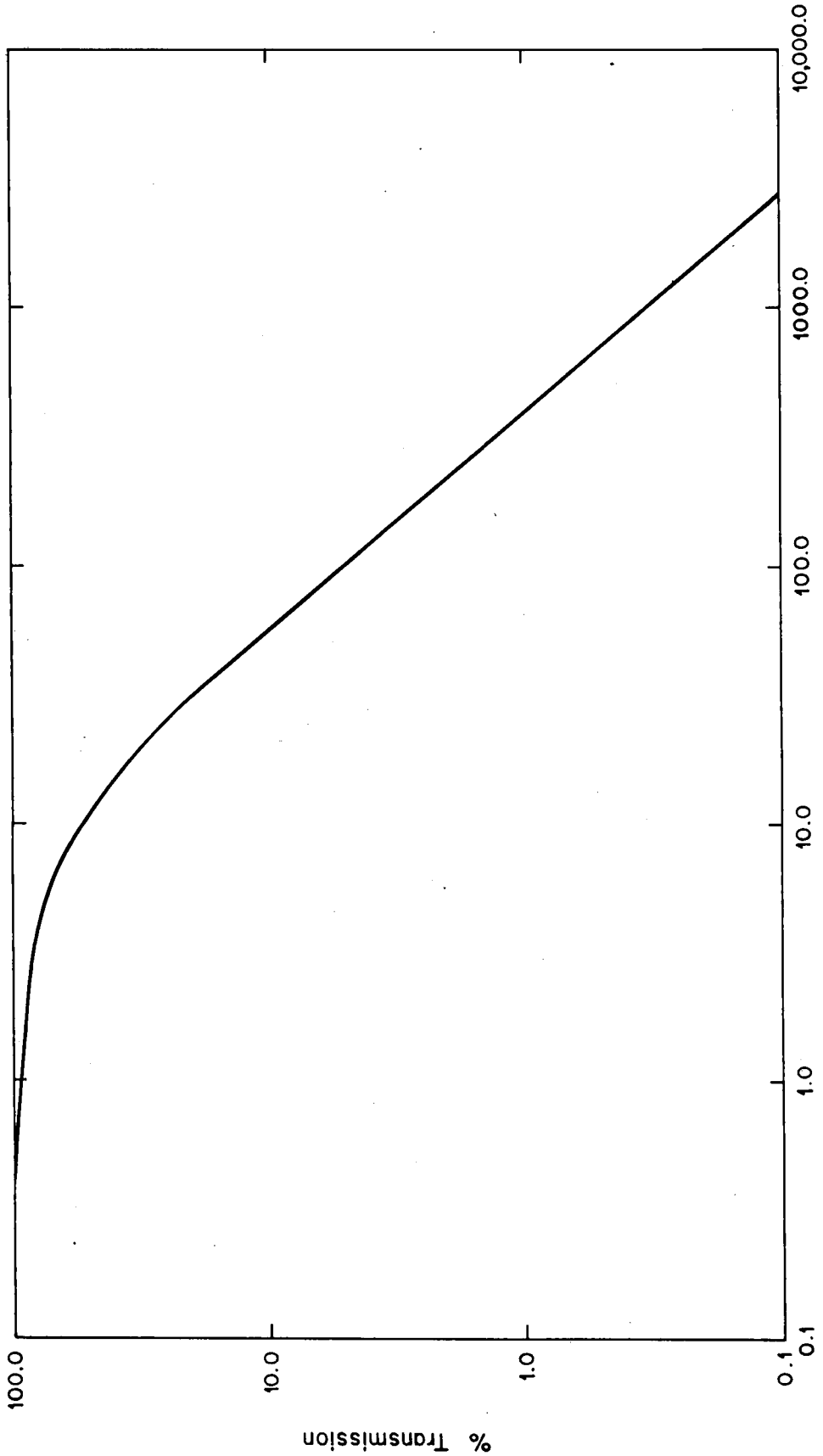


Figure 7. Calibration curve for plate response (data from Cabot Spectrographic Laboratory, University of Kentucky, Lexington).

(IE/IM), where IE is the spectral intensity of the trace element E, and IM the spectral intensity of the internal standard M. For this study, iron was chosen as the internal standard for both pyrite and pyrrhotite. One of the limitations of the laser microprobe is its lack of precision. This is directly related to the size of the crater produced each time a sample is hit by a laser burst. As quantitative analysis by the laser microprobe is directly proportional to the size of the crater produced, it is important to maintain either a constant crater diameter or calculate the ratio of the intensity of each trace element to the intensity of the internal standard for each sample (which is assumed to be a constant). As the burst of laser energy varies somewhat from shot to shot, so does the crater diameter; therefore, the intensity ratio method was used to overcome this problem. In other words, although the amount of sample vaporized each time varied, the ratio of the concentration of the trace element vaporized to the amount of internal standard vaporized remained constant (Bhatia, 1976).

Due to the relatively high scatter of the data, all data points that fell outside the 95 percent confidence limit of the mean (generally less than 10 percent of the total data) were eliminated. The scatter of data was probably due to a combination of inhomogeneities in the standards and imprecisions in the analytical equipment. This same procedure was used for each trace element at all concentration levels. These data were subsequently plotted against the log of the concentration of the trace element over its entire concentration range.

At low concentration levels the relationship between concentration and intensity was considered to be linear, therefore a least squares regression line could be fitted to the data, giving the working or standard curve for each element. The working curve for each element (Co, Ni, Mn, Pb, Ti, Sn, Ag, and Cu) is illustrated in Figure 8. The spectral lines used for trace element determinations, instrumentation, and laser microprobe settings used are given in Appendix D (Table D-1). The regression line equations, correlation coefficients, and 95 percent confidence limits for working curves are also given in Appendix D (Table D-2). Due to the poor precision of the data and hence, low correlation coefficient (Appendix D, Table D-2), copper was not included in this study. The fact that the most sensitive copper lines do not vary significantly with changes in concentration is probably the main reason for lack of precision of copper. It must be noted that the various regression lines plotted in Figure 8 do not generally fit the mean values very well. This is accounted for by the highly scattered data. Since the regression lines represent all of the data points, it is believed that they more closely approximate the true linear relationship rather than plotting a line through the mean values.

Precision and Accuracy. An attempt was made to check the precision and accuracy of the analytical method. Massive samples of pyrite and pyrrhotite were analyzed nine and six times, respectively, to check precision (Appendix D, Tables D-3). Assuming that the trace elements distributions are relatively homogeneous, the precision (using the intensity ratio method) appears to be reasonably good. The coefficients

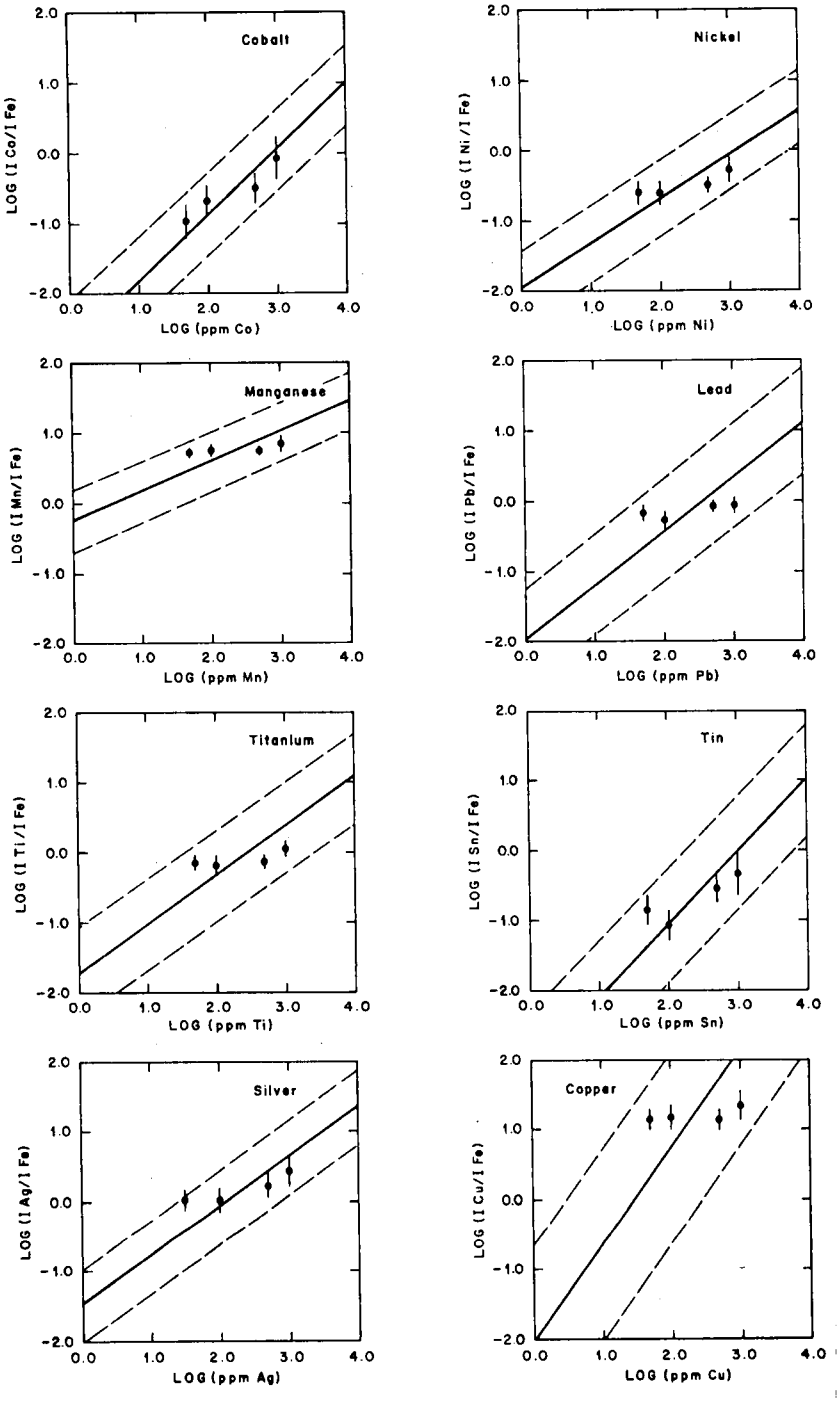


Figure 8. Standard working curves for Co, Ni, Mn, Pb, Ti, Sn, Ag, and Cu in pyrite and pyrrhotite. Dashed lines represent the 95 percent confidence limit on the regression lines. Both the regression lines and confidence limits for each element are based on all of the data points rather than the mean. Closed circles represent the mean plus one standard deviation (bar) for each standard. See Appendix D for statistical data on regression lines.

of variation (a measure of precision) average about 50 to 60 percent in pyrite and about the same for pyrrhotite.

A pyrite standard obtained from the Geology Department of Pennsylvania State University was used to check accuracy. The only data available were mean values for several elements of which only three elements (Co, Ni, and Mn) were used in this study. The ranges and standard deviations about the means were not available. An additional problem with this standard is the possibility of zoning. The mean data from the working curves appear to be reasonable when compared against the standard. The values are consistently about 50 percent below what the standard reports but one standard deviation nearly includes the reported value (Appendix D, Table D-4). From this data, it appears that the quantitative values are reasonable though the accuracy is not known. For this study the emphasis is placed on the relative values and the Co:Ni ratios for determining trends.

CHAPTER III

ORE PETROGRAPHY

According to Magee (1968), the ore deposits of the Ducktown district consist of approximately 65 percent massive sulfides and 35 percent gangue minerals. The ore minerals that make up the massive sulfide consist of approximately 60 percent pyrrhotite, 30 percent pyrite, 4 percent chalcopyrite, 4 percent sphalerite, 2 percent magnetite, traces of silver and gold, and other metallic minerals (galena, bornite, cubanite, molybdenite, arsenopyrite, stannite, and native bismuth). The following observations on the composition and textures of the sulfides that occur in the Ducktown district are summarized from Magee (1968), Carpenter (1974), Ringler (1979), Barton (pers. comm., 1982), Runyon (1983), and samples obtained for the present study.

Pyrrhotite

Carpenter (1974) identified three types of pyrrhotite in the Ducktown area. These include: hexagonal, monoclinic, and hexagonal + monoclinic intergrowths. He observed that the monoclinic and hexagonal + monoclinic varieties are most abundant in the lowest grades of metamorphism, whereas, the hexagonal and hexagonal with monoclinic rims varieties of pyrrhotite dominate higher grades of metamorphism (above garnet grade). Ringler (1979) found no evidence for the presence of monoclinic pyrrhotite in the Calloway orebody, as all pyrrhotite was

determined to be of the hexagonal type. Magee (1968) reported a composition of about $Fe_{11}S_{12}$ (average 47.8 atomic percent Fe).

In the country rocks (Ocoee Gorge) the pyrrhotite and pyrite usually occur in coarser and more quartz-rich layers in the metasedimentary rocks. The pyrrhotite is generally fine-grained and occurs as "streaks" parallel to S_1 and S_2 cleavage replacing several of the silicate phases (Figure 9a). Some of the pyrrhotite occurs of polycrystalline aggregates exhibiting polygonal boundaries and triple (120°) junctions implying annealing and recrystallization (Stanton, 1972). Runyon (1983) has suggested a synmetamorphic origin for the pyrrhotite.

In the orebody, pyrrhotite masses display a wide variety of complex forms, intergrowths, and grain-boundary relations. It commonly replaces gangue minerals (Figures 9b and 9c). Frequently, the pyrrhotite contains inclusions of pyrite, veinlets and fine-grained inclusions of chalcopyrite, sphalerite, galena, and various gangue minerals (Figure 9d). Much of the pyrrhotite consists of polycrystalline aggregates displaying polygonal boundaries, triple (120°) junctions, and deformation twinning (Figure 9e). Due to their relatively high ductility, pyrrhotite and chalcopyrite are commonly squeezed into fractures in pyrite (Figure 9f).

Pyrite

In the country rocks (Ocoee Gorge), pyrite is most abundant in the lower grades of metamorphism. As with pyrrhotite, the pyrite generally occurs in the coarser-grained and more quartz-rich metasediments. Pyrite is usually found as individual cubes (Figure 10a) and as

Figure 9. Photomicrographs of sulfide assemblages in the Great Smoky Group metasedimentary rocks and Ducktown orebodies. Uncrossed polars in reflected light unless otherwise noted. Scales are shown at bottom of figure. (A) "Streaks" of pyrrhotite parallel to S_1 cleavage; chlorite grade, Ocoee Gorge. (B) Pyrrhotite rimmed by chalcopyrite and minor sphalerite; upper level, Calloway orebody. (C) Pyrrhotite and minor chalcopyrite replacing gangue along cleavage traces; upper level, Calloway orebody. (D) Inclusions of chalcopyrite and sphalerite in pyrrhotite; upper level, Calloway orebody. (E) Deformation twinning in pyrrhotite (crossed polars); 27 level, Calloway orebody. (F) Pyrrhotite filling fractures in pyrite; Cherokee orebody.

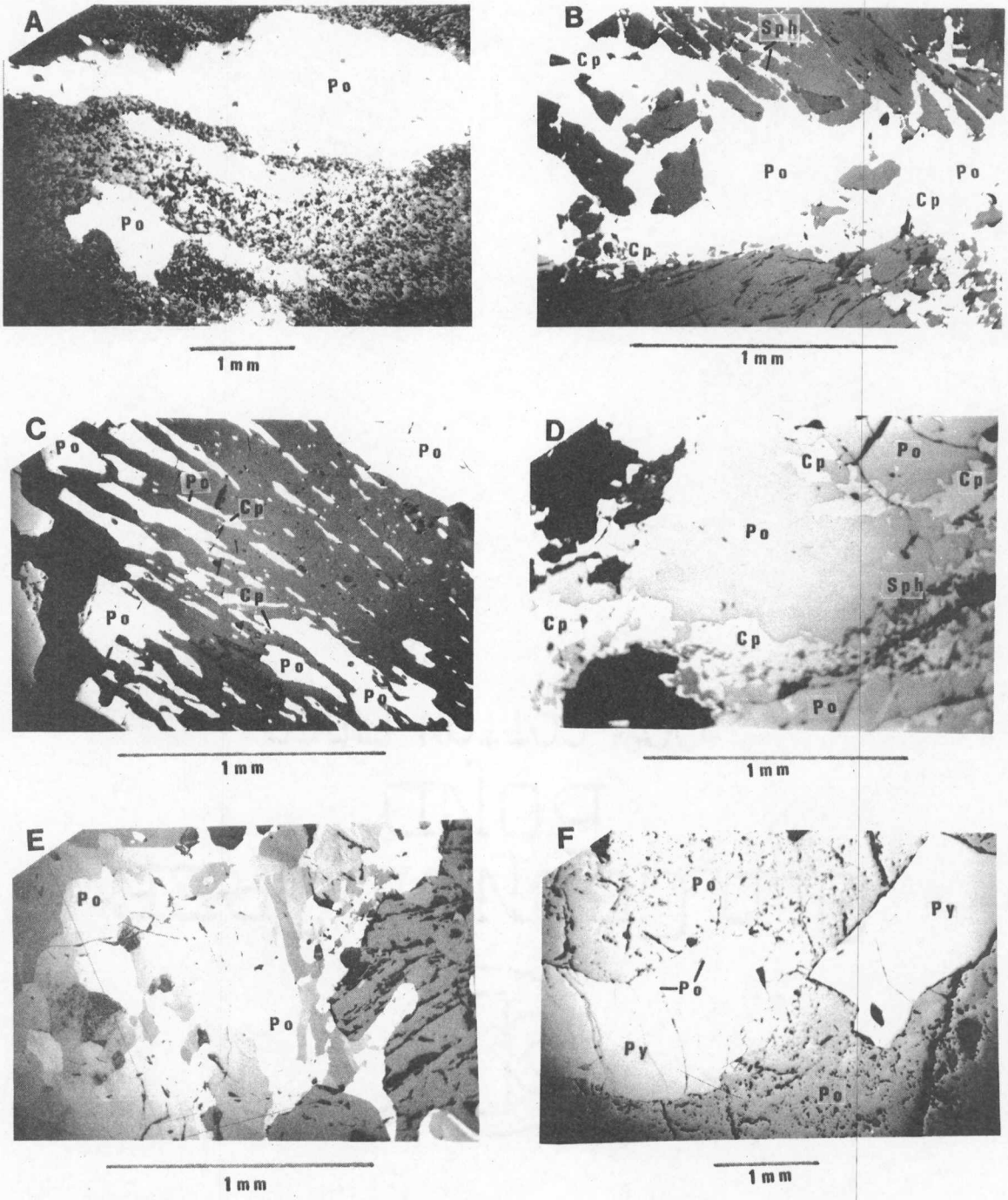

A
Po
Po
1 mm
B
Sph
Cp
Po
Po
Cp
Cp
1 mm
C
Po
Po
Po
Cp
Cp
Po
Po
Po
1 mm
D
Cp
Po
Cp
Po
Sph
Cp
Cp
Po
1 mm
E
Po
Po
1 mm
F
Po
Py
Po
Py
Po
1 mm

Figure 9.

Figure 10. Photomicrographs of sulfide assemblages in the Great Smoky Group metasediments and Ducktown orebodies. Uncrossed polars in reflected light unless otherwise noted. Scales are shown at bottom of figure. (A) Typical euhedral pyrite in metasedimentary rocks; chlorite grade, Ocee Gorge. (B) Synmetamorphic pyrite euhedra within a matrix of chalcopyrite; 27 level, Calloway orebody. (C) Subeuhedral pyrite in a matrix of pyrrhotite; Cherokee orebody. (D) Anhedral pyrite in a matrix of finely intergrown pyrrhotite and chalcopyrite; 22 level, Calloway orebody. (E) Pyrite grains with fractures filled in by pyrrhotite and chalcopyrite; 27 level, Calloway orebody. (F) Sphalerite, chalcopyrite, and galena inclusions in pyrite; upper level, Calloway orebody.

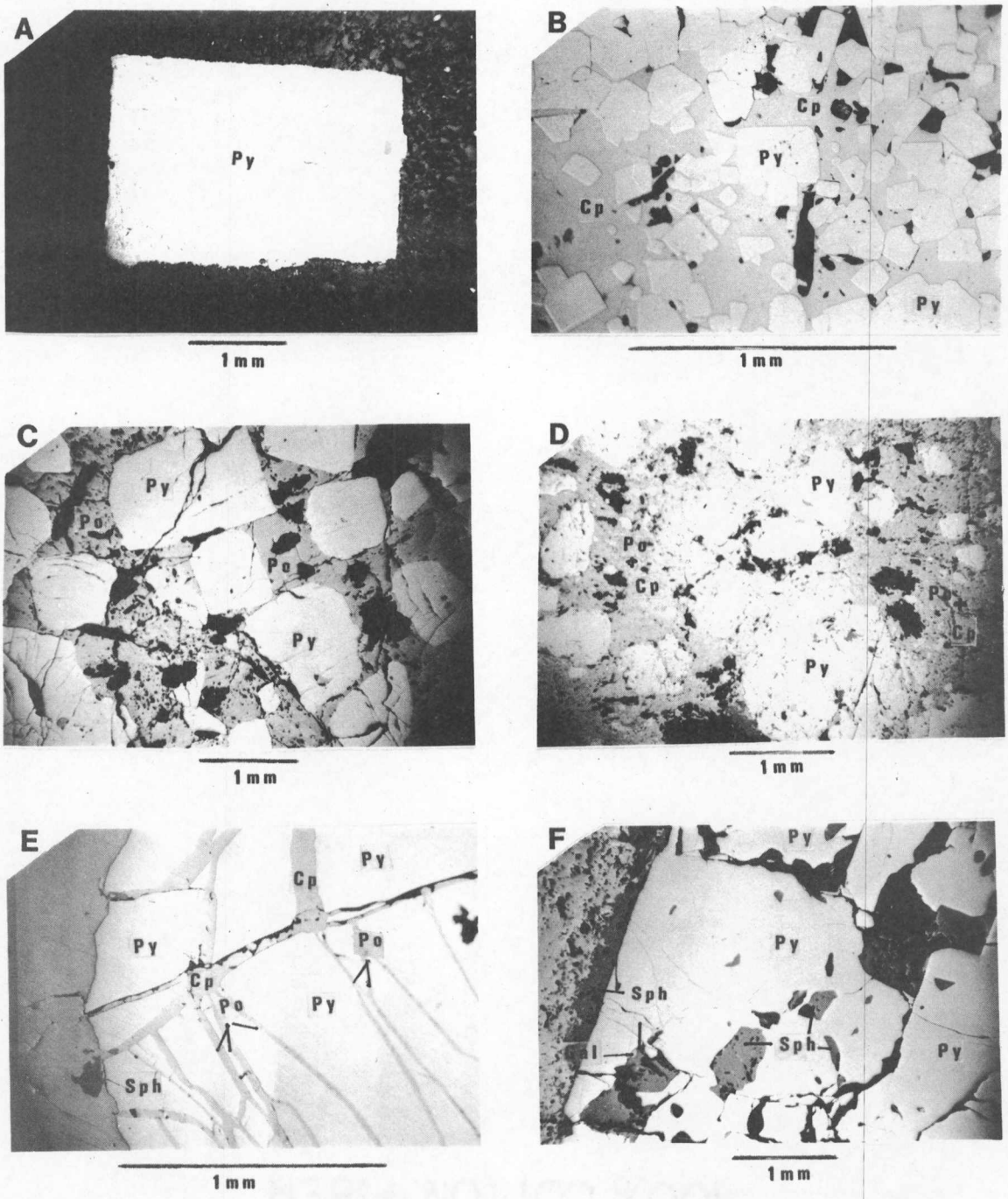

A
Py
1 mm
B
Cp
Py
Cp
Py
1 mm
C
Py
Po
Po
Py
1 mm
D
Py
Po
Cp
Py
Cp
Py
1 mm
E
Py
Cp
Py
Po
Cp
Po
Py
Sph
1 mm
F
Py
Py
Sph
Sph
Py
1 mm

Figure 10.

irregular aggregates of small cubes and it commonly shows replacement by silicates and other sulfides. Frequently, pyrite grains contain inclusions of other sulfide (pyrrhotite, galena, sphalerite, and chalcopyrite), oxide and silicate minerals. Runyon (1983) noted that with increase in metamorphic grade the pyrite becomes more irregularly shaped masses aligned parallel to S_1 cleavage. He also noted that, in the staurolite zone, pyrite is not a stable phase; it is found as a late fracture-filling phase and as an alteration product on pyrrhotite grains. Carpenter (1974) recognized two distinct generations of pyrite: (1) prograde pyrite (euhedral grains lacking embayments of other minerals and no specific orientation of inclusions, if present); and (2) retrograde pyrite (characterized by irregular serrated grain boundaries, replacement by later minerals, and included phases oriented along crystallographic directions of pyrite).

In the orebody, pyrite usually occurs as fine- to coarse-grained crystalline aggregates up to 1.3 centimeters across, but occasionally crystals up to 10 centimeters or more across are found. Pyritic zones, masses up to 15 meters wide, have been observed (Magee, 1968). Commonly, porphyroblasts of pyrite occur in a matrix of pyrrhotite and/or chalcopyrite, a texture which is considered typical of regionally metamorphosed massive sulfide deposits (Figures 10b and 10c). Pyrite grains which are generally anhedral to subeuhedral appear to have been replaced by other sulfides and/or gangue minerals (Figure 10d). The anhedral to subeuhedral variety of pyrite appears to be similar to the retrograde pyrite noted by Carpenter (1974). Additionally, many pyrite

grains contain small inclusions of sphalerite, chalcopyrite, galena, magnetite, and various gangue minerals (Figure 10f). Some of the pyrite appears brecciated, with fractures filled with pyrrhotite and/or chalcopyrite (Figure 10e). Annealed texture in pyrite, triple (120°) junctions, indicative of recrystallization was also noted in some samples.

An attempt was made to see if the trace element contents varied significantly with different textural varieties of pyrite (different generations of pyrite). No clear relationship could be established. It appears that the general trace element distribution pattern was established during the peak of prograde regional metamorphism and any subsequent retrograde metamorphism did not significantly affect the overall trace element distribution.

Chalcopyrite

In the country rocks (Ocoee Gorge), chalcopyrite generally occurs as small individual grains, as inclusions in pyrite and sphalerite, and rimming pyrrhotite patches (Runyon, 1983).

Chalcopyrite is the only significant copper mineral in the primary ore and is most frequently associated with pyrrhotite (Magee, 1968). The chalcopyrite occurs as intergrowths and veinlets in pyrrhotite, and as veinlets in the gangue minerals, especially quartz, calcite, and Ca-silicates, and occasionally pyrite (Figures 11a, 11d, 11e, and 11f). Chalcopyrite also occurs as oriented inclusions in sphalerite ("chalcopyrite disease") presumably due to exsolution from a sphalerite-chalcopyrite solid solution (Figure 11b). Experimental studies suggest

Figure 11. Photomicrographs of sulfide assemblages in the Ducktown orebodies. Uncrossed polars unless otherwise noted. Scales are shown at bottom of figure. (A) Intergrowths of chalcopyrite, sphalerite, and pyrrhotite; upper level, Calloway orebody. (B) Grains and rods of chalcopyrite oriented within sphalerite; upper level, Calloway orebody. (C) Typical sulfide assemblage of pyrrhotite, pyrite, sphalerite, and chalcopyrite; upper level, Calloway orebody. (D) Pyrrhotite, sphalerite, and chalcopyrite replacing gangue; upper level, Calloway mine. (E) Chalcopyrite replacing gangue along oriented grain boundaries; 27 level, Calloway orebody. (F) Euhedral grains of pyrite in a matrix of chalcopyrite and minor sphalerite; 27 level, Calloway orebody.

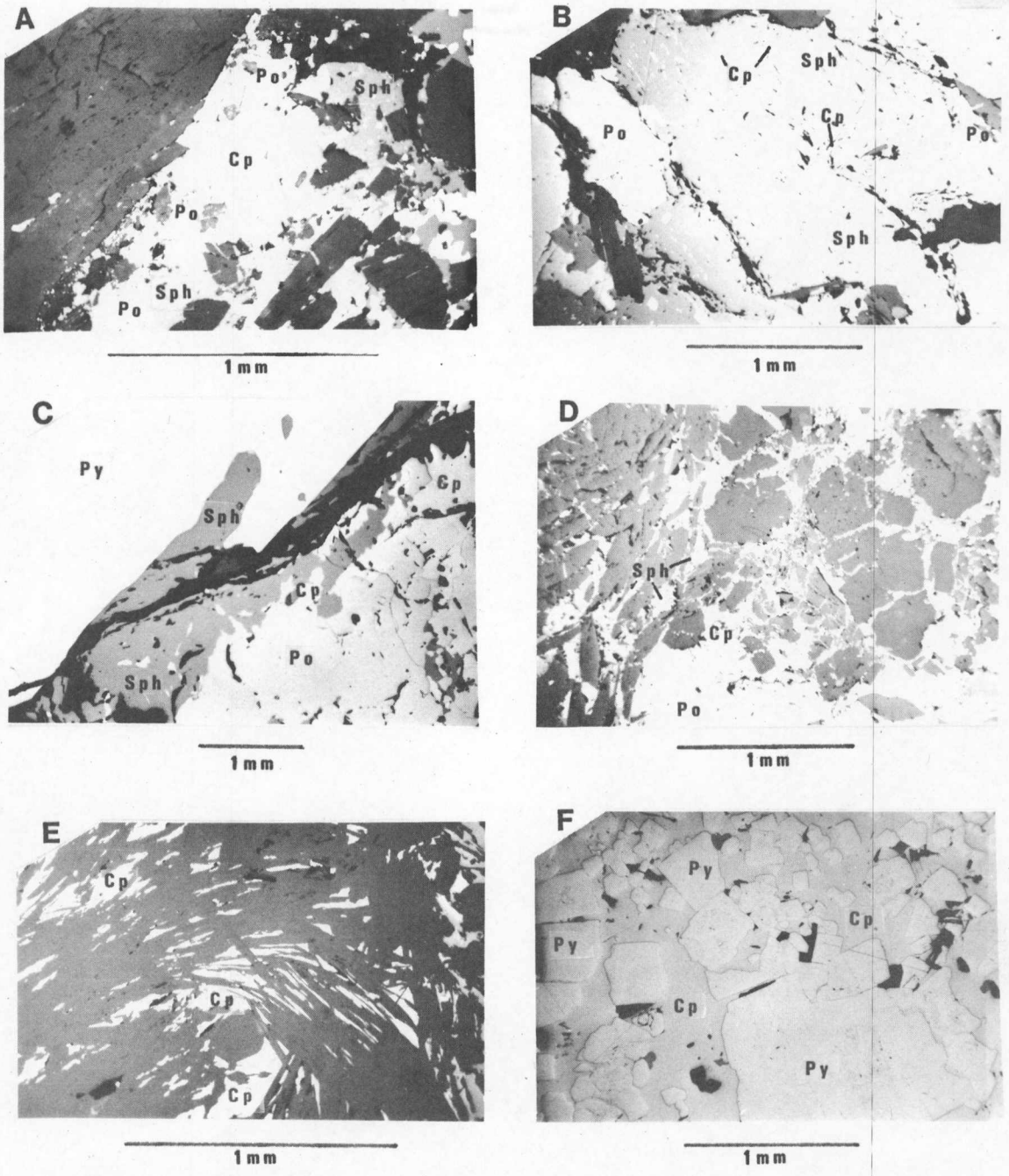

A
Po
Sph
Cp
Po
Sph
Po
1 mm
B
Cp
Sph
Cp
Po
Po
Sph
1 mm
C
Py
Sph
Cp
Cp
Po
Sph
1 mm
D
Sph
Cp
Po
1 mm
E
Cp
Cp
Cp
1 mm
F
Py
Cp
Py
Cp
Py
1 mm

Figure 11.

that significant solid solution of chalcopyrite in sphalerite occurs only above 500°C (Craig and Vaughan, 1981).

Sphalerite

In the country rocks (Ocoee Gorge), sphalerite is not a common phase. If present, it generally occurs as small patches associated with pyrrhotite (Runyon, 1983).

The sphalerite in the orebody is of the marmatite variety which has a high Fe content and is generally dark brown to black in color. It is the only zinc mineral in the ore (Magee, 1968). Ringler (1979) determined the FeS content of sphalerite from the Calloway orebody. It ranged from 8.22 to 8.96 mole percent FeS. He noted no significant zoning in terms of FeS content within single samples, suggesting that a high degree of compositional equilibration was achieved during metamorphism. In contrast to Ringler's study, P. Barton (pers. comm., 1982) analyzed sphalerite in doubly polished thin sections and noted a systematic variation in the FeS content of sphalerite, from about 14 mole percent FeS (orange-brown) at the core to about 9 mole percent FeS (yellow) at the rim in contact with pyrrhotite. In the same section, sphalerite completely enclosed in calcite, showed relatively uniform FeS content (13-14 mole percent FeS). The lower FeS content of sphalerite in contact with pyrrhotite seems to represent compositional reequilibration during retrograde metamorphism. It has been suggested that in metamorphosed massive sulfide deposits, some sulfide phases (chalcopyrite, galena, and pyrrhotite) would reequilibrate, whereas others

(sphalerite, pyrite or arsenopyrite) would not (P. Barton, pers. comm., 1982).

Sphalerite has the same general occurrence as chalcopyrite and is frequently associated with it. It occurs as intergrowths and inclusions in pyrrhotite and occasionally in pyrite (Figures 10f and 11c). Commonly, sphalerite contains tiny oriented inclusions of chalcopyrite ("chalcopyrite disease") (Figure 11b).

CHAPTER IV

TRACE ELEMENT DISTRIBUTION IN PYRITE AND PYRRHOTITE FROM THE DUCKTOWN MINING DISTRICT

The distribution of trace elements in the pyrite and pyrrhotite analyzed was examined with respect to: (1) variation from the country rocks (Ocoee Gorge) to the orebodies; (2) variation between the Cherokee and Calloway orebodies; (3) lateral variation of trace elements from the hanging wall to the footwall in the orebodies; (4) vertical variation from the upper to the lower levels of the Calloway orebody; and (5) cobalt and nickel contents and the Co:Ni ratio in terms of ore genesis. A general review of trace elements in pyrite and pyrrhotite is discussed in Appendix F.

Due to the relatively high variability of the analytical data, mean concentrations of the trace elements are utilized in this study to compare one sample to another and examine various geochemical trends. Although the ranges of values overlap each other it will be shown that the mean values are statistically different and represent the relative relationship between the trace elements and their geochemical environments.

It has been observed that most elements in minerals have distributions which are approximately log-normal (Price, 1972). Therefore, the frequency distribution of the present data was checked by graphical methods: (1) cumulative frequency histograms of the raw analytical data; (2) frequency histograms of log-transformed analytical data; and

(3) cumulative frequency curves plotted on log-probability paper (Sinclair, 1976). Examples of these plots are shown in Figures 12 and 13. From these plots it was concluded that the concentrations of the different trace elements in the studied sample groups generally approached a log-normal distribution rather than an arithmetic-normal distribution. Therefore, where groups of data are discussed (large number of observations) the geometric mean is used, whereas, for individual samples (relatively small numbers of observations) the arithmetic mean is used. Use of arithmetic means for the grouped data would have produced appreciably different mean values but not significantly different trends, whereas, for individual samples the difference between the geometric and arithmetic means is insignificant.

Figures depicting trace element variations are plotted in groups of elements (Co, Ni, Co:Ni ratio; Pb, Sn, Ag; and Mn, Ti) for ease of viewing. It is interesting to note that the elements in each group generally follow a similar pattern, indicating that they may be chemically related. It should be noted that the Co:Ni ratio is plotted in a different scale.

Variation in the Trace Element Contents of Pyrite and Pyrrhotite from the Ocoee Gorge Metasedimentary Rocks to the Orebodies

Samples of both pyrite and pyrrhotite were collected from the chlorite, biotite, and garnet grades of metamorphism in Ocoee Gorge (Figure 5, p. 7) and from staurolite-kyanite grades in the orebodies themselves. All of the data were combined from the individual grades

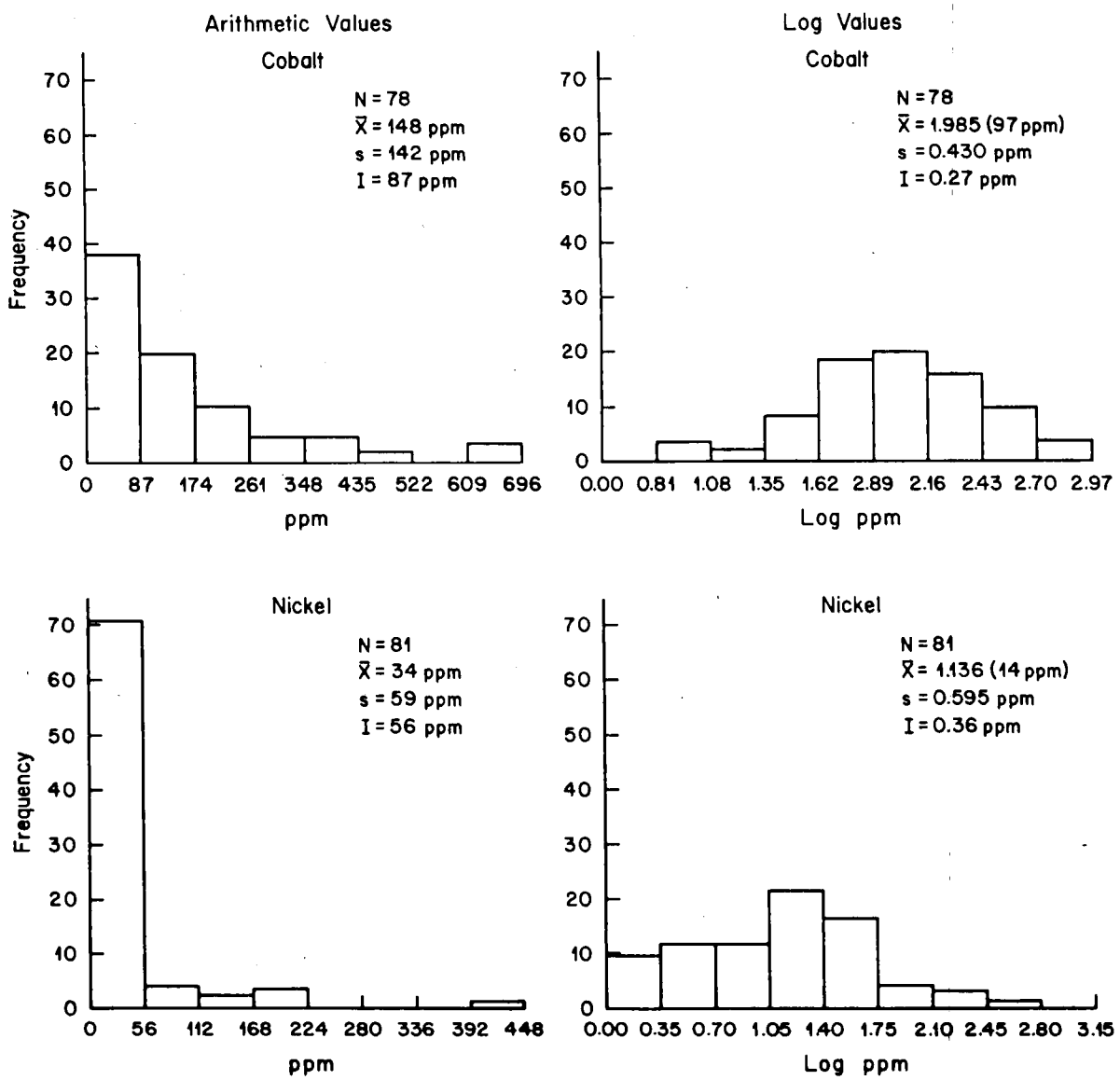


Figure 12. Frequency histograms of Co and Ni in pyrite from the Calloway orebody. Arithmetic and logarithmic data indicate that the data are log-normally distributed. The class interval was calculated using the formula I = R/1 + (3.222 x Log N); where I = Class Interval; R = Range of Observations; and N = Number of Observations.

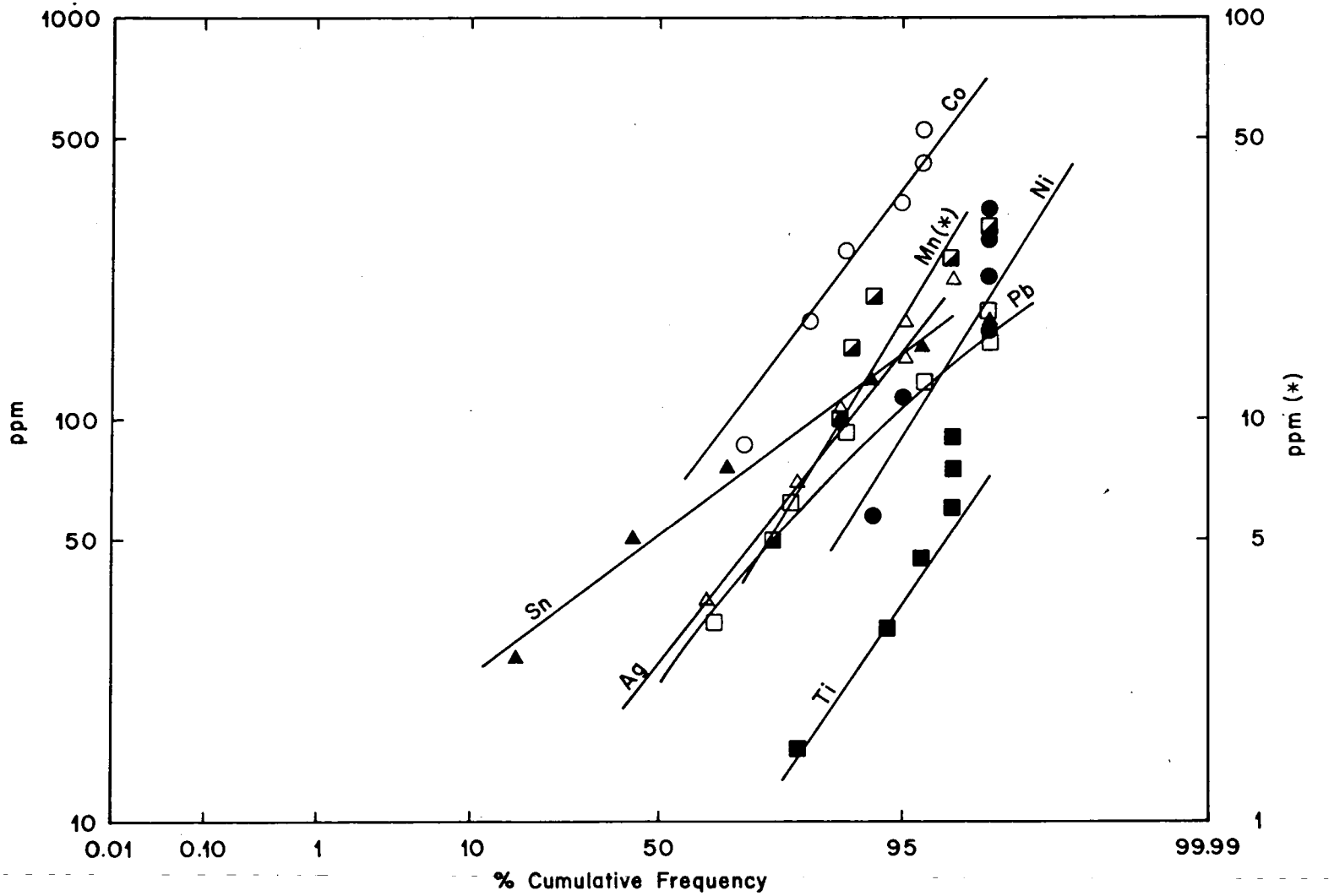


Figure 13. Log probability plots for nine trace elements in pyrite from the Calloway orebody. Most of the trace elements are log-normally distributed.

and orebodies and the geometric means were plotted on a logarithmic scale (Figures 14 and 15). The geometric mean data are summarized in Tables 2 and 3 and the raw analytical data are listed in Appendix G (Tables G-1 to G-6).

Pyrite. Pyrite was not analyzed from garnet grade due to its sparse occurrence and fine grain size. Pyrite in the garnet and higher grade zones is believed to be of metamorphic origin (G. Runyon, pers. comm., 1983). The following observations were made:

1. Co and Co:Ni ratio increase from the Ocoee Gorge to the orebodies (with increasing grade of metamorphism).

2. Ti, Mn, Sn, Pb, Ag, and Ni decrease from the Ocoee Gorge to the orebodies (with increasing grade of metamorphism).

Pyrrhotite. The following observations were made:

1. As in pyrite, the Co:Ni ratio increases from the Ocoee Gorge to the orebodies.

2. Co, Ni, Pb, Sn, Ag, Mn, and Ti decrease from the Ocoee Gorge to the orebodies.

Variations of Trace Element Contents of Pyrite and Pyrrhotite between the Calloway and Cherokee Orebodies

Figures 14 and 15 also show the trace element variation between the two orebodies studied; the geometric mean data are summarized in Tables 2 and 3 and the raw analytical data are listed in Appendix G (Tables G-1 to G-6).

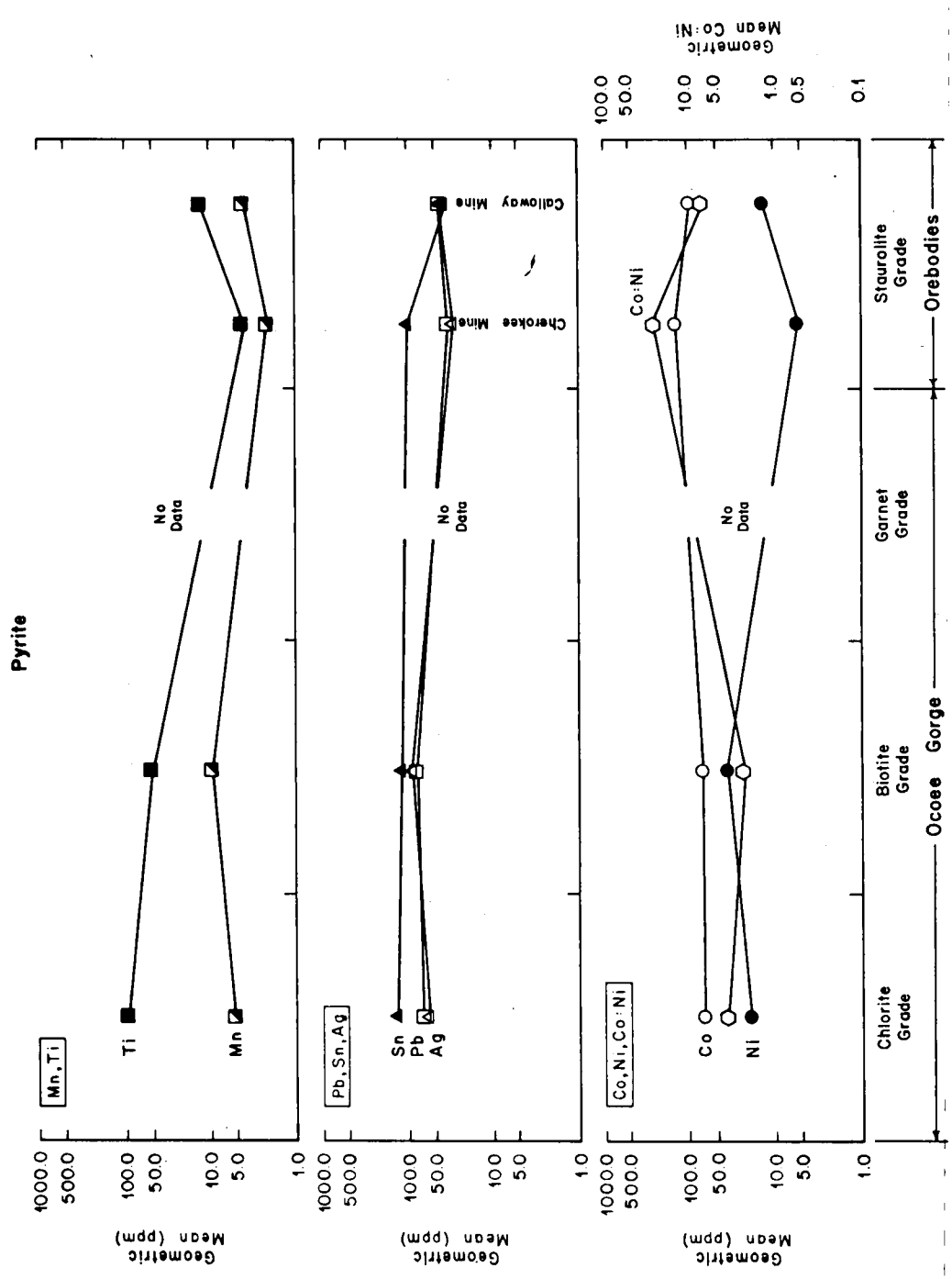


Figure 14. Variation of trace elements in pyrite from the metasedimentary rocks and orebodies of the Ducktown area as a function of increasing grade of metamorphism. See Appendix G for detailed analytical data.

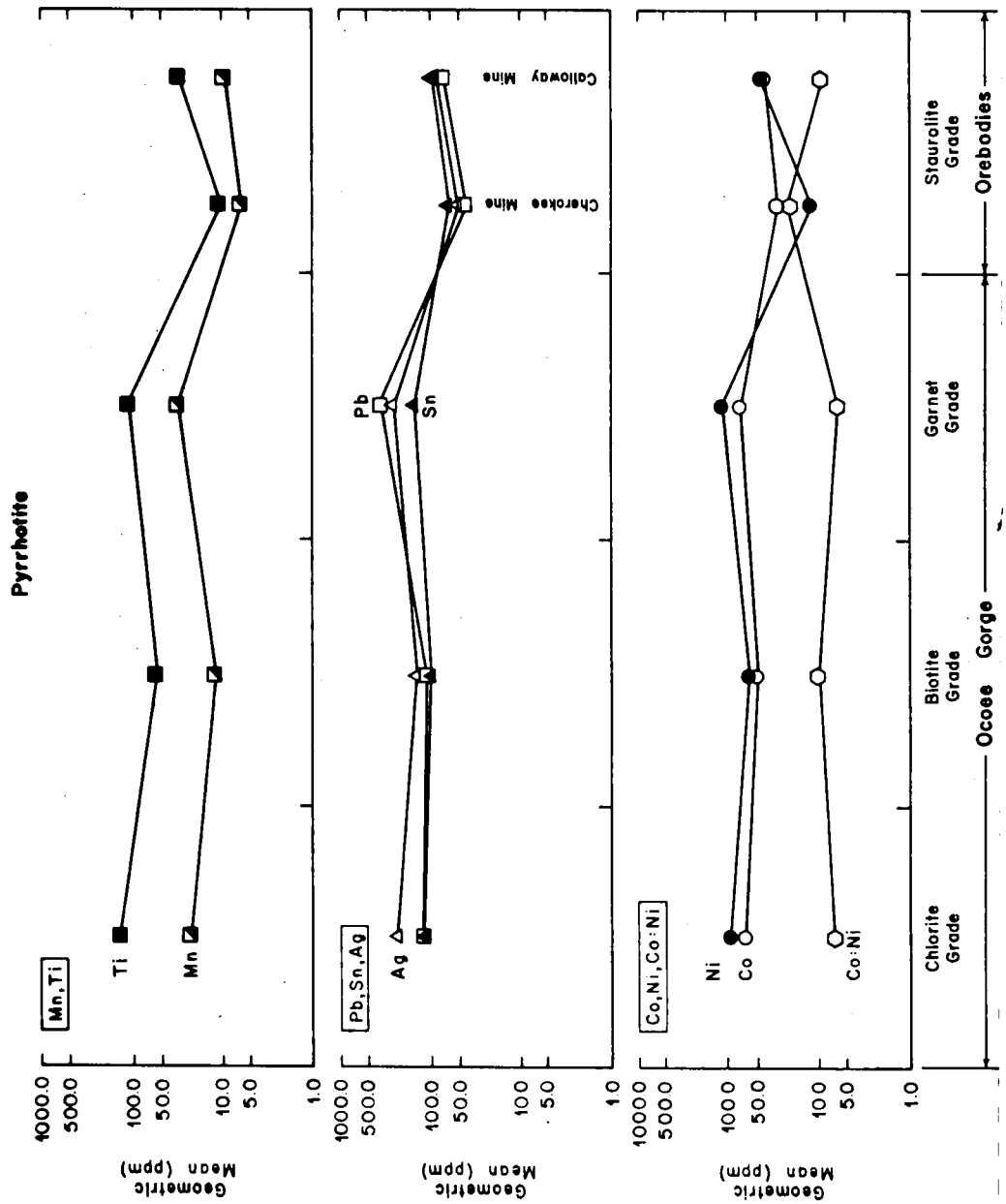


Figure 15. Variation of trace elements in pyrrhotite from the metasedimentary rocks and orebodies of the Ducktown area as a function of increasing grade of metamorphism. See Appendix G for detailed analytical data.

Table 2. Summary of Geometric Mean Data for Pyrite from the Ocoee Gorge Metasediments, and the Calloway and Cherokee Orebodies.

	Co	Ni	Mn	Pb	Ti	Sn	Ag	Co:Ni
Chlorite Grade	71	20	5	73	88	130	58	3.55
Biotite Grade	73	38	9	78	49	113	87	2.22
Garnet Grade	No samples analyzed from the garnet grade							
Staurolite Grade								
Calloway Orebody	97	14	4	43	12	78	42	7.36
Cherokee Orebody	149	6	2	31	4	99	38	25.52

Note: For details see Appendix G, Tables G-1 to G-3.

Table 3. Summary of Geometric Mean Data for Pyrrhotite from the Ocoee Gorge Metasediments, and the Calloway and Cherokee Orebodies.

	Co	Ni	Mn	Pb	Ti	Sn	Ag	Co:Ni
Chlorite Grade	64	93	19	116	125	108	200	0.67
Biotite Grade	49	59	11	102	51	106	136	0.98
Garnet Grade	74	112	28	313	98	146	252	0.62
Staurolite Grade								
Calloway Orebody	39	43	9	72	28	95	85	0.92
Cherokee Orebody	28	12	6	40	10	65	51	2.20

Note: For details see Appendix G, Tables G-4 to G-6.

Pyrite. The following observations were made:

1. Ni, Pb, Ag, Mn, and Ti show a marked increase from the Cherokee to the Calloway orebody.

2. Co, Sn, and the Co:Ni ratio show a decrease from the Cherokee to the Calloway orebody.

Pyrrhotite. The following observations were made:

1. Co, Ni, Mn, Pb, Ti, Sn, and Ag increase from the Cherokee to the Calloway orebody.

2. Co:Ni ratio show an overall decrease from the Cherokee to the Calloway orebody.

The data from pyrite and pyrrhotite analyses along the traverse from the Ocoee Gorge to the orebodies were also checked statistically using the Student t-test (Appendix J, Table J-1). It was determined that nearly all mean values were statistically different at the 95 percent significance level when comparing the Ocoee Gorge sulfides to the orebodies and comparing the Cherokee orebody to the Calloway orebody.

The analytical data have also been examined for correlations among elements. Correlation coefficients (r) calculated for each pair are shown in Appendix J (Tables J-2 and J-3). Pertinent observations may be summarized as follows: in pyrite, (1) from the Ocoee Gorge only Co-Ni, Ag-Ni, Ag-Pb, and Ag-Sn show significant correlations; (2) there are many elemental pairs that show statistically significant correlations in the Calloway orebody, the pairs that show the highest degree of correlation are Ti-Mn, Sn-Mn, and Sn-Ti; and (3) the only elemental pairs

that show any significant correlation in the Cherokee orebody are Ti-Mn, Sn-Mn, and Sn-Ti. These are the same elemental pairs that show the highest degree of correlation in the Calloway orebody. In pyrrhotite, (1) from the Ocoee Gorge, as in the orebodies, there are many elemental pairs that show statistically significant correlations; and (2) the elemental pairs that show the highest degree of correlation are in the Cherokee orebody, these include Pb-Ni, Ag-Ni, and Ag-Pb.

Variations in the Trace Element Contents of Pyrite and Pyrrhotite from the Hanging Wall to the Footwall of the Calloway Orebody

Over 40 samples of pyrite and pyrrhotite were systematically collected and analyzed from 4 sets of cores (628/629, 300/301, 469/470, and 965/966) through the Calloway orebody (Plate 1).

The arithmetic mean data are summarized in Tables 4 and 5 and the raw analytical data are listed in Appendix H (Tables H-1 to H-4 and H-6 to H-9). All of the data has been plotted on a logarithmetic scale separately for pyrite and pyrrhotite (Figures 16 to 23). Due to the small number of analyses for each individual sample, the arithmetic mean is used. The trends in the trace element data observed were visually estimated and then tested by regression analysis. The sulfide sample collected furthest toward the hanging wall of the orebody was fixed as origin of the plot and subsequent samples were measured from that point. Examples of the type of regression plots used are illustrated in Figure 24. The statistical data are listed in Appendix I (Tables I-1 and I-2). Trace element variations in pyrite and pyrrhotite from the

Table 4. Summary of Arithmetic Mean Data for Pyrite from the Calloway and Cherokee Orebodies.

Core	Sample*	Co	Ni	Mn	Pb	Ti	Sn	Ag	Co:Ni
CA-628	165-170	236	51	5	170	24	135	116	9.93
	100-105	812	27	8	147	25	94	107	45.89
CA-629	145-150	557	13	8	58	15	94	52	84.10
	270-275	710	7	14	22	14	76	45	237.96
CA-300	150-160	81	854	4	108	17	97	63	0.84
	30-40	115	27	3	63	9	92	39	3.88
	10-20	47	292	8	238	26	90	372	0.81
CA-301	0-10	49	78	6	44	14	83	36	7.94
	80-90	31	22	1	18	2	68	61	1.33
CA-469	20-25	64	89	9	83	10	84	74	1.14
	50-55	57	3	1	36	3	85	38	19.69
	85-90	74	20	8	55	27	83	93	9.86
CA-965	80-85	157	11	10	71	14	96	73	15.56
	70-75	116	63	16	64	71	189	163	6.95
	65-70	56	55	13	232	60	79	73	2.69
	35-40	311	18	5	35	16	104	7	57.92
	15-20	70	34	5	116	91	222	80	2.18
CA-966	10-15	103	6	14	22	21	62	84	74.88
	45-50	36	5	7	13	21	54	22	7.26
	70-75	49	8	4	17	12	60	36	9.49
	95-100	112	14	6	59	15	69	139	68.0
CH-857	40-45	578	117	2	27	9	130	96	127.36
CH-858	20-25	77	6	6	34	24	195	32	17.06
	25-30	160	9	2	40	3	85	38	40.39
	30-35	174	6	4	41	14	99	50	41.33

*All data are listed from the hanging wall to the footwall of the orebody for each core.

Note: For details see Appendix H, Tables H-1 to H-5.

Table 5. Summary of Arithmetic Mean Data for Pyrrhotite from the Calloway and Cherokee Orebodies.

Core	Sample*	Co	Ni	Mn	Pb	Ti	Sn	Ag	Co:Ni
CA-628	210-215	59	84	39	254	118	144	164	1.68
	130-135	49	64	79	136	40	134	83	0.92
	110-105	34	28	30	68	53	98	74	2.12
	15-20	109	30	2	79	16	123	38	3.26
CA-629	75-80	52	22	10	215	56	189	143	2.08
	140-145	66	109	6	135	50	112	210	0.72
	210-215	45	30	7	85	43	107	65	1.71
	270-275	67	22	3	37	26	101	61	5.95
	330-335	42	16	12	86	36	93	54	2.29
	370-375	78	40	68	59	35	130	105	1.93
CA-300	150-160	49	426	5	100	16	82	67	0.52
	80-90	59	439	17	135	116	142	200	0.32
CA-301	80-90	69	164	11	29	22	147	79	0.72
	100-110	67	243	55	61	57	161	80	0.39
	130-140	35	130	12	180	61	116	161	0.61
CA-470	135-140	59	262	48	247	99	84	284	0.24
	55-60	23	55	8	138	32	93	75	0.43
CA-469	20-25	24	41	33	57	10	87	78	0.77
	50-55	20	65	2	75	6	69	49	1.05
	85-90	49	27	5	46	7	105	68	2.37
	110-115	24	1043	12	64	26	105	211	0.05
CA-965	45-50	23	27	147	88	26	73	62	1.23
	15-20	57	58	10	234	73	180	100	1.21
CA-966	10-15	40	19	36	46	38	74	105	6.80
	45-50	64	56	11	24	19	72	165	1.44
	95-100	41	11	5	42	34	98	103	8.14
	130-135	51	26	17	60	70	85	63	1.75
	140-145	121	36	17	77	71	76	97	3.48
	180-185	44	41	11	53	61	101	89	1.52
CH-857	40-45	17	12	99	38	18	63	55	2.41
	5-10	44	22	44	17	12	499	42	4.64
CH-858	0-5	46	15	3	21	8	83	35	9.12
	10-15	48	22	7	48	31	67	74	6.95
	25-30	217	7	2	59	4	88	38	45.24
	30-35	12	8	5	30	16	47	36	2.05
	40-45	16	13	16	41	11	68	74	1.00
	70-75	35	178	6	85	30	50	120	0.41

*All data are listed from the hanging wall to the footwall of the orebody for each core.

Note: For details see Appendix H, Tables H-6 to H-10.

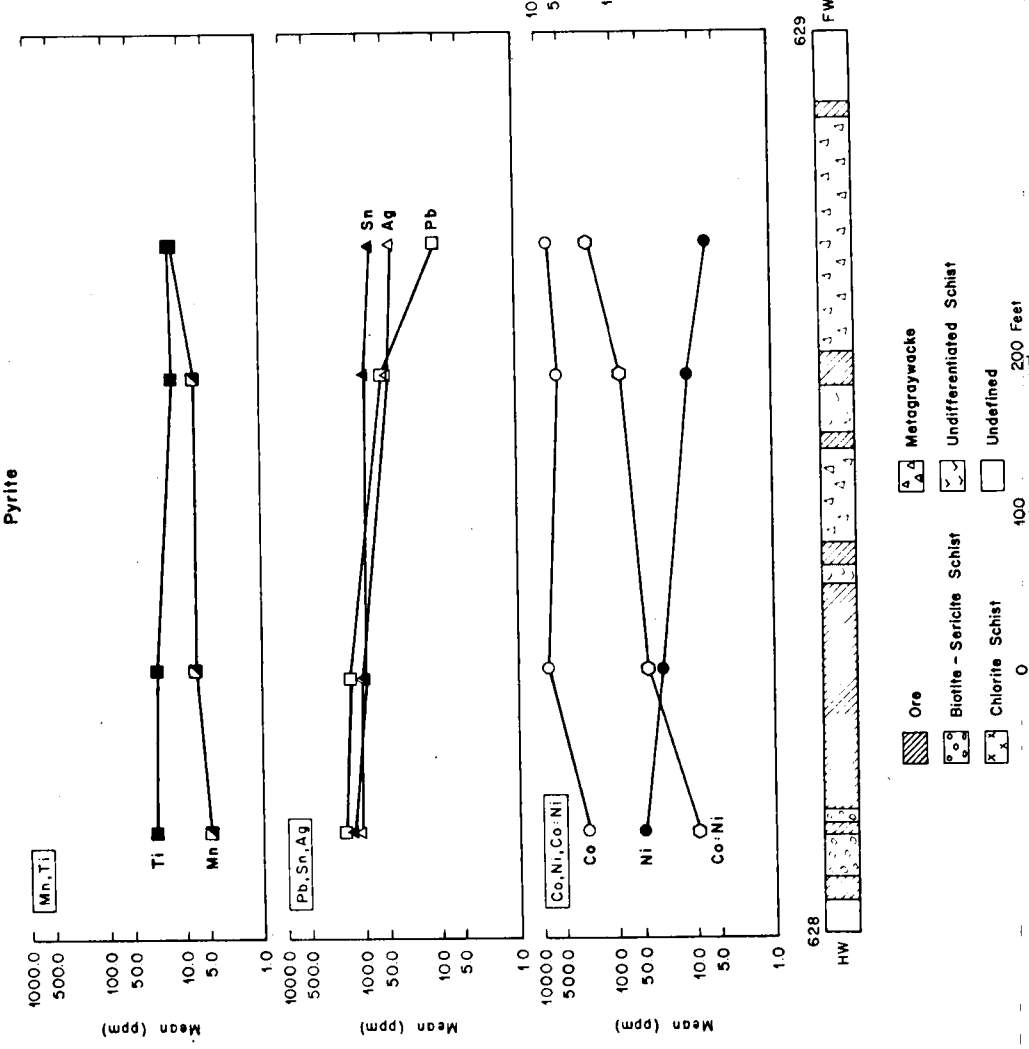


Figure 16. Variation of trace elements in pyrite from the hanging wall to the footwall in core 628/629 from the Calloway orebody. See Appendix H for detailed analytical data.

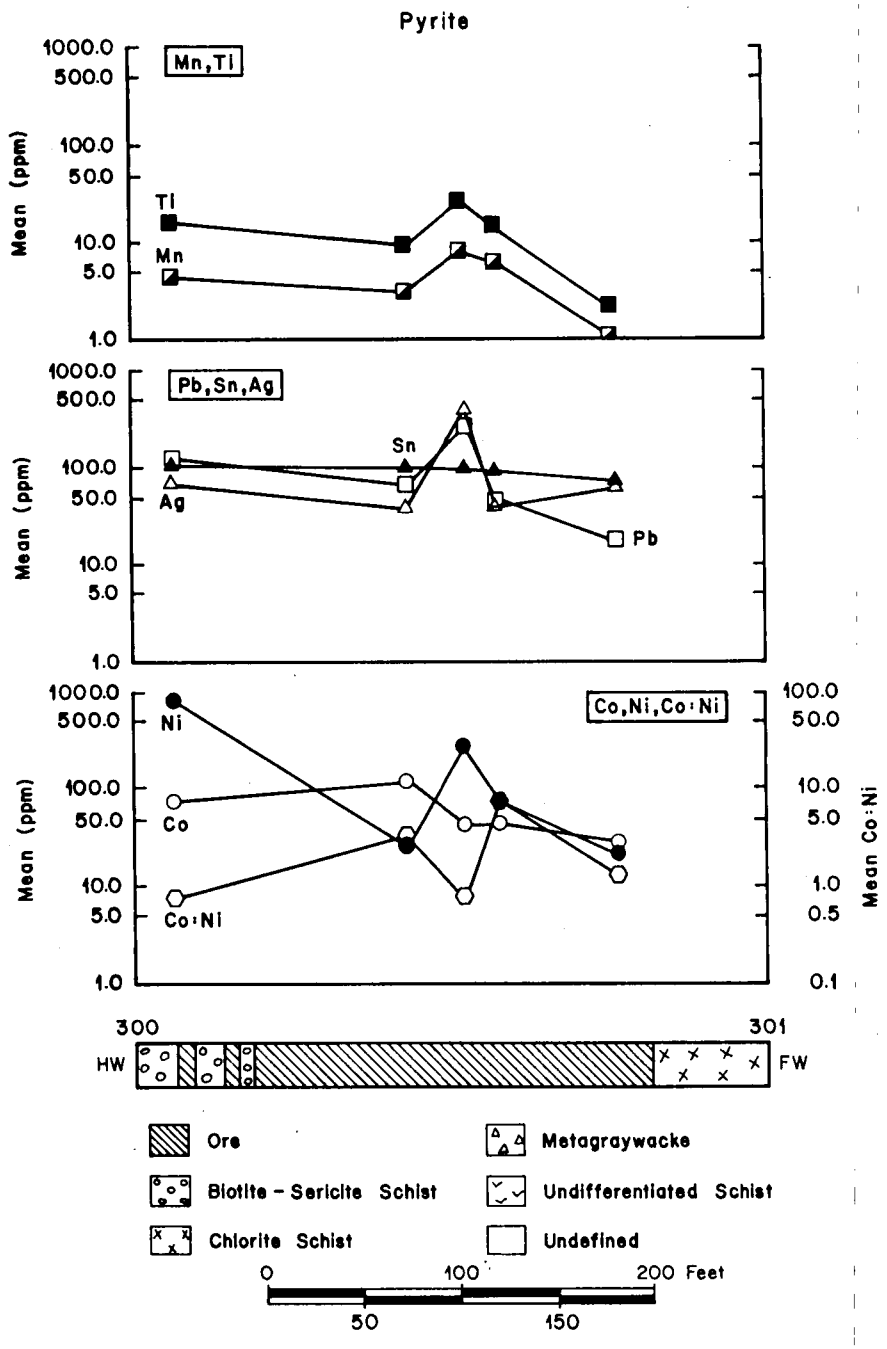


Figure 17. Variation of trace elements in pyrite from the hanging wall to the footwall in core 300/301 from the Calloway orebody. See Appendix H for detailed analytical data.

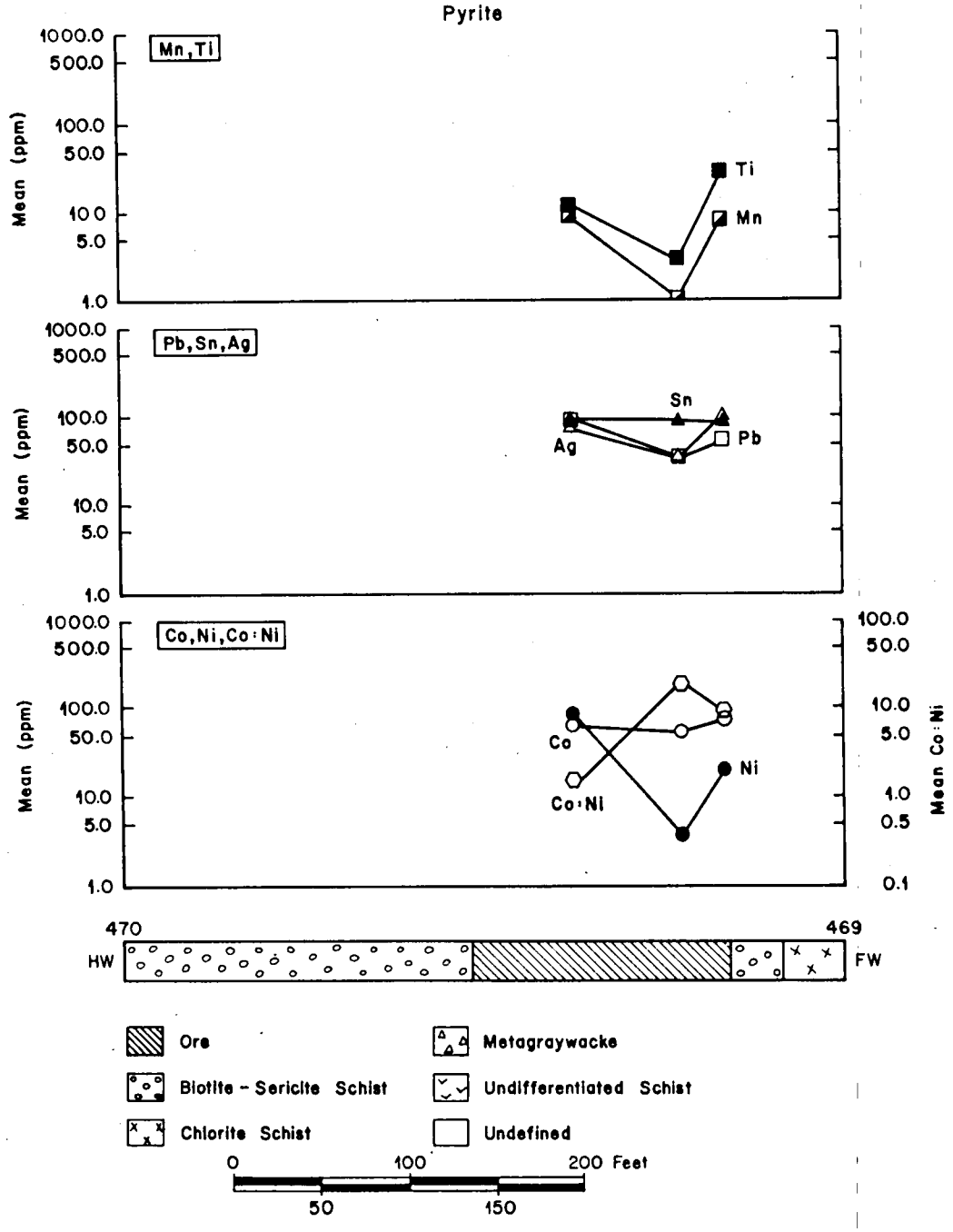


Figure 18. Variation of trace elements in pyrite from the hanging wall to the footwall in core 469/470 from the Calloway orebody. See Appendix H for detailed analytical data.

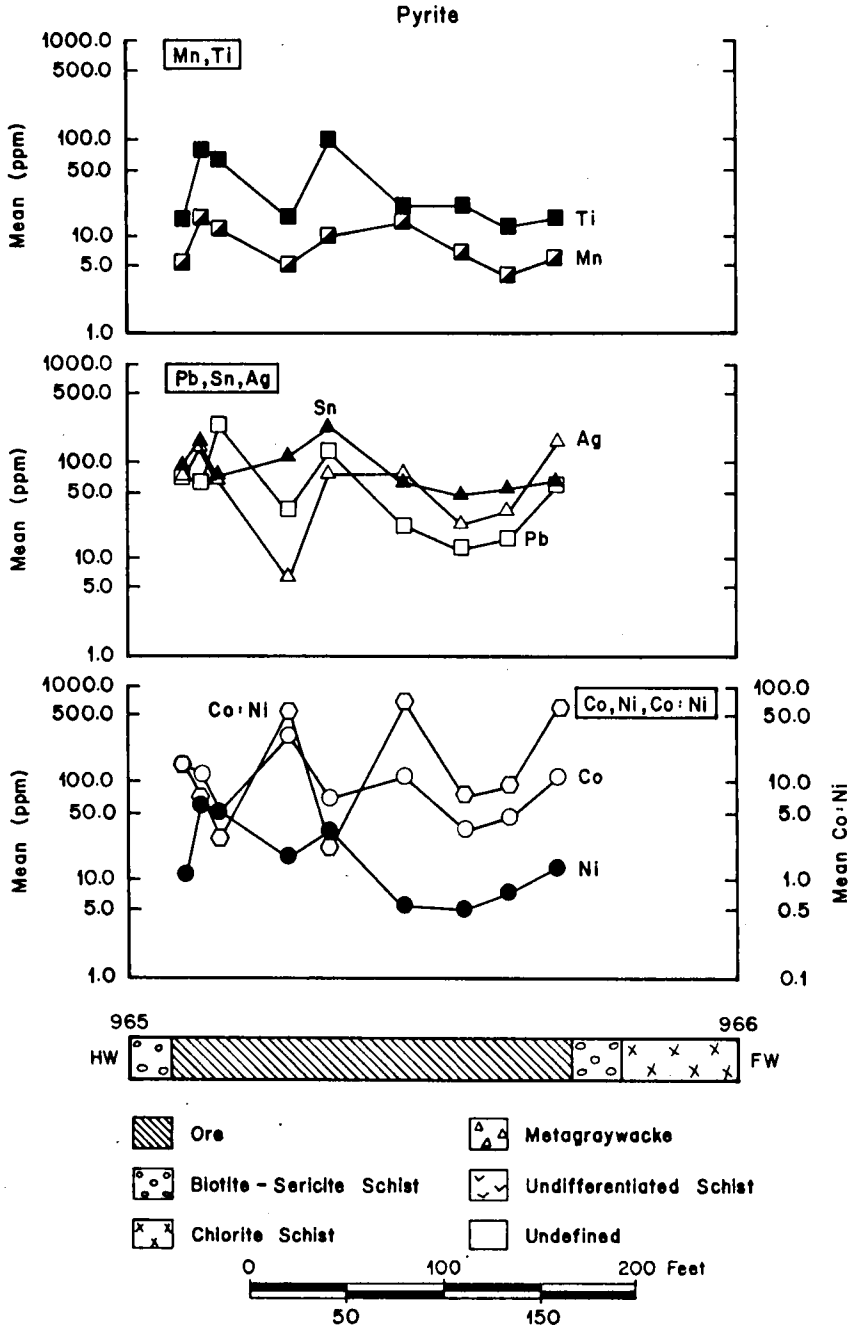


Figure 19. Variation of trace elements in pyrite from the hanging wall to the footwall in core 965/966 from the Calloway orebody. See Appendix H for detailed analytical data.

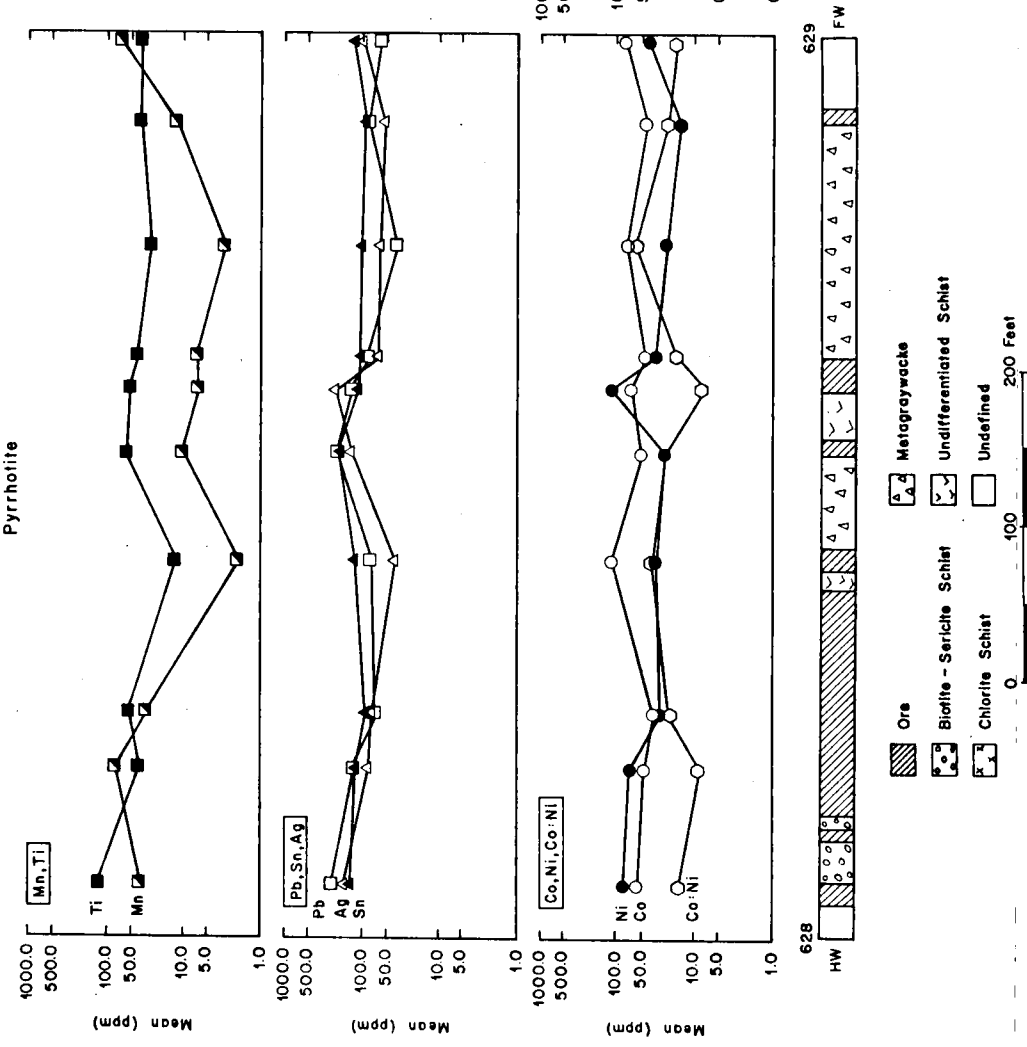


Figure 20. Variation of trace elements in pyrrhotite from the hanging wall to the footwall in core 628/629 from the Calloway orebody. See Appendix H for detailed analytical data.

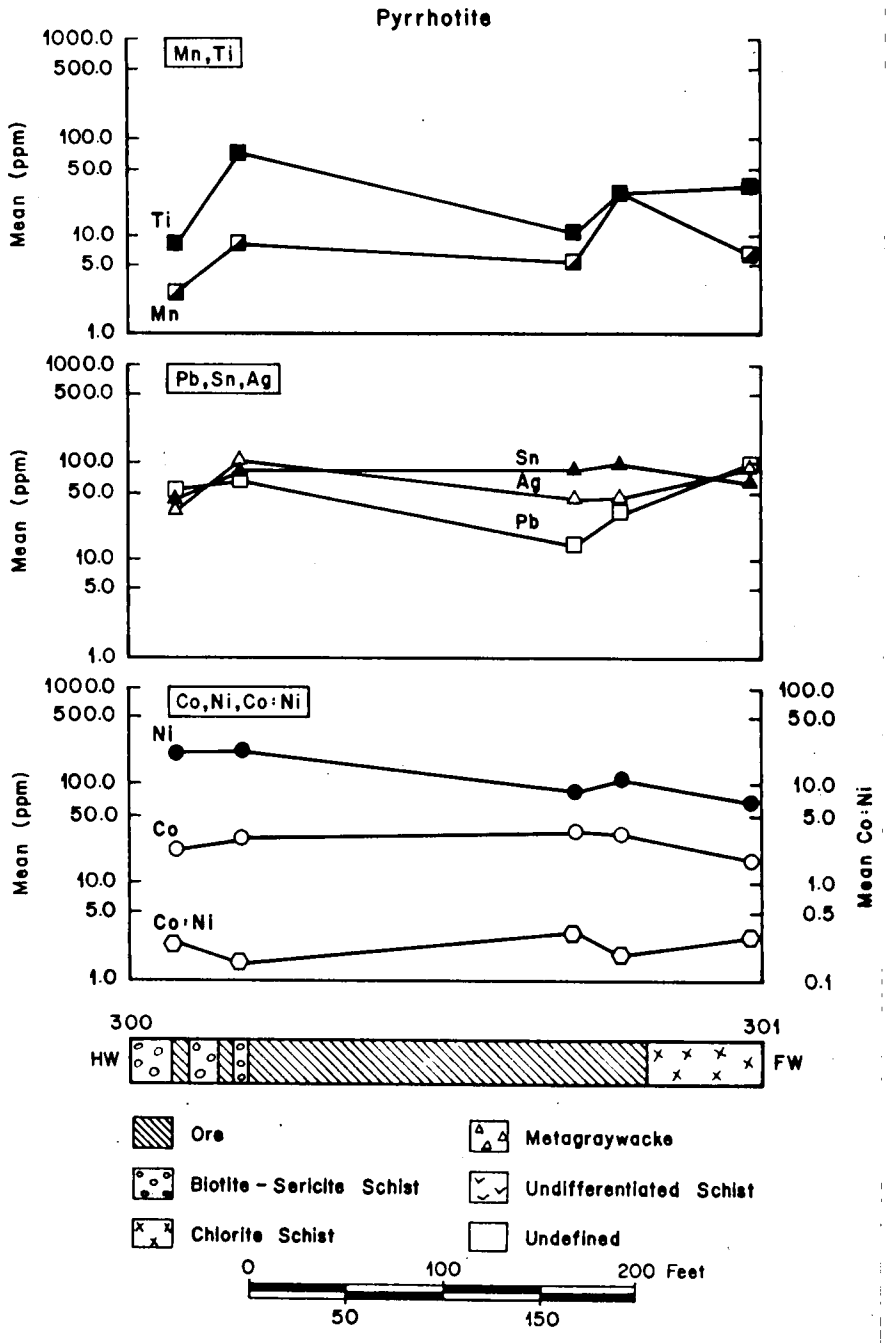


Figure 21. Variation of trace elements in pyrrhotite from the hanging wall to the footwall in core 300/301 from the Calloway orebody. See Appendix H for detailed analytical data.

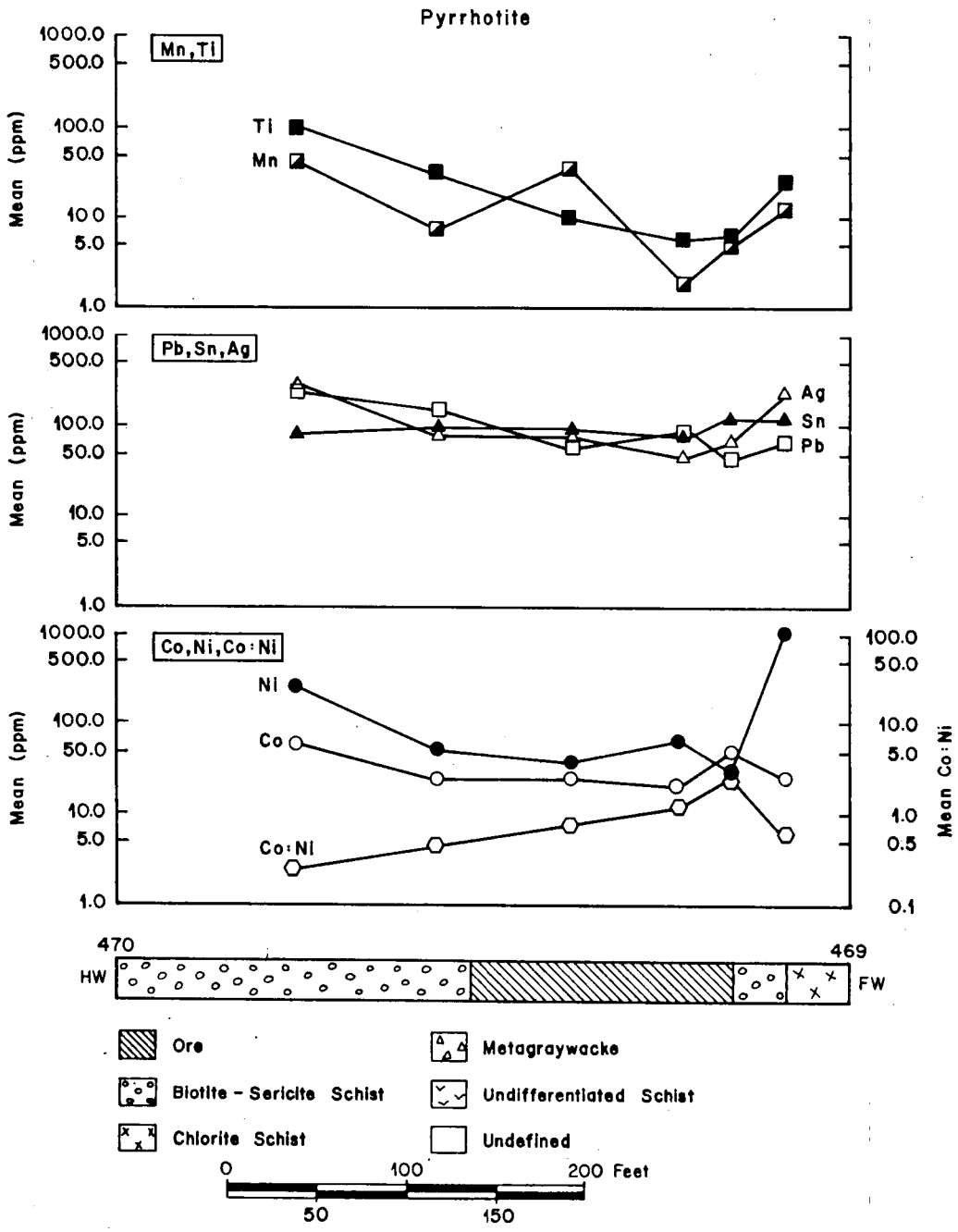


Figure 22. Variations of trace elements in pyrrhotite from the hanging wall to the footwall in core 469/470 from the Calloway orebody. See Appendix H for detailed analytical data.

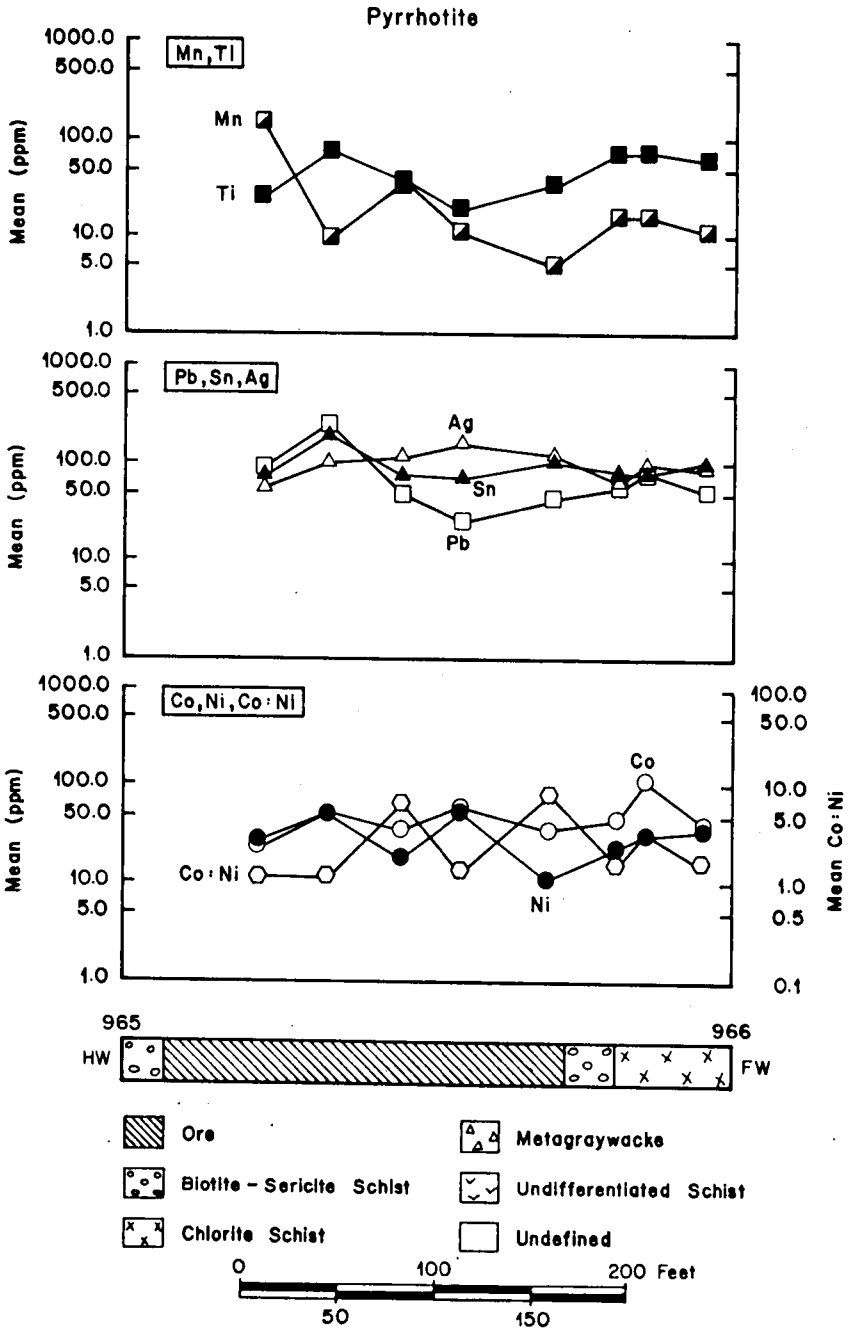


Figure 23. Variations of trace elements in pyrrhotite from the hanging wall to the footwall in core 965/966 from the Calloway orebody. See Appendix H for detailed analytical data.

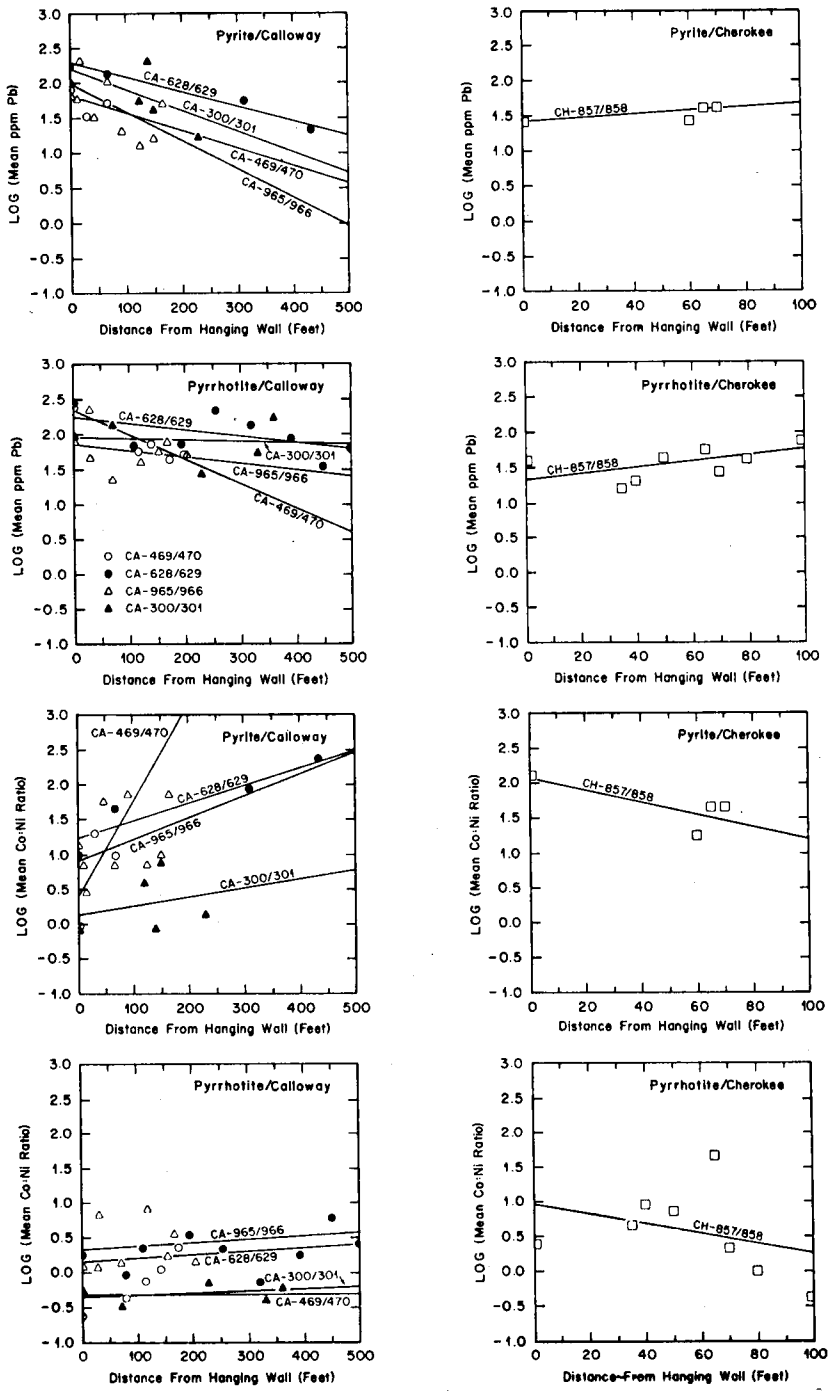


Figure 24. Examples of least squares regression plots used to statistically study the trends observed in Figures 17 to 25. See Appendix I for detailed statistical data.

hanging wall to the footwall in the Calloway orebody may be summarized as follows:

Pyrite. The data for pyrite appears to be somewhat scattered but show some trends from the hanging wall to the footwall of the orebody. The observations may be summarized as follows:

1. the Co:Ni ratio shows an overall increase;
2. Ni, Mn, Pb, Ti, and Sn show an overall decrease; and
3. Co and Ag show no apparent trend.

Pyrrhotite. Pyrrhotite being the dominant phase in these orebodies, there is much more data for pyrrhotite than for pyrite. As for pyrite, the pyrrhotite data appear to be quite variable but show similar trends observed in pyrite. The observations may be summarized as follows:

1. the Co:Ni ratio shows an overall increase;
2. Ni, Pb, Ag, and Mn show an overall decrease; and
3. Co, Ti, and Sn show no apparent trend.

Variations in Trace Element Contents of Pyrite and Pyrrhotite from the Hanging Wall to the Footwall of the Cherokee Orebody

Only eight samples of pyrite and pyrrhotite from a single set of cores (857/858) through the Cherokee orebody were analyzed (Plate 2). The arithmetic mean data are summarized in Tables 4 and 5, pp. 46 and 47, and the raw analytical data are listed in Appendix H (Tables H-5 and H-10). All of the data have been plotted on a logarithmic scale

separately for pyrite and pyrrhotite (Figures 25 and 26). The trends in the trace element data observed were visually estimated and then tested by regression analysis. The sulfide sample collected furthest toward the hanging wall of the orebody was fixed as origin of the plot and subsequent samples were measured from that point. Examples of the type of regression plots used are illustrated in Figure 24. The statistical data are listed in Appendix I (Tables I-1 and I-2). Trace element variations from the hanging wall to the footwall in the Cherokee orebody may be summarized as follows:

Pyrite. Due to the few samples of pyrite analyzed from this orebody it is difficult to make any generalizations as to possible trends, therefore none are made (Figure 25).

Pyrrhotite. The following observations were made:

1. Pb, Ag, and Ni show an overall increase;
2. Mn, Sn, and the Co:Ni ratio show an overall decrease; and
3. Co and Ti show no apparent trend.

Variations in the Trace Element Contents of Pyrite and Pyrrhotite from the Upper to the Lower Levels of the Calloway Orebody

The data for Calloway cores were used to check if there was any change in the trace element contents of the sulfide phases with depth. The geometric mean data are summarized in Tables 6 and 7, and the raw analytical data are listed in Appendix G (Tables G-2 and G-5). The data for each set of cores were grouped together for pyrite and pyrrhotite, respectively, and plotted as a function of depth (Figures 27 and 28).

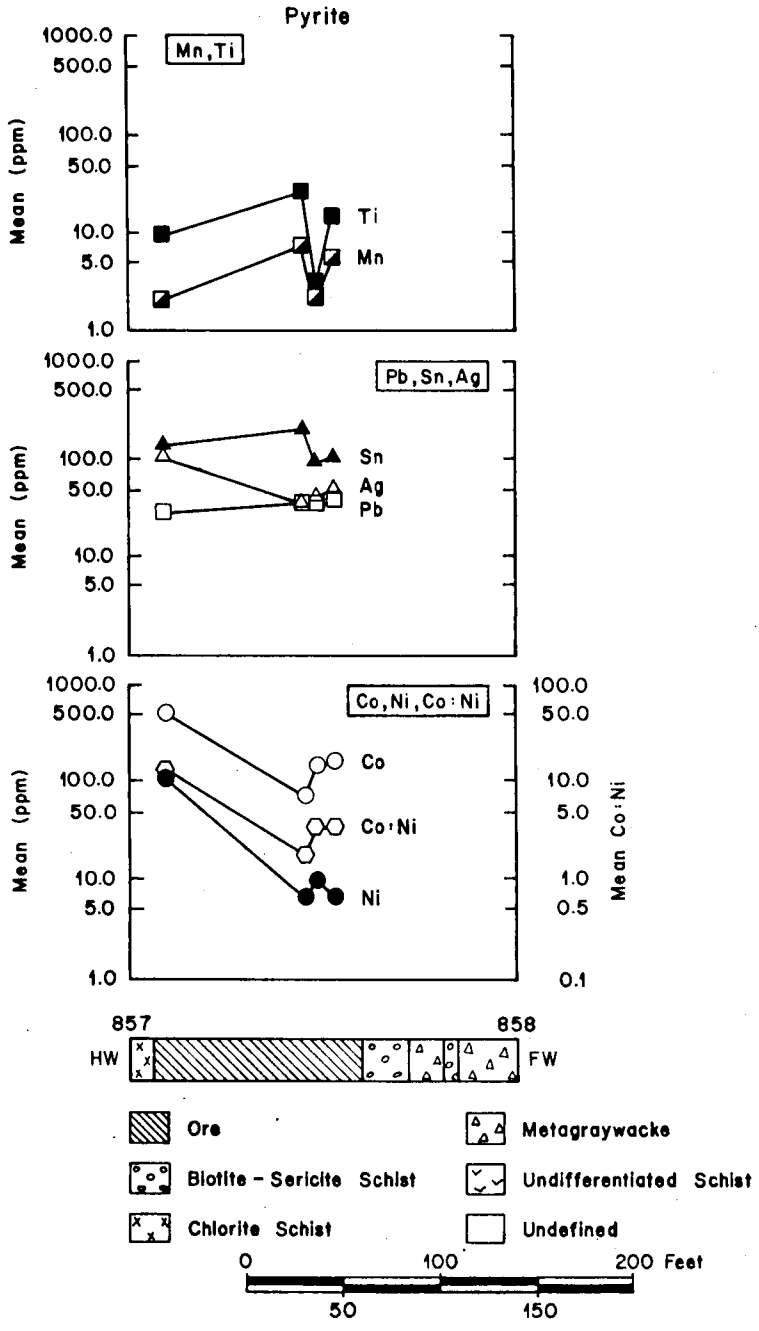


Figure 25. Variation of trace elements in pyrite from the hanging wall to the footwall in core 857/858 from the Cherokee orebody. See Appendix H for detailed analytical data.

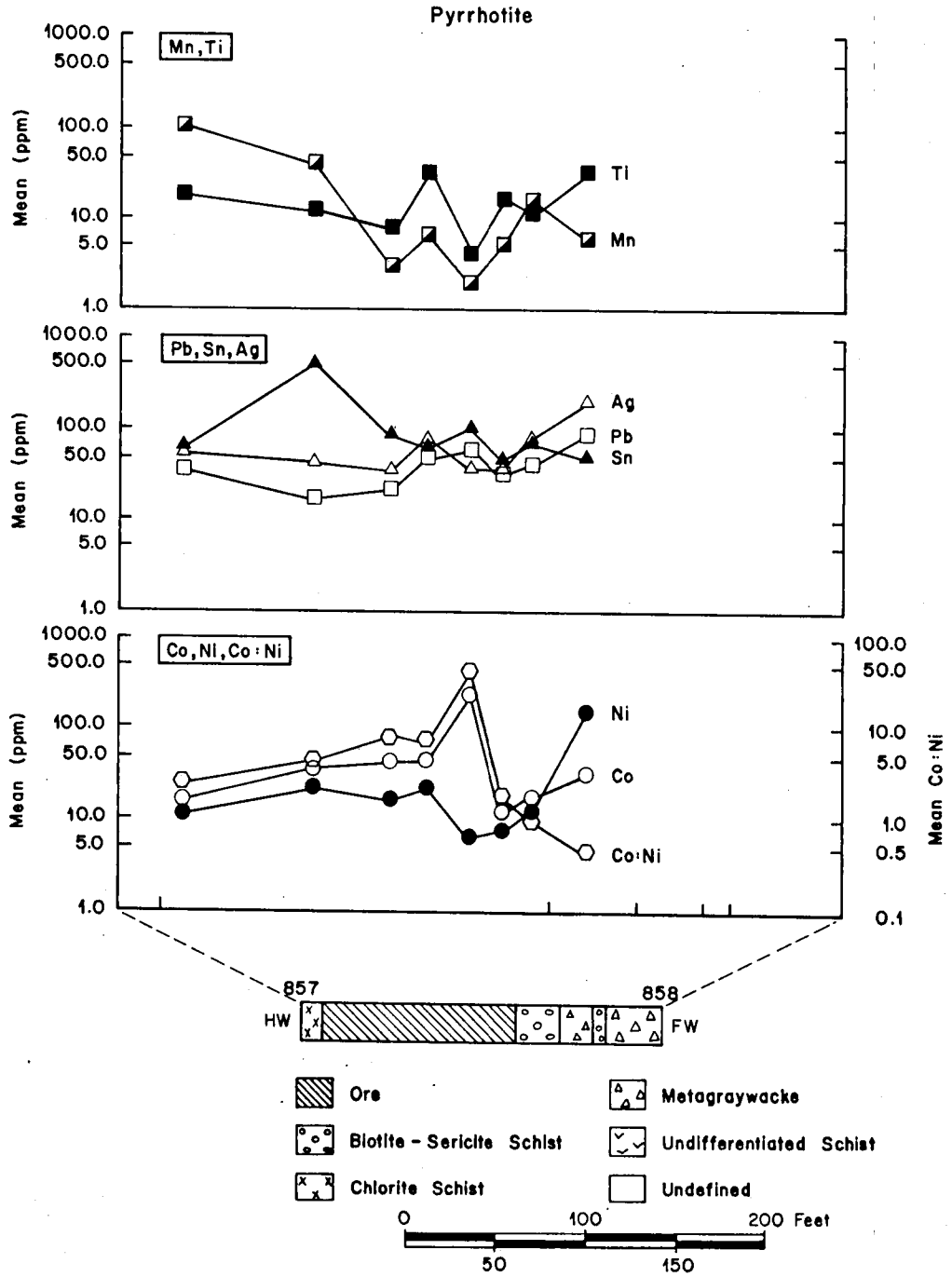


Figure 26. Variations of trace elements in pyrrhotite from the hanging wall to the footwall in core 857/858 from the Cherokee orebody. See Appendix H for detailed analytical data.

Table 6. Summary of the Geometric Mean Data for Pyrite from the Four Sets of Cores Sampled from the Calloway Orebody.

Core	Co	Ni	Mn	Pb	Ti	Sn	Ag	Co:Ni
CA-628/629	431	18	5	61	17	88	62	27.29
CA-300/301	45	40	3	53	8	82	45	0.91
CA-469/470	61	11	5	47	8	84	54	7.60
CA-965/966	106	10	5	34	15	75	34	10.96

Note: For details see Appendix G, Table G-2.

Table 7. Summary of the Geometric Mean Data for Pyrrhotite from the Four Sets of Cores Sampled from the Calloway Orebody.

Core	Co	Ni	Mn	Pb	Ti	Sn	Ag	Co:Ni
CA-628/629	50	31	9	93	34	110	82	1.33
CA-300/301	45	193	9	95	33	117	107	0.27
CA-469/470	30	61	8	83	17	90	93	0.42
CA-965/966	41	34	14	53	38	96	86	1.66

Note: For details see Appendix G, Table G-5.

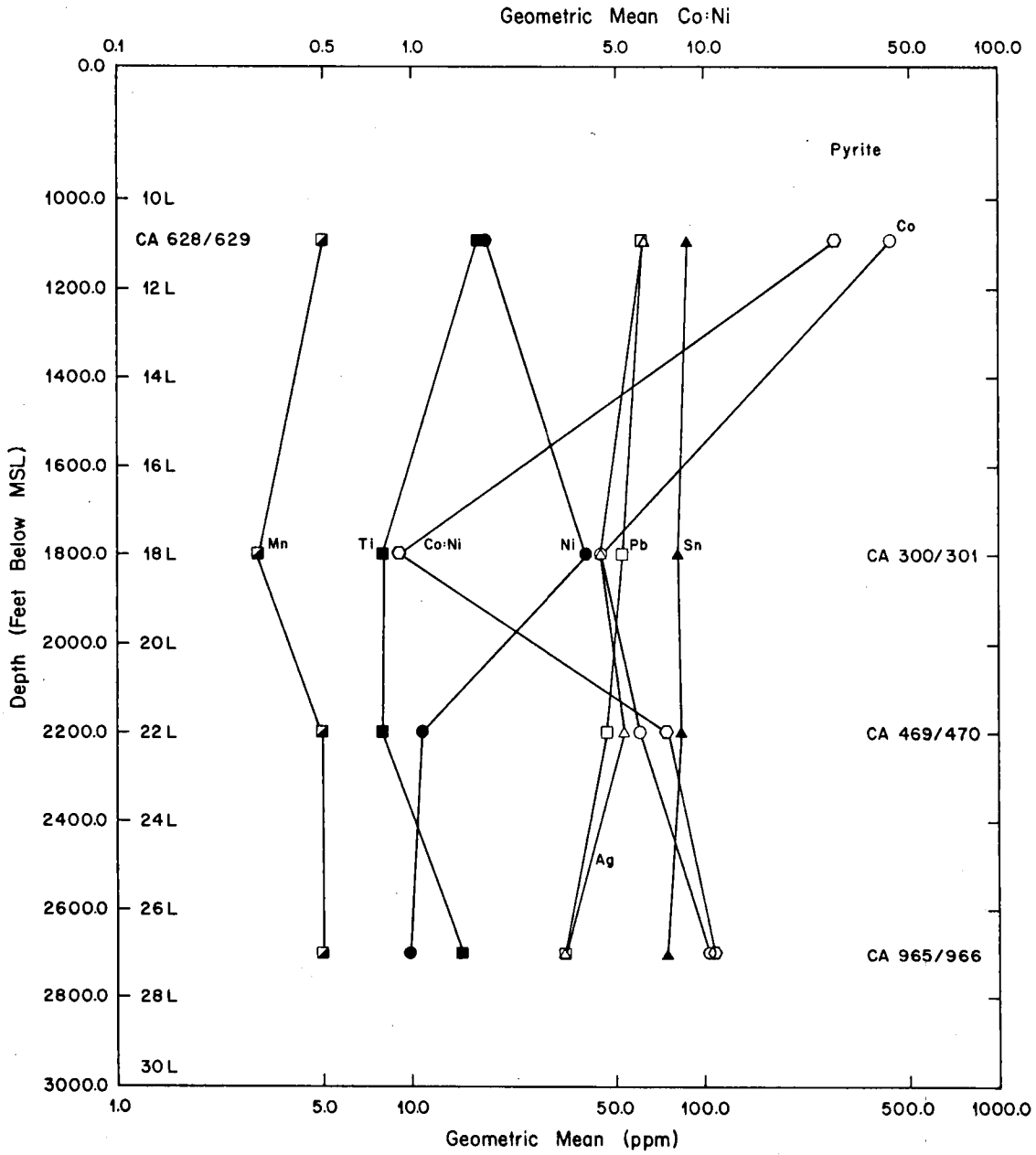


Figure 27. Variations of trace elements in pyrite from the upper levels to the lower levels in the Calloway orebody. See Appendix G for detailed analytical data.

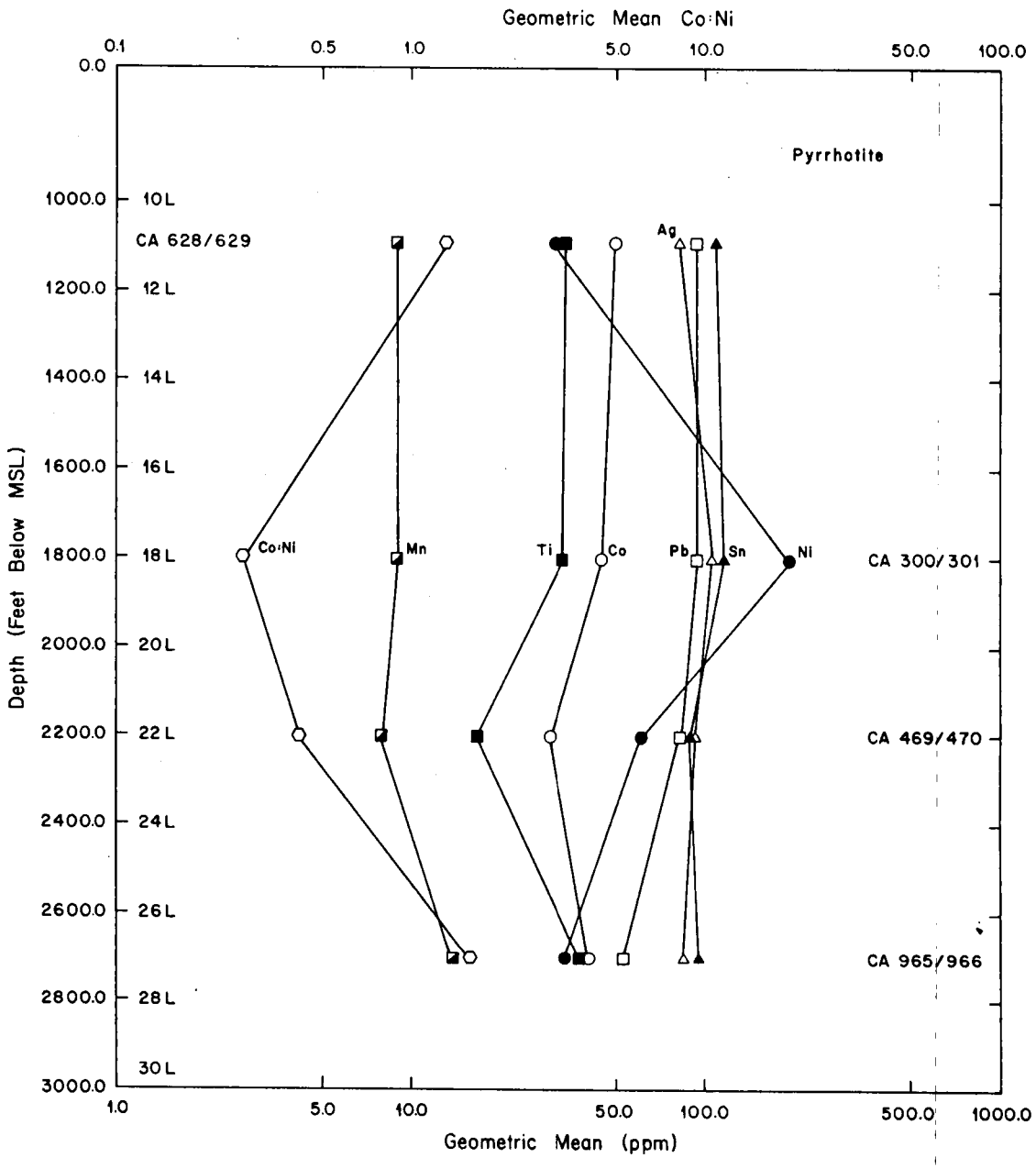


Figure 28. Variations of trace elements in pyrrhotite from the upper levels to the lower levels in the Calloway orebody. See Appendix G for detailed analytical data.

Pyrite. The trace element data for the uppermost level (core 628/629) are quite different from the lower levels. This may be due to the fact the pyrite data are not representative as very little pyrite could be found in the samples from this core; the sulfides in this core are dominantly pyrrhotite with subordinate amounts of chalcopyrite and sphalerite. In addition, this part of the orebody is structurally more complex and there is no alteration zone present (Plate 1). Thus the pyrite analyzed from this core may be of different generation compared to pyrites in the other cores. Due to these differences, the upper level is not included in the following summary. Generalized trends for the lower level cores (300/301, 469/470, and 965/966) were visually estimated and include:

1. Co, Mn, Ti, and the Co:Ni ratio show an overall increase with depth;
2. Pb, Ag, and Ni show an overall decrease with depth; and
3. Sn shows no apparent trend with depth.

Pyrrhotite. As in the case of pyrite, the trace element contents of the sulfide phases in the upper level are very different from the lower levels. This may be due to increased deformation and possible mobilization of trace elements in this part of the orebody. Therefore, the following summary is based only on the lower-level cores (300/301, 469/470, and 965/966):

1. Mn and the Co:Ni ratio show and overall increase with depth;
2. Ni and Pb show an overall decrease with depth; and
3. Co, Ti, Sn, and Ti show no apparent trend with depth.

Cobalt, Nickel, and the Co:Ni Ratio in Pyrite and Pyrrhotite

The cobalt and nickel contents and the Co:Ni ratio of both pyrite and pyrrhotite are given in Table 8. The raw analytical data are listed in Appendix G (Tables G-1 to G-6).

Table 8. Comparison of Cobalt and Nickel Contents and the Co:Ni Ratios of Pyrite and Pyrrhotite from the Ocoee Gorge Metasediments, and the Calloway and Cherokee Orebodies.

	Ocoee Gorge	Calloway Orebody	Cherokee Orebody
Pyrite			
Mean Co (ppm)	64	97	149
Mean Ni (ppm)	21	14	6
Mean Co:Ni Ratio	2.67	7.36	25.52
Pyrrhotite			
Mean Co (ppm)	53	39	28
Mean Ni (ppm)	70	43	12
Mean Co:Ni Ratio	0.73	2.20	0.92

Note: All values listed are geometric means.

CHAPTER V

INTERPRETATION AND DISCUSSION

Interpretation of the data obtained in this study must account for the following observations: (1) differences in the trace element contents of pyrite and pyrrhotite between the country rocks and the orebodies; (2) differences between the Calloway and Cherokee orebodies; and (3) trends observed within the Calloway orebody. The above must also be evaluated with regard to the various hypotheses that have been proposed for the genesis of the Ducktown massive sulfide deposits.

Comparison of the Country Rocks and the Orebodies

Much, if not all, of the pyrrhotite in the country rocks appears to have formed from pyrite during regional metamorphism (Runyon, 1983). Textural evidence does indicate such an origin for some of the pyrrhotite in the orebodies, but available data do not permit ascribing such an origin to all the pyrrhotite in the orebodies. Thus, it is difficult to evaluate the trace element contents of pyrrhotite between the country rocks and the orebodies. A comparison of the trace element contents of pyrite is more meaningful and is emphasized in the following discussion.

Data presented earlier clearly show that the trace element contents of pyrite in the country rocks is quite different from those of pyrite in the orebodies. One possible explanation is that the two pyrite populations are genetically unrelated. For example, based solely on the nickel and cobalt concentrations in pyrite, Doe (1962) concluded that

the pyrite in the orebodies at Balmat, New York, is genetically unrelated to the disseminated pyrite in the surrounding country rocks. An alternative explanation, and the one preferred for the Ducktown area, is that the trace element variations may be related to regional metamorphism. The main reason for this interpretation is that the trace element variations appear to be related to metamorphic grade.

The most important features of the trace element distribution pattern in pyrite may be summarized as follows (Figure 14, p. 41): with increasing metamorphic grade cobalt content increases whereas nickel content decreases, resulting in a marked increase in the Co:Ni ratio. This pattern is entirely consistent with what has been observed by many other workers (see Appendix F).

Comparison of the Calloway and the Cherokee Orebodies

In terms of the trace element contents of pyrite and pyrrhotite, the Calloway and Cherokee orebodies appear to be quite different when studied visually (Figures 14 and 15, pp. 41 and 42) and statistically (Table J-1, Appendix J). The Cherokee orebody contains pyrite which is higher in Co and has a much higher Co:Ni ratio, possibly indicating a higher temperature of formation (Figures 14 and 15).

The trace element distribution among orebodies in a single mining district has been studied by several authors, such as, Doe (1962), Cambel and Jarkovsky (1967, 1969), Rose (1967, 1970), Johnson (1972), Price (1972), Both (1973), Bhatia (1976, 1981), Thole (1976), Sinclair et al. (1977), and Bralia et al. (1979). To account for comparable

differences observed in the orebodies from the Broken Hill district in Australia, Both (1973) suggested a chemical differentiation among the ore lenses which were syngenetic with the enclosing sediments but represent a sequence in time. The chemical differences observed between these horizons can then be explained by variations in the relative proportions of elements being transported into the depositional environment and/or variations in the depositional environment itself.

Magee (1968) and Slater (1982) have summarized the differences between the Calloway and Cherokee orebodies. According to Magee (1968), these two orebodies may represent two distinctly different ore horizons, one of high-copper ores (Burra Burra, London, East Tennessee, Calloway and Mary-Polk) and the other of low-copper ores (Eureka, Boyd, and Cherokee). The characteristics of these different horizons include: (1) higher copper and zinc assays (av. 1.6 percent Cu and 1.2 percent Zn), less magnetite (av. 1 percent), less massive sulfides versus gangue, and less pyrite in the high-copper ores; and (2) lower copper and zinc assays (av. 0.7 percent Cu and 0.5 percent Zn), more magnetite (3 percent), more massive sulfides versus gangue, and more pyrite in the low-copper ores.

If the Burra Anticlinorium is unfolded it appears that the Cherokee orebody would be stratigraphically lower, and therefore, older than the Calloway orebody (Figure 4, p. 6). The Cherokee deposit may have been part of the earliest phase of ore formation, formed at higher temperature and possibly closer to the source of fluids than the Calloway

orebody. These processes may have been similar to those that produce the pyrite ore (ryukako) of Kuroko Deposits, described by Franklin, Lyndon and Sangster (1981), accounting for higher temperature characteristics of the low-copper ores in the Ducktown District.

Vertical Zoning from the Hanging Wall to the Footwall within the Calloway and Cherokee Orebodies

These orebodies are interpreted to have been originally deposited as horizontal layers and later folded to their present orientation. Thus, variation in the present down-dip direction of an orebody actually represents lateral variation in terms of its original deposition.

The trace elements that appear to show the most distinctive trends are Pb, Ni and the Co:Ni ratio (Figures 16 to 24, pp. 48 to 56). In general, Pb and Ni decreases, whereas the Co:Ni ratio increases from the hanging wall to the footwall in the Calloway orebody. A general zonation pattern has tentatively been recognized from the hanging wall to the footwall of several of the orebodies. The zonation pattern, based on limited data, indicates copper rich mineralization along the footwall of the orebody and zinc rich mineralization along the hanging wall of the orebody (Slater, 1982). Bulk copper and zinc assay data were obtained from the Tennessee Chemical Company for the four sets of cores analyzed from the Calloway orebody. The Zn:Cu ratios (Figure 29), although quite variable, generally indicate that the footwall is slightly enriched in copper (Zn:Cu < 1), whereas the hanging wall is slightly enriched in zinc (Zn:Cu > 1). The samples analyzed for cores CA-965/966 (Figure 29) show a distinctly reversed pattern which is not

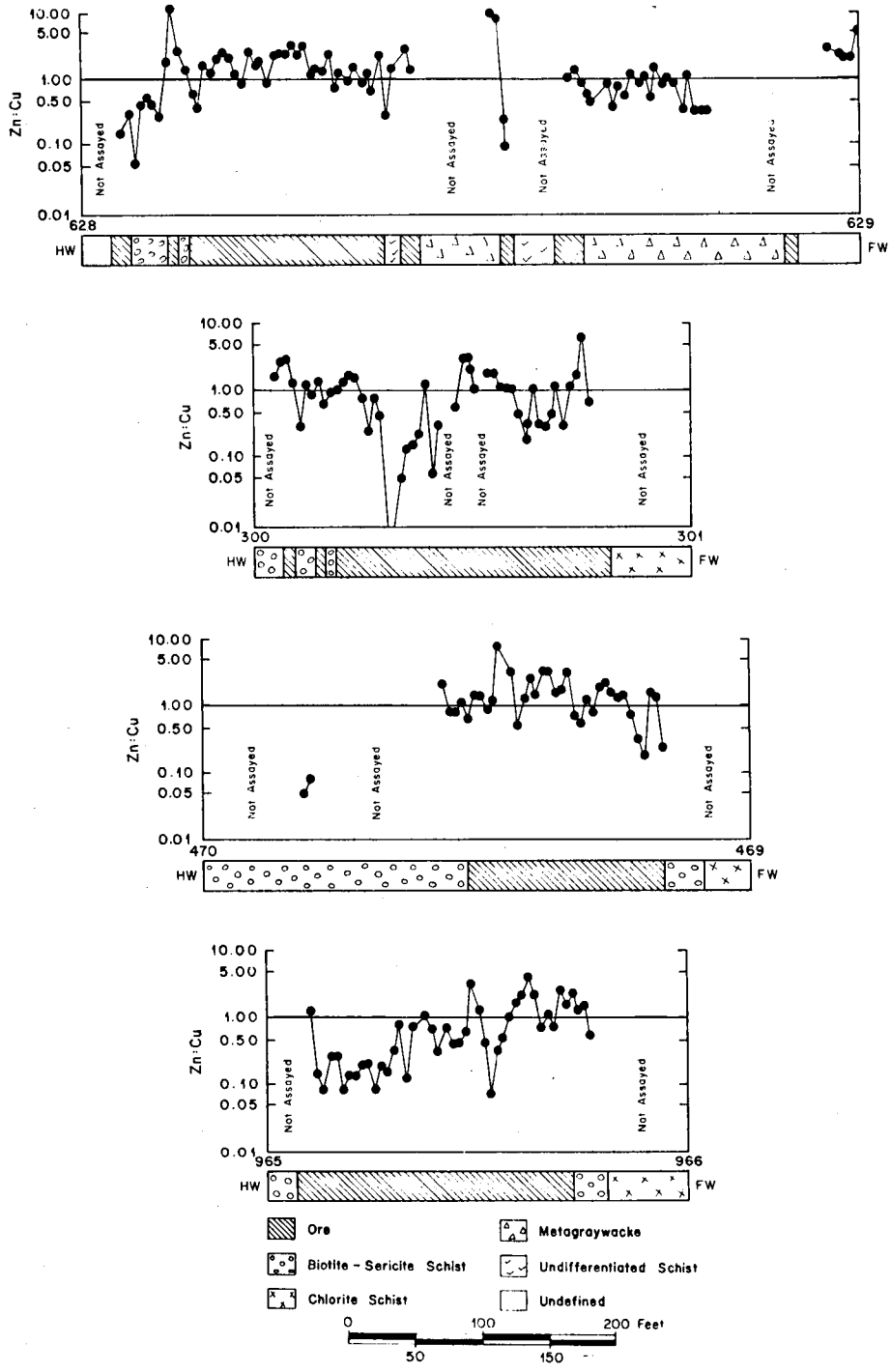


Figure 29. Zn:Cu ratios from bulk assay data for the four cores (628/629, 300/301, 469/470, and 965/966) from the Calloway Orebody obtained from the Tennessee Chemical Company.

reflected in the trace element data and is not fully understood. Since the data presented in Figure 29 represents only a very small sample of the Calloway orebody, it is likely that the overall zonation pattern recognized in the Ducktown orebodies (discussed above) is more distinct. This base metal zoning pattern along with the alteration patterns developed around the orebody, chlorite schist along the hanging wall and sericite schist along the footwall, has led researchers to believe that hydrothermal processes are responsible for the patterns observed (Mauger, 1972; Addy, 1977; and others). Mauger (1972) postulated, based on sulfur isotope data, that variations across the orebody may be related to original stratigraphy prior to metamorphism. Because Pb and Zn have a marked geochemical affinity, the patterns observed are not unreasonable. The presence of these elements in increasing amounts towards the hanging wall and the prevalence of elements like copper in the footwall might indicate several things, including, (1) stratigraphic up direction, (2) decreasing temperature towards the hanging wall, and (3) direction of hydrothermal fluid flowage. Factors, such as elemental zoning, alteration patterns, and isotope data, appear to fit with the syngenetic-premetamorphic origin proposed by Mauger (1972) and Addy (1977). One of the problems with the premetamorphic origin was pointed out by Tung (1968). He noted the presence of sulfide minerals replacing both high grade metamorphic mineral assemblages and later stage alteration minerals (chlorite and biotite). Tung (1968) suggested that the ore deposits were formed during or after metamorphism. This brings up another question as to the timing of the alteration zone itself. Was

the alteration zone produced by the ore-forming fluids or formed later on during metamorphism? Interestingly, the Cherokee orebody shows reversed metal zoning and alteration patterns. The chlorite schist is located along the hanging wall of the orebody which is generally enriched in copper with respect to the footwall. The trace element data from pyrite and pyrrhotite also show a reversed pattern (Figures 24 to 26, pp. 56, 59, and 60). This would indicate that the Cherokee orebody is on an overturned limb of the Burra Anticlinorium (Figure 4, p. 6) and that the orebodies were present prior to metamorphism. It appears that whatever was controlling the bulk chemistry of these deposits also may have had a similar effect on the trace element distribution.

Slater (1978, 1982) relates the base metal zoning and alteration patterns, along with the occurrence of some localized amphibolite bodies, as being indicative of a possible volcanogenic origin. These features are similar to those observed in the classic volcanogenic massive sulfide deposits, such as the mineralogical and alteration patterns observed in the Noranda district, Canada.

The trace element data along with bulk copper and zinc data, and alteration patterns established around the orebodies, aid in understanding the origin of these deposits. The trends observed in the orebodies are probably related to the original horizontal orientation within a sedimentary pile and subsequent tilting during periods of deformation. The origin of the hydrothermal fluids that formed the orebodies is uncertain.

Lateral Zoning within the Calloway Orebody

The trace element data in the sulfides (this study) are distinctly different in the uppermost part of the orebody, especially the extremely high values of cobalt and the Co:Ni ratio. This might indicate higher temperatures of formation in this part of the orebody (Mookherjee and Philip, 1979; Thole, 1976). The upper part of the orebody is morphologically different than the lower parts (Plate 1). Addy (1977) observed that this part of the orebody is structurally more complex, lacks an alteration zone, and that there is no isotope depletion present in this part of the orebody. Towards the lower levels of the orebody (flanks? of the orebody), there is an overall decrease in Pb and Ni in pyrite and pyrrhotite and an increase in the Co and Co:Ni ratio in pyrrhotite (Figures 27 and 28, pp. 62 and 63). Similarly, there is a net decrease in the bulk Zn towards the lower levels, indicating a similar metal zoning pattern as observed from the hanging wall towards the footwall of the orebody.

Interpretation of lateral metal zoning patterns within orebodies is very difficult due to the apparent lack of data in the literature. It does appear, however, that the distinct differences between the upper and lower parts of the orebody are complex and probably involve several processes.

Proposed Model for the Ducktown District

Many models have been proposed for the Ducktown district. Based on the data generated from this and other studies one comes to realize that this area has had a very complex history. Due to the effects of

metamorphism, many of the original characteristics of the district have been destroyed. An additional problem in the district is the lack of understanding of the stratigraphy of the area. However, based on structural, petrologic, and geochemical data, some interpretation of these deposits will be attempted.

Hutchinson (1980) classifies the Ducktown deposits into the Kieslagar or Besshi-type Exhalative Volcanogenic group. According to his definition, these deposits are "deposited in unstable subsiding basins with thick sedimentary sequences of greywackes and volcanoclastic rocks." Although the metal zoning and alteration patterns are similar to volcanogenic massive sulfide deposits, there is not enough evidence for the presence of igneous rocks (except the presence of localized amphibolite bodies) to call this a true volcanogenic massive sulfide deposit.

Sawkins (1976) classifies the Ducktown deposits as Sullivan-type deposits related to rifting tectonics. Both of the classic examples he sites for this group of deposits, the Sullivan and the Mt. Isa, are major lead-zinc-silver deposits. The Mt. Isa deposit in Australia occurs in a thick sequence of volcanics and the Sullivan deposit, in Canada, occurs near a series of basaltic intrusives cross cutting the ore. The Ducktown deposits have very little zinc, and practically no lead or silver. As previously mentioned, the only occurrence of igneous-type rocks in the area, are localized occurrences of amphibolites. The precursor rock is presumed to be basaltic in composition, but this is not known for certain. If these deposits were associated

with igneous activity, it must have been in the form of magmatic fluids migrating for some distance from the source through a sedimentary pile. This could account for the metal zoning, alteration zones, and relatively high Co:Ni ratio in pyrite. The ore horizon concept might be accounted for by a sedimentary (syngenetic) origin as proposed by Both (1973). If one compares the differences between proximal and distal ores presented by Large (1977), the Ducktown deposits do not fit either category. From these considerations it would appear that these deposits may have formed by exhalative processes but not directly within the center of igneous activity.

Many workers have discussed the application of Co:Ni ratios in pyrites to providing constraints on their origin (Appendix F). A similar attempt for the Ducktown ores is illustrated in Figure 30 which compares the composition (Co, Ni) of the Ducktown pyrites to that of pyrites from known environments as reported in literature. The pyrite from the Ducktown country rocks plots in the region of overlap between volcanic-exhalative and sedimentary-syngenetic fields, which is consistent with, but not an evidence for, the interpretation that this pyrite is sedimentary-syngenetic in origin. Pyrites from the Ducktown orebodies plot in the volcanic-exhalative field, but this does not necessarily mean that the Ducktown ores are volcanic-exhalative in origin. The ore pyrites clearly show an increase in Co, a decrease in Ni and an increase in Co:Ni ratios which, as discussed earlier, may well be ascribed to regional metamorphism of sedimentary-syngenetic pyrite. This change in pyrite composition is compatible with metamorphic

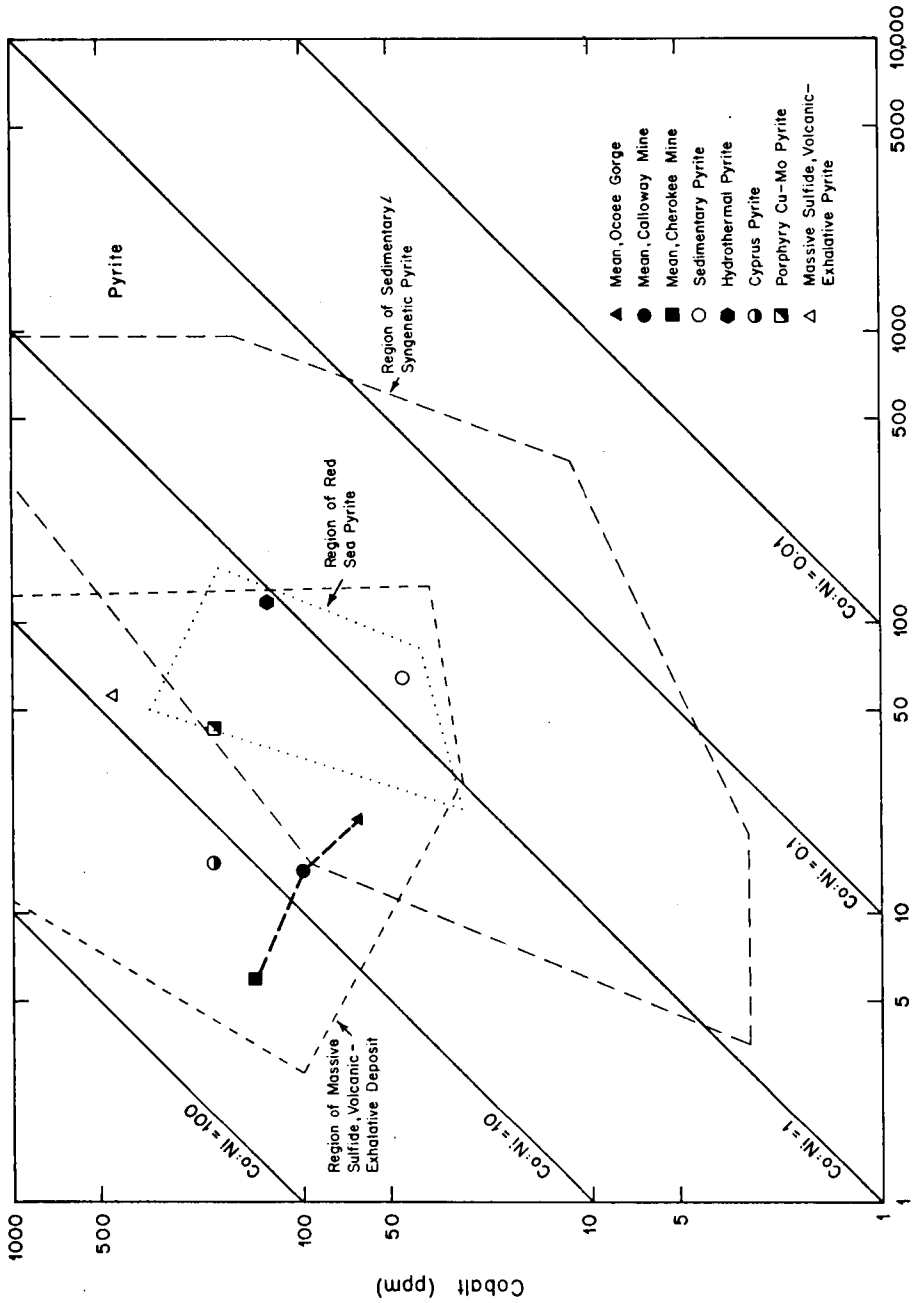


Figure 30. Comparison of cobalt and nickel contents of syngenetic, hydrothermal, and volcanic-exhalative (massive sulfide) pyrite with pyrite from the metasedimentary rocks and orebodies in the Ducktown area, Tennessee. All symbols are plotted as geometric mean values. Data for the various fields are from Price (1972).

mobilization of ore constituents from the country rocks to the sites of orebodies, as suggested by Runyon and Misra (1981) and Runyon (1983).

CHAPTER VI

SUMMARY

Pyrite and pyrrhotite from the country rocks and orebodies in the Ducktown district were analyzed for selected trace elements (Co, Ni, Mn, Pb, Ti, Sn, Ag). Various trends in the trace element distribution were visually and statistically evaluated along with other data in terms of ore genesis of the Ducktown massive sulfide deposits. The results are listed below:

1. The trace element contents of pyrite and pyrrhotite from the country rocks (Ocoee Gorge) are different than those from the orebodies. This is evident from both trend plots and statistical analysis.

2. The trace element contents of pyrite and pyrrhotite from the Calloway orebody are different than those from the Cherokee orebody. This is also evident from both trend plots and statistical analysis.

3. The trace elements in pyrite and pyrrhotite show several trends from the hanging wall to the footwall in the Calloway orebody, in particular Pb, Ni, and the Co:Ni ratio.

4. The trace elements in pyrite and pyrrhotite show several trends from the upper to the lower levels of the Calloway orebody, particularly Co, Pb, Ni, and Co:Ni ratio. The trace element data from the uppermost level is substantially different than the lower levels.

5. Trace elements in pyrite and pyrrhotite also show several trends from the hanging wall to the footwall in the Cherokee orebody, but appear to be reversed from those observed in the Calloway orebody.

This data along with bulk copper data and alteration patterns indicate that the Cherokee orebody is probably overturned.

6. Pyrite from the Cherokee orebody have the highest Co contents and Co:Ni ratio. The pyrite from the country rocks have the lowest Co contents and Co:Ni ratio.

7. Pyrrhotite from the country rocks have the highest Co and Ni contents and the lowest Co:Ni ratio.

8. The Co, Ni, and Co:Ni ratio data for pyrites from the Ducktown country rocks plot in the region of overlap between the volcanic-exhalative and sedimentary-syngenetic fields, whereas the pyrites for the Ducktown orebodies plot in the volcanic-exhalative field. The pyrites for the orebodies clearly show an increase in Co, a decrease in Ni and an increase in Co:Ni ratios when compared to the pyrites from the country rocks. These observations are consistent with metamorphic mobilization of ore constituents from the country rocks to the orebodies.

The Ducktown deposits have had a complex history and cannot be explained by any single genetic model. It is believed that the deposits were originally deposited prior to metamorphism in a sedimentary environment removed from any volcanic center. They were formed by a mixture of meteoric and magmatic ore-forming fluids. Subsequent prograde metamorphism may have remobilized the disseminated sulfides, including trace elements, from the country rocks into the orebodies, resulting in some addition to the orebodies.

BIBLIOGRAPHY

BIBLIOGRAPHY

Addy, S. K., 1973, The problem of ore genesis at Ducktown, Tennessee, interpretation of stable isotopes ($^{18}O/^{16}O$, $^{13}C/^{12}C$ and D/H), microprobe, and textural data: Ph.D. Thesis, Columbia Univ., New York, 219p.

--------, and Ypma, P. J. M., 1977, Origin of massive sulfide deposits at Ducktown, Tennessee: An oxygen, carbon, and hydrogen isotope study: Econ. Geol., v. 72, p. 1245-1268.

Adler, I., 1966, X-Ray Emission Spectrography in Geology: Elsevier Publishing Company Inc., New York, 258p.

Arkin, H., and Colton, R. R., 1970, Statistical Methods: Barnes and Noble Books, New York, 344p.

Bethke, P. M., and Barton, P. B., 1971, Distribution of some minor elements between coexisting sulfide phases: Econ. Geol., v. 66, p. 140-163.

Bhatia, D. M. S., 1976, Geochemistry, paragenetic relationship, spatial distribution and factor analysis of selected trace elements at the Magmont mine southeast Missouri: Ph.D. Thesis, Univ. of Missouri, Rolla, 306p.

--------, and Hagni, R. D., 1981, Laser probe determinations of trace element concentrations in sulfide minerals from the Magmont mine, Viburnum Trend, southeast Missouri: Soc. of Mining Eng. of AIME, Trans., v. 268, p. 1847-1855.

Blackburn, W. H., 1968, Spectrochemical determinations in garnets using a laser microprobe: Applied Spectroscopy, v. 22, no. 4, p. 278-283.

--------, and Schwendeman, James F., 1977, Trace-element substitution in galena: Canadian Mineral., v. 15, p. 365-373.

Both, R. A., 1973, Minor element geochemistry of sulphide minerals in the Broken Hill lode (N. S. W.) in relation to the origin of the ore: Min. Dep. (Berl.), v. 8, p. 349-369.

Bralia, G. S., Sabiti, G., and Troja, F., 1979, The revaluation of the Co:Ni ratio in pyrite as a geochemical tool in ore genesis problems: Min. Dep. (Berl.), v. 14, p. 353-374.

Brown, H. S., 1961, Wall rock alteration at the Calloway mine, Ducktown district: Cities Service Company, Copperhill Operations, Unpub. Company Rept., 24p.

Butler, J. R., 1972, Age of Paleozoic metamorphism in the Carolinas, Georgia and Tennessee, Southern Appalachians: Am. Jour. Sci., v. 272, p. 319-333.

--------, 1973, Paleozoic deformation and metamophism in part of the Blue Ridge thrust sheet, North Carolina: Am. Jour. Sci., v. 273-A, p. 78-88.

Cambel, B., and Jarkovsky, J., 1965, Rare elements in pyrite from the west Carpathian ore deposits and their possible use in the study of the mineralization genesis: Geokhim. Ada. Nauk. SSR. Inst. Geokhim. i, Analit Khim, p. 245-266.

--------, 1967, Geochemie der Pyrite einiger Lagerstatten der Tschechoslowakei. VSAV, Bratislava.

--------, 1969, Geochemistry of pyrrhotite of various genetic types: Geol. Instit. of the Komensky University monograph, Bratislava, p. 167-183.

Carpenter, R. H., 1974, Pyrrhotite isograd in southeastern Tennessee and southwestern North Carolina: Geol. Soc. Amer. Bull., v. 85, p. 451-456.

--------, 1970, Metamorphic history of the Blue Ridge Province of Tennessee and North Carolina: Geol. Soc. Amer. Bull., v. 81, p. 749-762.

Carr, M. H., and Turekian, K. K., 1961, The geochemistry of cobalt: Geochim. Cosmochim. Acta, v. 23, p. 9-60.

Craig, J., and Vaughn, D. J., 1981, Ore Microscopy and Ore Petrography: John Wiley and Sons, New York, 406p.

Dallmeyer, R. D., 1975, $^{40}Ar/^{39}Ar$ incremental release ages of biotite from Cherokee orebody, Ducktown, Tennessee; their bearing on the age of sulfide mineralization: Econ. Geol., v. 70, p. 341-345.

Doe, B. R., 1962, Distribution and composition of sulfide minerals at Balmat, New York: Geol. Soc. of Am., Bull., v. 73, p. 833-854.

Emmons, W. H., and Laney, F. B., 1926, Geology and ore deposits of the Ducktown mining district, Tennessee: U.S. Geological Survey Prof. Paper 139, 114p.

Ermin, N. I., 1975, Quantitative analysis by means of the laser micro-analyzer LMA-1: Min. Mag., v. 40, p. 312-314.

Espenshade, G. H., 1963, Geology and composition of some copper deposits in North Carolina, Virginia, and Alabama: U.S. Geol. Survey Bull. 1142-I.

Estes, E. L., 1972, Diagenetic alteration of Mercenaria Mercenaria as determined by laser microprobe analysis: Ph.D. Thesis, Univ. of North Carolina, 87p.

Fleischer, M., 1955, Minor elements in some sulfide minerals: Econ. Geol. 50th Anniv. Vol., p. 970-1024.

Franklin, J. M., Lydon, J. W., and Sangster, D. M., 1981, Volcanic-associated massive sulfide deposits: Econ. Geol. 75th Anniv. Vol., p. 485-628.

Fullagar, P. D., Brown, H. S., and Hagner, A. F., 1967, Geochemistry of wallrock alteration and the role of sulfurization in the formation of the Ore Knob sulfide deposit: Econ. Geol., v. 62, p. 798-825.

Ghosh-Dastidar, P., Pajari, G. E., and Trembath, L. T., 1970, Factors affecting the trace element partition coefficients between coexisting sulfides: Econ. Geol., v. 65, p. 815-837.

Harding-Barlow, I., Snetsinger, K. G., and Keil, K., 1973, Laser microprobe instrumentation; in Andersen, C. A., Ed., Microprobe Analysis: John Wiley and Sons, New York, p. 423-455.

Harvey, C., 1975, Petrography, structure, and trace element content of the wall rock biotites from the Boyd and Calloway ore bodies, Ducktown, Tennessee: Master's Thesis, Univ. of North Carolina, 75p.

Hatcher, R. D., Jr., Butler, J. R., Fullagar, R. D., Secor, D. T., and Snoke, A. W., 1980, Geologic synthesis of the Tennessee-Carolinas-Northeast Georgia Southern Appalachian; in Proceedings "the Caledonides in the U.S.A.," ed. D. R. Wones: Virginia Polytech. Inst. and State Univ., Dept. of Geol. Sciences Mem. No. 2, p. 83-90.

Hawley, J. E., and Nichol, I., 1961, Trace elements in pyrite, pyrrhotite and chalcopyrite of different ores: Econ. Geol., v. 56, p. 467-487.

Hernon, R. M., 1968, Geology of the Ducktown, Isabella, and Persimmon Creek quadrangles, Tennessee and North Carolina: U.S. Geol. Survey, Open File Report, 71p.

Holcombe, R. J., 1973, Mesoscopic and microscopic analysis of deformation and metamorphism near Ducktown, Tennessee: Ph.D. Thesis, Standford Univ., 225p.

Hurst, V. J., 1955, Stratigraphy, structure, and mineral resources of the Mineral Bluff quadrangle, Georgia: Georgia Geol. Survey, Bull. no. 63, 137p.

--------, and Schlee, J. S., 1962, Ocoee metasediments--North Central Georgia--Southeast Tennessee: Guidebook No. 3, Geol. Soc. America, Southeastern Sec. Am. Mtg., 10p.

Hutchinson, R. W., 1980, Massive base metal sulfide deposits as guides to tectonic evolution: Geol. Assoc. of Canada Special Paper 20, p. 659-684.

Itoh, S., and Kanheira, K., 1967, Trace elements in sulfide minerals from the Tsuchikura mine, Shiga Prefecture, with special reference to the contents of cobalt and nickel: Min. Geol. of Japan, v. 17, p. 251-260.

Itoh, S., 1971, Chemical composition of country rocks and minor elements in sulfide minerals from bedded cupriferous pyrite deposits in Tenryu River basin: Geol. Survey of Japan, Bull., v. 22, p. 117-132.

Johnson, A. E., 1972, Origin of Cyprus deposits: 24th IGC, section 4, p. 291-298.

Keil, K., and Snetsinger, K. G., 1973, Applications of the laser microprobe to geology; in Andersen, C. A., Microprobe Analysis: John Wiley and Sons, New York, p. 457-476.

Kinkel, A. R., Jr., Thomas, H. H., Marvin, R. F., and Watshall, F. G., 1965, Age and metamorphism of some massive sulfide deposits in Virginia, North Carolina, and Tennessee: Geochim. Cosmochim. Acta, v. 20, p. 717-724.

Large, R. R., 1977, Chemical evolution and zonation of massive sulfide deposits in volcanic terrains: Econ. Geol., v. 72, p. 549-572.

Lenker, E. S., 1962, A trace element study of selected sulfide minerals from the eastern United States: Ph.D. Thesis, Pennsylvania State Univ., 144p.

Loftus-Hills, G., and Solomon, M., 1967, Cobalt, nickel, and selenium in sulfides as indicators of ore genesis: Min. Dep., v. 2, p. 228-242.

Magee, N., 1968, Geology and ore deposits of the Ducktown district, Tennessee; in Ridge, J. D., Ed., Ore deposits of the United States: 1933-1967 (Graton-Sales Vol.): Am. Inst. Min. Metall. Pet. Eng., New York, p. 207-241.

Mauger, R. L., 1972, A sulfur isotope study of the Ducktown, Tennessee, district, USA: Econ. Geol., v. 67, p. 497-510.

Merschat, C. E., and Weiner, L. S., 1973, Provisional geologic map of the Ocoee Supergroup southwestern North Carolina and southeastern Tennessee (abs.): Geol. Soc. America Abs. with Programs, v. 5, p. 420.

Misra, K. C., and Fleet, M. E., 1973, The chemical composition of synthetic and natural pentlandite assemblages: Econ. Geol., v. 68, p. 518-539.

Mookherjee, A., and Philip, R., 1979, Distribution of copper, cobalt, and nickel in ores and host-rocks, Ingladhal, Karnataka, India: Mineral. Dep. (Berl.), v. 14, p. 33-55.

Nesbitt, B. E., 1979, Regional metamorphism of the Ducktown, Tennessee, massive sulfides and adjoining portions of the Blue Ridge Province: Ph.D. Thesis, Univ. of Mich., 216p.

--------, and Kelly, W. C., 1980, Metamorphic generation of sulfides, oxides, and graphite in and around the orebodies at Ducktown, Tennessee: Econ. Geol., v. 75, p. 1010-1021.

--------, and Essene, E. J., 1982, Metamorphic thermometry and barometry of a portion of the southern Blue Ridge Province: Am. Jour. Sci., v. 282, p. 701-729.

Pearson, E. S., and Hartley, H. O., eds., 1956, Biometrika tables for statisticians, Vol. 1: Cambridge University Press, 238p.

Price, B. J., 1972, Minor elements in pyrites from the Smithers map area, B. C. and exploration applications of minor element studies: Master's Thesis, Univ. of British Columbia, 270p.

Reed, J. C., Jr., 1970, The Blue Ridge and the Reading Prong; in Studies of Appalachian Geology, central and southern: Intersci. Publ., New York, p. 195-197.

Ringler, R. W., 1979, Sphalerite geobarometry of the Calloway Mine, Ducktown, Tennessee: Econ. Geol., v. 74, p. 937-942.

Rose, A. A., 1967, Trace elements in sulfide minerals from the Central district, New Mexico and the Bingham district, Utah: Geochim. Cosmochim. Acta, v. 31, p. 547-586.

--------, 1970, Origin of trace element distribution patterns in sulfides of the Central and Bingham districts, Western U.S.A.: Min. Dep., v. 5, p. 157-163.

Runyon, G. A., 1983, The distribution and variation of sulfide constituents of the Great Smoky Group, Ducktown area, Tennessee, with respect to metamorphic grade: Master's Thesis, The Univ. of Tenn., Knoxville, 115p.

Runyon, G. A., and Misra, K. C., 1981, Metamorphic mobilization of sulfide constituents in metasediments of the Great Smoky Group, Ducktown area, Tennessee: Geol. Soc. America Abs. with Programs, v. 13, p. 33.

Sawkins, F. J., 1976, Massive sulfide deposits in relation to geotectonics: Geol. Assoc. Canada, Spec. Paper, no. 14, p. 221-240.

Sawyer, R. A., 1951, Experimental Spectroscopy: Prentice Hall Inc., New York, 358p.

Sinclair, A. J., 1976, Applications of Probability Graphs in Mineral Exploration: Assoc. of Expl. Geochemists Spec. Vol., no. 4, 95p.

--------, Fletcher, W. K., Price, B. J., Bentzen, A., and Wong, S. S., 1977, Minor elements in pyrites from some porphyry-type deposits, British Columbia: Trans. of SME, v. 262, p. 94-100.

Slater, R., 1978, Cherokee north open pit (Cities Service Co.), Ducktown district, southeast Tennessee: I.A.G.O.D. 5th Symposium Guidebook for Eastern Field Excursion A-2, p. 1-10.

--------, 1982, Massive sulfide deposits of the Ducktown mining district, Tennessee, in Exploration for Metallic Resources in the Southeast: University of Georgia, Dept. of Geology and Center for Continuing Education, p. 91-99.

Stanton, R. L., 1972, Ore Petrology: McGraw-Hill, New York, 713p.

Thole, R. H., 1976, The geology of the Shamrocke Mine, Rhoedesia--a stratiform copper deposit: Econ. Geol., v. 71, p. 202-228.

Tilden, J. E., 1971, Distribution of certain trace elements in sulfide minerals from selected ore deposits of the southeastern United States: Master's Thesis, North Carolina State Univ., 43p.

Tsui, T. F., et al., 1975, Laser microprobe analysis of fluid inclusions: Geol. Soc. of America Annual Meetings, Salt Lake City.

Tung, J. P., 1968, A study of the wall rocks and relationship to the ore body at the Calloway Mine, Ducktown, Tennessee: Master's Thesis, The Univ. of Tennessee, Knoxville, 66p.

Weiner, L. S., and Merschat, C. E., 1978, Summary of geology between the Great Smoky Mountain fault at Parksville, Tennessee, and basement rocks of the Blue Ridge at Glade Gap, North Carolina: Tennessee Div. Geol., Rept. Invs. 37, 86p.

APPENDICES

APPENDIX A

SAMPLE PREPARATION

SAMPLE PREPARATION

A. Standards

1. Standard material (powder) was previously ground to -325 mesh and homogenized by the manufacturer (Chemplex Industries, Inc.). Each of their sets of standards contained material made at various concentration levels, i.e., 50, 100, 500, and 1,000 ppm.

2. Each standard was again thoroughly mixed by the author.

3. 1 gram of standard material was weighed out and placed in a pellet die along with boric acid as the backing material.

4. This material was then pressed in a Carver Laboratory Press to 30,000 pounds for 30 seconds producing a pressed pellet or disc roughly 1 inch in diameter.

5. This procedure was followed for each standard pellet produced. The standard pellets were made in increasing concentration levels, i.e., 50, 100, 500, then 1,000 ppm in order to reduce problems with subsequent contamination. The pellet die was thoroughly cleaned and dried between each use.

B. Unknowns

When using the laser microprobe for analysis it has been determined that polished sections produce the best results (Bhatia, 1976). Polished sections were also used to study the opaque mineralogy under reflected light.

Each polished section was made to approximately 1 inch in diameter and prepared using standard techniques. The final polishing, however,

was done on a low-speed, automatic Stellapol lap to prevent the sample from heating up and reduce and deformational effects due to polishing.

APPENDIX B

STATISTICAL TERMS AND EQUATIONS

STATISTICAL TERMS AND EQUATIONS USED IN THIS STUDY

1. Geometric Mean (G_m):

$$G_m = \sqrt[n]{x_1 \cdot x_2 \cdot x_3 \cdots x_n} \; ; \quad \text{Log } G_m = \frac{\text{Log } x_1 + \text{Log } x_2 + \ldots \text{Log } x_n}{n}$$

2. Arithmetic Mean ($\bar{x}$):

$$\bar{x} = \frac{\sum_{i=1}^{n} x_i}{n}$$

3. Standard Deviation (s or σ):

$$s = \frac{\sqrt{\sum_{i=1}^{n} (x_i - \bar{x})^2}}{n - 1}$$

4. Coefficient of Variation (V):

$$V = \frac{s}{\bar{x}} \cdot 100$$

5. Class Interval (I):

$$\frac{r}{1 + (3.222 \times \log n)}$$

6. Correlation Coefficient (r):

$$r = \frac{n\Sigma xy - \Sigma x \Sigma y}{\sqrt{[n \cdot \Sigma x^2 - (\Sigma x)^2][n \cdot \Sigma y^2 - (\Sigma y)^2]}}$$

7. Variance (s^2 or σ^2):

$$s^2 = \frac{\sum_{i=1}^{n} (x_i - \bar{x})^2}{n}$$

8. Least Squares Equation:

General Equation: $\hat{y} = mx + b$

$$m = \frac{\Sigma x\, y - (\Sigma x)(\Sigma y)/n}{\Sigma x^2 - (\Sigma x)^2/n}$$

$$b = \bar{y} - b\bar{x}$$

9. Standard Error of Estimate (S_y): $Sy = 1.96 \sqrt{\frac{SS}{n}}$

(95 Percent Confidence Interval on Regression Line)

10. Student's t-Test (Log Transformation) Equation:

$$t = \frac{\log_e \bar{x}_1 - \log_e \bar{x}_2}{\sqrt{\left(\frac{S_1^2}{n_2} + \frac{S_2^2}{n_2}\right) \times \left(\frac{n_1 + n_2}{n_1 + n_2 - 2}\right)}}$$

where, $\bar{x}_1 > \bar{x}_2$

n = total number of items

Σ = "sum of"

x,y = data expressed as individual values

SS = sum of the errors squared

m = slope of line

b = Y-intercept

t = t-statistic

$\hat{y}$ = value of y predicted by the regression line for the corresponding x

APPENDIX C

CHEMICAL ANALYSES OF INITIAL SET OF STANDARDS

Table C-1. Chemical Analyses of Samples Selected for the Initial Set of Standards Chosen for LMP Analysis.

Sample Type	Fe(%)	Cu(%)	Cu(ppm)	Zn(%)	Zn(ppm)	S(%)	Co(ppm)	Ni(ppm)	Mn(ppm)	Pb(ppm)	Ti(ppm)	Sn(ppm)	Ag(ppm)	Au(ppm)	V(ppm)	Mo(ppm)	Cr(ppm)	As(ppm)	Se(ppm)	Cd(ppm)	In(ppm)	Sb(ppm)	Bi(ppm)	Si(%)
Zn Concentrate (Mill)	23.90	1.29	-----	36.30	-----	33.80	74	5	1800	1300	40	9	13.0	37	<10	3	15	9	40	760	87	0.8	13.0	0.80
Zn Concentrate (Mill)	24.20	1.30	-----	36.80	-----	34.20	71	4	1800	1300	40	6	13.0	37	10	3	14	9	40	810	86	1.0	14.0	0.70
Cu Concentrate (Mill)	41.00	14.60	-----	1.41	-----	34.90	89	2	450	4500	30	80	33.0	90	10	71	9	11	52	36	15	1.4	62.0	1.10
Cu Concentrate (Mill)	40.30	14.30	-----	1.37	-----	34.40	88	2	450	4300	30	80	33.0	80	8	68	8	13	51	36	15	1.3	48.0	1.15
Fe Concentrate (Mill)	55.30	-----	930.	-----	2700.	37.90	220	7	260	100	100	<3	2.5	3	7	<1	15	29	24	17	1	0.4	12.0	0.90
Fe Concentrate (Mill)	54.70	-----	880.	-----	2800.	38.80	210	5	250	98	100	3	2.5	2	8	<1	17	32	26	17	1	0.3	9.0	0.95
Massive Po+/-Cp (Cherokee)	54.40	0.94	-----	-----	3500.	37.10	71	<1	1200	100	10	6	5.0	12	10	<1	8	6	32	19	1	0.2	8.0	2.10
Massive Po+/-Cp (Cherokee)	54.70	0.96	-----	-----	3500.	37.20	69	<1	1200	100	20	<3	5.0	14	10	<1	6	6	28	19	1	0.2	8.0	2.05
Massive Py+Po (Cherokee)	45.40	-----	3500.	-----	2600.	44.30	190	<1	660	280	10	3	1.5	4	14	<1	5	110	35	14	<1	0.8	5.0	1.95
Massive Py+Po (Cherokee)	46.10	-----	3500.	-----	2500.	44.10	198	<1	650	280	10	3	1.5	2	7	<1	7	110	33	14	<1	0.7	7.0	1.80

Po = Pyrrhotite
Cp = Chalcopyrite
Py = Pyrite
(Cherokee) = Samples from Cherokee Orebody

APPENDIX D

INSTRUMENTATION, WORKING CURVE, PRECISION, AND ACCURACY DATA

Table D-1. Spectral Lines, Instrumentation,[a] and Laser Microprobe Settings Used[b] for Trace Element Determinations.

Element	Wavelength (Angstroms)
Fe	2912
Co	2582
Ni	3414
Mn	2801
Pb	4057
Ti	3088
Sn	3262
Ag	3280

[a] Instrumentation

Jarrell-Ash Laser Microprobe Mark II
Model No. 45-604
Neodymium-Yag Laser Rod

Jarrell-Ash, 1.0 Meter Czerny-Turner Emission Spectrograph
Model No. 75-150

Kodak Spectrum Analysis Plates No. 3 (4 x 10 in.)
Cat. No. 172 9599
Recording Range 2,400 to 4,000 Angstroms

Kodak Fixer
Cat. No. 197 1746

Kodak Developer D-19
Cat. No. 146 4593

Plate Development per Cabot Spectrographic Laboratory Procedures

[b] Laser Microprobe Settings Used

Slit Width: 20
Electrode Gap: 2 mm
Excitation: 2000 volts (Setting No. 1)
Laser Power: 0.5 joules (Setting No. 3)
Slit Height: 3 mm

Table D-2. Best Fit Line Equations, Correlation Coefficients, and Confidence Limits for Working Curves.

El	Equations	N	Correlation Coefficient (r)	95% Confidence Interval on (r)	95% Minimum Statistically Significant (r)	Sum of Errors Squared	95% Confidence Limit of the Regression Line
Co	Log (ICO/IFE) = (0.962) * Log Conc-Co - 2.798	68	0.76	(0.87,0.64)	0.236	7.75	± 0.66
Ni	Log (INI/IFE) = (0.621) * Log Conc-Ni - 1.907	52	0.59	(0.74,0.46)	0.268	9.07	± 0.82
Mn	Log (IMN/IFE) = (0.420) * Log Conc-Mn - 0.231	63	0.39	(0.59,0.17)	0.244	14.40	± 0.94
Pb	Log (IPB/IFE) = (0.775) * Log Conc-Pb - 1.961	59	0.42	(0.61,0.18)	0.252	13.10	± 0.92
Ti	Log (ITI/IFE) = (0.690) * Log Conc-Ti - 1.710	62	0.43	(0.62,0.19)	0.246	14.09	± 0.93
Sn	Log (ISN/IFE) = (1.041) * Log Conc-Sn - 3.135	69	0.66	(0.76,0.49)	0.234	10.68	± 0.77
Ag	Log (IAG/IFE) = (0.714) * Log Conc-Ag - 1.486	68	0.68	(0.80,0.54)	0.236	9.74	± 0.74
Cu	Log (ICU/IFE) = (1.282) * Log Conc-Cu - 1.808	69	0.24	(0.47,0.03)	0.234	17.31	± 0.98

Table D-3. Precision Data for a Typical Sample of Pyrite and Pyrrhotite.

El	N	Range (ppm)	Mean (ppm)	Std. Dev. (ppm)	Coeff. of Var. (%)
		Core Sample: CA-965, 35-40 (Pyrite)			
Co	9	224-461	311	92	29.58
Ni	9	1-61	18	21	116.67
Mn	9	1-11	5	4	80.00
Pb	9	22-45	35	9	25.71
Ti	9	9-29	16	8	50.00
Sn	9	69-208	104	41	39.42
Ag	9	4-13	7	3	42.86
Co:Ni	8	3.93-206.0	57.92	70.72	122.10
		Core Sample: CA-629, 210-215 (Pyrrhotite)			
Co	6	21-97	45	29	64.44
Ni	6	7-61	30	19	63.33
Mn	6	3-14	7	5	71.43
Pb	6	60-131	85	26	30.59
Ti	6	17-77	43	26	60.47
Sn	6	69-144	107	32	29.91
Ag	6	36-102	65	24	36.92
Co:Ni	6	1.05-3.19	1.71	0.80	46.78

Table D-4. Comparison of a Pyrite Standard Analyzed by the Laser Microprobe (LMP) and Atomic Absorption (AA).

El	N (LMP)	Range Pyrite Standard (LMP) (ppm)	Mean Pyrite ± Standard Dev. (ppm)	Mean Pyrite Standard (AA) (ppm)
Co	9	10-115	45 ± 36	91
Ni	8	6-104	32 ± 32	74
Mn	8	3-28	10 ± 8	20
Co:Ni	8	0.16-4.0	1.39 ± 1.43	1.23

APPENDIX E

OPAQUE MINERALOGY

Table E-1. Opaque Mineralogy of Samples Used in This Study, Ducktown Area, Tennessee.

Sample		Py	Po	Cp	Sph	Gal	Oxides
Ocoee Gorge							
DT-1C		x	x				x
DT-2D		x					
DT-12A			x				
DT-4B		x					x
119A			x				
DT-3C		x	x				
DT-4C		x	x				
122			x				
DS#1			x				
DT-9F			x				
DT-9H			x				x
Calloway Orebody							
CA-628	210-215		x				
	165-170	x	x	x	x	x	x
	130-135	x	x	x	x		
	100-105	x	x	x	x	x	
	15-20		x	x	x	x	
CA-629	75-80		x	x	x	x	
	140-145		x	x	x		
	145-150	x	x	x	x	x	
	210-215		x	x	x		
	270-275	x	x		x	x	x
	330-335		x		x		
	370-375		x		x		
CA-300	150-160	x	x	x	x	x	
	80-90	x	x	x			
	30-40	x	x	x	x	x	
	10-20	x	x				
CA-301	0-10	x	x	x	x		
	80-90	x	x	x	x	x	
	100-110		x	x	x	x	
	130-140		x	x			
CA-470	135-140		x				
	55-60		x		x		
CA-469	20-25	x	x	x	x	x	
	50-55	x	x	x	x	x	
	85-90	x	x	x	x	x	
	110-115		x				

Table E-1 (continued)

Sample		Py	Po	Cp	Sph	Gal	Oxides
CA-965	80-85	x	x	x	x		
	70-75	x	x	x	x		
	65-70	x	x	x	x		
	45-50		x	x	x		
	35-40	x		x	x		
	15-20	x	x	x	x		
CA-966	10-15	x	x	x			
	45-50	x	x	x			
	70-75	x	x	x	x	x	
	95-100	x	x	x	x		
	130-135	x	x				
	140-145		x	x			
	180-185		x				
CH-857	40-45	x	x	x	x	x	
	5-10		x	x			
CH-858	0-5		x	x	x		
	10-15		x	x	x		
	20-25	x	x				
	25-30	x	x				
	30-35	x	x	x			
	40-45	x	x	x	x		
	70-75		x				x

Py = Pyrite
Po = Pyrrhotite
Cp = Chalcopyrite
Sph = Sphalerite
Gal = Galena

APPENDIX F

TRACE ELEMENT REVIEW

TRACE ELEMENTS IN PYRITE AND PYRRHOTITE: A REVIEW

The trace elements in sulfide ores and sulfide minerals have been studied for over one hundred years. The earlier workers were primarily involved in qualitative analysis in order to find new elements and new resources of the rarer elements. Later, in the 1940's and 50's, the emphasis shifted to quantitative analysis for obtaining information about the processes of ore formation (Fleischer, 1955).

Mode of Occurrence of Minor Elements

Fleischer (1955) noted that the most widely recognized modes of occurrence of trace elements in minerals are as "trace minerals" and as atomic substitutions for the major elemental components of minerals in regular lattice positions. An additional mode of occurrence is as individual atoms or small groups of atoms that occur in lattice defects of the host mineral.

The "trace minerals" generally occur as separate microscopic mineral phases that are included within the crystal of the host mineral. These contaminants can generally be avoided by carefully mapping each mineral phase before the analysis is performed.

Trace elements that occur as atomic substitutions for the major elemental components of host minerals are more likely to exhibit a consistent distribution and provide more meaningful information on the factors involved in the genesis of the mineral deposits.

The third mode of occurrence, as individual atoms or small groups of atoms in lattice defects of the host minerals, would be greatly

affected by the number and nature of such defects. In part, this may account for greater variability of elements observed in some sulfide minerals (Bhatia, 1976). For a much more detailed discussion on the modes of occurrence of trace elements in sulfides see Fleischer (1955), Cambel and Jarkovsky (1967, 1969), and Price (1972).

Selected Trace Elements Contained in Pyrite and Pyrrhotite

The following observations are summarized from Fleischer (1955), Hawley and Nichol (1961), Cambel and Jarkovsky (1967, 1969), and Price (1972) and will emphasize those elements used in this study (Co, Ni, Mn, Pb, Ti, Sn, and Ag).

Pyrite. Trace elements that have been identified in pyrite include: As, Sb, Bi, Co, Cu, Sr, Ba, Tl, Cr, Ga, Cd, In, Pb, Mn, Ni, Ag, Sn, V, Zn, Au, Mo, Ti, U, Th, Hg, Se, and Pt-group elements.

Cobalt. Cobalt is believed to substitute for iron in the pyrite crystal structure. This element, along with nickel, is of great interest due to its somewhat systematic variation in different types of mineral deposits. It has been noted by many authors that the cobalt content and the Co:Ni ratio appear to be characteristic of individual deposits.

Nickel. Nickel in pyrite is also believed to be due to atomic substitution for iron. In general, the pyrite structure accommodates more cobalt than nickel. There appears to be a less systematic

variation of nickel with different types of deposits but, as previously mentioned, the Co:Ni ratio is somewhat characteristic.

Manganese. According to Price (1972), there should be only limited substitution of iron by manganese in the pyrite lattice. Since both sphalerite and magnetite can contain appreciable amounts of manganese in solid solution, some of the manganese in pyrite may be attributed to inclusions of these minerals. Also limonite, manganese oxide stains or tarnish on pyrite could account for anomalously high concentrations on manganese in pyrite.

Lead. It is believed that the lead content of pyrite is most probably due to minute inclusions of galena or other lead-bearing sulfides. However it must be pointed out that in the present study, great care was taken to avoid pyrite grains with tiny inclusions of galena and that another mode of occurrence might be possible.

Titanium. There is very little information on the occurrence of titanium in pyrite. It has been observed that titanium is commonly found in pyrite and is relatively regularly distributed.

Tin. Due to the dissimilar ionic charge and covalent radius, extensive substitution of tin for iron in pyrite is not likely and that most analyses of tin in the literature are less than 300 ppm. Tin-bearing minerals, such as cassiterite and stannite, may occur as microinclusions in pyrite and produce anamolously high concentrations of tin.

Silver. Due to the large size of the silver ion and differences in the charges, only limited substitution of silver for iron is expected. It is believed that much of the silver in pyrite reported in the literature is due to the presence of microinclusions of admixed silver-sulfosalts and galena.

Pyrrhotite. Trace elements that have been identified in pyrrhotite include: Sb, As, Bi, Cr, Co, Cu, Ge, Au, Pb, Mn, Mo, Ni, Re, Se, Ag, Tl, Sn, Ti, W, V, Zn, and the Pt-group metals.

Cobalt. Cobalt in pyrrhotite, as in pyrite, is believed to be due to atomic substitution for iron. Reported values of cobalt in pyrrhotite exceeding 1 percent are rare. Cobalt together with nickel in pyrrhotite is believed to reflect genetic, geological and physical-chemical conditions of pyrrhotite formation.

Nickel. Nickel in pyrrhotite (up to 1 percent) is also believed to be due to atomic substitution for iron. Other sources of nickel in pyrrhotite are believed to be microinclusions of pentlandite and other nickel-bearing phases. It is also believed that the amount of nickel present in pyrrhotite is dependent on the temperature of pyrrhotite formation or equilibration (Misra and Fleet, 1973).

Manganese. There appears to be a lack of atomic substitution of iron by manganese in pyrrhotite. The presence of manganese is better explained by a heterogeneous admixture. But due to the persistence of manganese in pyrrhotite and the relatively uniform occurrence in

pyrrhotite of different genetic types, it is believed that some manganese may be bound isomorphously.

Lead. Very little information is available on the lead contents in pyrrhotite, but it is believed to have a heterogeneous occurrence in pyrrhotite, mainly as tiny inclusions of lead-bearing minerals.

Titanium. It is presumed that titanium is present as an admixture (heterogeneous constituent) in pyrrhotite. Commonly, ilmenite is present in mineral deposits, as tiny inclusions in pyrrhotite. Generally, pyrrhotite contains more titanium than does pyrite.

Tin. Tin in pyrrhotite, as in pyrite, is erratic in its occurrence and appears to be restricted to deposits that contain cassiterite, stannite, or other tin-bearing minerals. Tin probably occurs in these tin-bearing phases as tiny microinclusions in pyrrhotite.

Silver. Little data is available on the silver content of pyrrhotite but it has been observed to increase with depth.

Cobalt, Nickel, Co:Ni Ratio and the Genesis of Ore Deposits

It is believed that the trace element contents of sulfides reflect the trace composition of the ore-forming fluids from which the sulfides directly crystallize. Therefore, it may be possible to use the trace elements as indicators of ore genesis if the fluids which transport and deposit different types of mineral deposits differ significantly in their trace element content, though possibly depositing the same major elements (Loftus-Hills and Solomon, 1961).

The cobalt, nickel, and Co:Ni ratio in pyrite and pyrrhotite have been used as an indication of the environment of deposition for many years. The following data are summarized from Fleischer (1955), Loftus-Hills and Solomon (1967), Cambel and Jarkovsky (1967, 1969), Price (1972), Johnson (1972), Thole (1976), and Bralia et al. (1979).

Pyrite

Sedimentary pyrites. These pyrites are characterized by relatively low values of cobalt and nickel and a Co:Ni ratio < 1 (average 0.63). Also cobalt and nickel are strongly correlated to each other in sedimentary pyrites with $r > 0.90$.

Hydrothermal pyrites. These pyrites show highly variable contents of both cobalt and nickel and therefore, their Co:Ni ratio is also highly variable but generally < 5.

Massive sulfide and volcanic-exhalative pyrites. These pyrites are characterized by cobalt being higher than nickel (with nickel usually less than 100 ppm) and Co:Ni ratio between 5 and 50 (average 8.70).

Although these observations have been observed by many researchers and are generally accepted by the scientific community, caution is advised when using these criteria for interpretive purposes. Also, the Co:Ni ratio alone is not diagnostic of the depositional environment (Loftus-Hills and Solomon, 1967).

Table F-1 which follows is summarized from Price (1972).

Table F-1. Comparison of Cobalt and Nickel Contents and Co:Ni Ratios from Sedimentary (Syngenetic), Hydrothermal, and Volcanic-Exhalative (Massive Sulfide) Pyrite (Summarized from Price, 1972).

	Sedimentary	Hydrothermal	Massive Sulfide
Co	41 ppm	141 ppm	486 ppm
Ni	65 ppm	121 ppm	56 ppm
Co:Ni	0.63	1.17	8.70

Note: The listed data are geometric means.

Pyrrhotite

Compared to pyrite, available data on pyrrhotite are rather limited. Cambel and Jarkovsky (1969) analyzed over 275 pyrrhotite samples from different types of deposits. It appears from their data that pyrrhotite shows some of the same characteristics as pyrite. Pyrrhotites from volcanogenic environments (high temperature) displays high cobalt and nickel contents and Co:Ni ratios less than 1. Pyrrhotites of hydrothermal origin commonly display low cobalt and nickel contents (average <100 ppm) and Co:Ni ratios greater than 1.

Effects of Metamorphism on Trace Elements in Pyrite and Pyrrhotite

This subject is not covered adequately in the published literature. It is, however, discussed in some detail by Cambel and Jarkovsky (1967 and 1969), Itoh and Kanehira (1967), Itoh (1971), and Bralia et al. (1979). All of the data pertains to cobalt, nickel, and the Co:Ni ratio. No data on other elements could be found.

The following is a summary of the observations made on the effects of metamorphism on the trace element distribution in pyrite and pyrrhotite:

1. Cobalt content of pyrite increases, and nickel content of pyrite decreases, resulting in a large increase in the Co:Ni ratio of pyrite with increasing grade of metamorphism.

2. In the metamorphic conversion of pyrite to pyrrhotite, cobalt is concentrated in pyrite, whereas nickel is concentrated in pyrrhotite.

3. In some instances, it appears that metamorphism has redistributed cobalt and nickel from a log normal to a more "arithmetic" normal distribution.

Distribution of Trace Elements between Coexisting Pyrite and Pyrrhotite

The distribution of trace elements between coexisting sulfides has been studied in detail by Fleischer (1955), Hawley and Nichol (1961), Cambel and Jarkovsky (1967 and 1969), Ghosh-Dastidar et al. (1970), Bethke and Barton (1971), and Mookerjee and Philip (1979). Their conclusions may be summarized as follows:

1. Cobalt is preferentially concentrated in pyrite over pyrrhotite.

2. Nickel is preferentially concentrated in pyrrhotite over pyrite. This is due to the fact that nickel can substitute for iron completely in pyrrhotite solid solutions (Hawley and Nichol, 1961).

It is believed that the distribution of cobalt and nickel between coexisting pyrite and pyrrhotite may be a function of metamorphism (Cambel and Jarkovsky, 1967 and 1969).

3. Lead is preferentially concentrated in pyrite over pyrrhotite.

4. Titanium, manganese, and tin are preferentially concentrated in pyrrhotite over pyrite.

No data on the distribution of silver between coexisting pyrite and pyrrhotite could be found.

APPENDIX G

GEOMETRIC MEAN DATA

Table G-1. Geometric Mean Data for Pyrite from the Ocoee Gorge Metasediments.

El	N	Range (ppm)	Geometric Mean (ppm)	Std. Dev. (± ppm)
			Chlorite Grade	
Co	11	57-121	1.849 (71)	0.115 (92,54)
Ni	12	4-107	1.300 (20)	0.954 (179,2)
Mn	12	1-25	0.695 (5)	0.490 (15,2)
Pb	12	22-379	1.865 (73)	0.403 (185,29)
Ti	12	31-247	1.944 (88)	0.310 (179,43)
Sn	11	91-176	2.115 (130)	0.102 (165,103)
Ag	12	13-257	1.766 (58)	0.417 (152,22)
Co:Ni	10	0.59-16.50	0.550 (3.55)	0.521 (11.78,1.07)
			Biotite Grade	
Co	15	21-200	1.861 (73)	0.314 (150,35)
Ni	14	9-178	1.580 (38)	0.419 (100,14)
Mn	14	2-76	0.962 (9)	0.474 (27,3)
Pb	15	20-258	1.891 (78)	0.322 (163,37)
Ti	15	29-141	1.693 (49)	0.261 (90,27)
Sn	14	69-208	2.054 (113)	0.155 (162,79)
Ag	13	53-174	1.939 (87)	0.154 (124,61)
Co:Ni	15	0.46-11.08	0.346 (2.22)	0.454 (6.31,0.78)
			Ocoee Gorge (All Pyrite)	
Co	25	21-144	1.806 (64)	0.227 (108,38)
Ni	24	4-107	1.322 (21)	0.414 (54,8)
Mn	26	1-31	0.766 (6)	0.469 (17,2)
Pb	26	20-258	1.853 (71)	0.331 (153,33)
Ti	25	14-188	1.761 (58)	0.273 (108,31)
Sn	26	24-188	2.029 (107)	0.197 (168,68)
Ag	25	13-187	1.815 (65)	0.306 (132,32)
Co:Ni	25	0.46-16.50	0.427 (2.67)	0.482 (8.11,0.88)

Table G-2. Geometric Mean Data for Pyrite from the Calloway Orebody.

El	N	Range (ppm)	Geometric Mean (ppm)	Std. Dev. (± ppm)
			Core: CA-628/629	
Co	17	121-1205	2.634 (431)	0.303 (865,214)
Ni	16	4-110	1.254 (18)	0.456 (51,6)
Mn	16	1-36	0.683 (5)	0.471 (14,2)
Pb	16	15-234	1.786 (61)	0.340 (134,28)
Ti	15	6-53	1.222 (17)	0.278 (32,8)
Sn	16	35-188	1.944 (88)	0.201 (140,55)
Ag	17	20-230	1.794 (62)	0.312 (128,30)
Co:Ni	17	1.10-602.50	1.436 (27.29)	0.717 (142.23,5.24)
			Core: CA-300/301	
Co	17	7-240	1.657 (45)	0.470 (134,15)
Ni	16	2-662	1.598 (40)	0.645 (175,9)
Mn	17	1-12	0.452 (3)	0.406 (7,1)
Pb	16	15-283	1.723 (53)	0.370 (124,23)
Ti	17	1-61	0.883 (8)	0.481 (23,3)
Sn	16	35-176	1.915 (82)	0.202 (131,52)
Ag	16	12-220	1.656 (45)	0.348 (101,20)
Co:Ni	17	0.04-22.00	-0.042 (0.91)	0.727 (4.84,0.17)
			Core: CA-469/470	
Co	10	29-90	1.782 (61)	0.167 (89,41)
Ni	10	1-169	1.056 (11)	0.714 (59,2)
Mn	10	1-22	0.402 (3)	0.514 (8,1)
Pb	10	20-139	1.672 (47)	0.264 (86,26)
Ti	10	2-36	0.899 (8)	0.444 (22,3)
Sn	10	69-101	1.922 (84)	0.059 (96,73)
Ag	10	17-161	1.735 (54)	0.284 (104,28)
Co:Ni	9	1.35-29.00	0.881 (7.60)	0.525 (25.47,2.27)
			Core: CA-965/966	
Co	39	36-461	2.024 (106)	0.345 (234,48)
Ni	39	1-134	0.983 (10)	0.575 (36,3)
Mn	38	1-33	0.693 (5)	0.441 (14,2)
Pb	38	7-142	1.536 (34)	0.387 (84,14)
Ti	36	3-111	1.172 (15)	0.342 (33,7)
Sn	36	24-208	1.876 (75)	0.180 (114,50)
Ag	39	4-259	1.535 (34)	0.530 (116,10)
Co:Ni	37	0.61-115.25	1.040 (10.96)	0.623 (46.03,2.61)

Table G-2 (continued)

El	N	Range (ppm)	Geometric Mean (ppm)	Std. Dev. (± ppm)
			Calloway Orebody (All Pyrite)	
Co	78	7-644	1.985 (97)	0.430 (260,36)
Ni	81	1-410	1.136 (14)	0.595 (54,3)
Mn	81	1-36	0.605 (4)	0.458 (12,1)
Pb	79	4-234	1.631 (43)	0.361 (98,19)
Ti	80	1-114	1.088 (12)	0.414 (32,5)
Sn	80	24-208	1.891 (78)	0.194 (122,50)
Ag	82	4-259	1.624 (42)	0.455 (120.15)
Co:Ni	79	0.21-206.00	0.867 (7.36)	0.755 (41.88,1.29)

Table G-3. Geometric Mean Data for Pyrite from the Cherokee Orebody.

El	N	Range (ppm)	Geometric Mean (ppm)	Std. Dev. (± ppm)
			Core: CH-857/858	
Co	13	36-445	2.173 (149)	0.264 (274,81)
Ni	13	2-24	0.768 (6)	0.346 (13,3)
Mn	13	1-7	0.281 (2)	0.288 (4,1)
Pb	13	20-45	1.491 (31)	0.132 (42,23)
Ti	13	1-23	0.635 (4)	0.500 (14,1)
Sn	13	58-187	1.997 (99)	0.117 (130,76)
Ag	13	20-66	1.578 (38)	0.163 (55,26)
Co:Ni	14	3.10-260.50	1.407 (25.52)	0.536 (87.70,7.43)

Table G-4. Geometric Mean Data for Pyrrhotite from the Ocoee Gorge Metasediments.

El	N	Range (ppm)	Geometric Mean (ppm)	Std. Dev. (± ppm)
			Chlorite Grade	
Co	6	21-200	1.803 (64)	0.339 (139,29)
Ni	6	24-662	1.970 (93)	0.471 (276,32)
Mn	6	12-27	1.283 (19)	0.127 (26,14)
Pb	6	69-222	2.065 (116)	0.171 (172,78)
Ti	6	83-333	2.097 (125)	0.227 (211,74)
Sn	6	58-166	2.032 (108)	0.169 (159,73)
Ag	6	125-475	2.301 (200)	0.205 (321,125)
Co:Ni	6	0.03-8.33	-0.171 (0.67)	0.800 (4.26,0.11)
			Biotite Grade	
Co	12	14-168	1.693 (49)	0.343 (109,22)
Ni	11	16-169	1.771 (59)	0.316 (122,29)
Mn	12	1-79	1.023 (11)	0.646 (47,2)
Pb	12	24-466	2.008 (102)	0.461 (294,35)
Ti	12	6-306	1.706 (51)	0.607 (206,13)
Sn	11	47-209	2.025 (106)	0.166 (155,74)
Ag	12	32-613	2.132 (136)	0.453 (385,48)
Co:Ni	12	0.16-4.63	-0.010 (0.98)	0.414 (2.54,0.38)
			Garnet Grade	
Co	9	51-97	1.868 (74)	0.087 (90,60)
Ni	9	61-247	2.051 (112)	0.187 (173,73)
Mn	10	6-100	1.444 (28)	0.418 (73,11)
Pb	10	168-537	2.496 (313)	0.150 (443,222)
Ti	10	31-581	1.991 (98)	0.403 (248,39)
Sn	10	80-250	2.163 (146)	0.170 (215,98)
Ag	10	110-623	2.402 (252)	0.228 (427,149)
Co:Ni	9	0.22-1.01	-0.211 (0.62)	0.192 (0.96,0.40)
			Ocoee Gorge (All Pyrrhotite)	
Co	26	14-113	1.721 (53)	0.264 (97,29)
Ni	26	9-247	1.842 (70)	0.333 (150,32)
Mn	25	1-79	1.141 (14)	0.476 (41,5)
Pb	27	24-466	2.174 (149)	0.383 (361,62)
Ti	26	6-333	1.830 (68)	0.455 (193,24)
Sn	26	12-209	2.014 (103)	0.244 (181,59)
Ag	26	28-536	2.224 (167)	0.332 (360,78)
Co:Ni	25	0.16-4.63	-0.134 (0.73)	0.370 (1.72, 0.31)

Table G-5. Geometric Mean Data for Pyrrhotite from the Calloway Orebody.

El	N	Range (ppm)	Geometric Mean (ppm)	Std. Dev. (± ppm)
			Core: CA-628/629	
Co	34	14-249	1.700 (50)	0.302 (100,25)
Ni	37	7-178	1.496 (31)	0.371 (74,13)
Mn	38	1-139	0.974 (9)	0.619 (39,2)
Pb	36	27-300	1.967 (93)	0.285 (179,48)
Ti	35	9-98	1.529 (34)	0.290 (66,17)
Sn	36	47-260	2.042 (110)	0.170 (163,74)
Ag	36	19-335	1.915 (82)	0.291 (161,42)
Co:Ni	36	0.18-11.08	0.125 (1.33)	0.438 (3.66,0.49)
			Core: CA-300/301	
Co	21	14-113	1.653 (45)	0.279 (86,24)
Ni	20	2-2137	2.285 (193)	0.601 (769,48)
Mn	21	1-88	0.971 (9)	0.585 (36,2)
Pb	20	20-499	1.977 (95)	0.355 (215,42)
Ti	20	5-276	1.525 (33)	0.462 (97,12)
Sn	20	58-301	2.070 (117)	0.203 (187,74)
Ag	21	51-717	2.031 (107)	0.373 (254,45)
Co:Ni	19	0.04-1.52	-0.566 (0.27)	0.516 (0.89,0.08)
			Core: CA-469/470	
Co	19	14-97	1.479 (30)	0.238 (52,17)
Ni	20	13-475	1.787 (61)	0.528 (207,18)
Mn	21	2-73	0.927 (8)	0.565 (31,2)
Pb	20	29-300	1.917 (83)	0.294 (163,42)
Ti	21	3-127	1.239 (17)	0.500 (55,5)
Sn	20	47-155	1.955 (90)	0.151 (128,64)
Ag	21	31-367	1.967 (93)	0.360 (212,40)
Co:Ni	20	0.06-4.54	-0.378 (0.42)	0.504 (1.34,0.13)
			Core: CA-965/966	
Co	28	14-99	1.609 (41)	0.250 (72,23)
Ni	27	7-126	1.527 (34)	0.335 (73,16)
Mn	29	1-261	1.137 (14)	0.590 (53,4)
Pb	29	17-262	1.722 (53)	0.345 (117,24)
Ti	29	5-151	1.579 (38)	0.345 (84,17)
Sn	28	47-208	1.984 (96)	0.178 (145,64)
Ag	28	27-213	1.934 (86)	0.231 (146,50)
Co:Ni	29	0.23-14.50	0.221 (1.66)	0.471 (4.92,0.56)

Table G-5 (continued)

El	N	Range (ppm)	Geometric Mean (ppm)	Std. Dev. (± ppm)
			Calloway Mine (All Pyrrhotite)	
Co	107	7-192	1.587 (39)	0.316 (80,19)
Ni	106	7-1119	1.629 (43)	0.552 (152,12)
Mn	105	1-139	0.962 (9)	0.551 (33,3)
Pb	106	11-300	1.856 (72)	0.338 (156,33)
Ti	107	1-151	1.442 (28)	0.427 (74,10)
Sn	106	24-301	1.980 (95)	0.194 (149,61)
Ag	107	15-367	1.931 (85)	0.306 (173,42)
Co:Ni	103	0.06-15.25	-0.034 (0.92)	0.547 (3.26,0.26)

Table G-6. Geometric Mean Data for Pyrrhotite from the Cherokee Orebody.

El	N	Range (ppm)	Geometric Mean (ppm)	Std. Dev. (± ppm)
			Core: CH-857/858	
Co	30	2-184	1.451 (28)	0.432 (76,10)
Ni	31	1-143	1.091 (12)	0.577 (47,3)
Mn	31	1-142	0.776 (6)	0.555 (21,2)
Pb	31	9-168	1.603 (40)	0.338 (87,18)
Ti	31	2-43	0.990 (10)	0.378 (23,4)
Sn	31	24-123	1.812 (65)	0.202 (103,41)
Ag	31	15-162	1.706 (51)	0.264 (93,28)
Co:Ni	31	0.20-34.78	0.343 (2.20)	0.603 (8.83,0.55)

APPENDIX H

ARITHMETIC MEAN DATA

Table H-1. Arithmetic Mean Data for Pyrite from the 628/629 Core in the Calloway Orebody.

El	N	Range (ppm)	Mean (ppm)	Std. Dev. (ppm)	Coeff. of Var. (%)
		Core, Sample: CA-628, 165-170			
Co	5	121-354	236	94	39.83
Ni	5	16-110	51	39	76.47
Mn	4	2-8	5	3	60.00
Pb	5	42-419	170	147	86.47
Ti	4	6-53	24	20	83.33
Sn	4	101-144	135	38	28.15
Ag	5	41-170	116	53	45.69
		Core, Sample: CA-628, 100-105			
Co	3	224-1068	812	511	62.93
Ni	3	13-44	27	16	59.26
Mn	3	4-12	8	4	50.00
Pb	3	87-234	147	77	52.38
Ti	3	6-38	25	17	68.00
Sn	3	47-123	94	41	43.62
Ag	3	44-230	107	107	100.00
		Core, Sample: CA-629, 145-150			
Co	6	224-771	557	209	37.52
Ni	6	4-24	13	9	69.23
Mn	6	1-27	8	10	125.00
Pb	6	34-91	58	26	44.83
Ti	6	3-25	15	9	60.00
Sn	6	47-188	94	49	52.13
Ag	6	20-96	52	28	53.85
		Core, Sample: CA-629, 270-275			
Co	3	313-1205	710	454	63.94
Ni	3	2-13	7	6	85.71
Mn	3	1-36	14	19	135.71
Pb	3	15-34	22	10	45.45
Ti	3	8-19	14	6	42.86
Sn	3	35-134	76	52	68.42
Ag	3	27-80	45	30	66.67

Note: Samples are listed from the hanging wall to the footwall of the orebody.

Table H-2. Arithmetic Mean Data for Pyrite from the 300/301 Core in the Calloway Orebody.

El	N	Range (ppm)	Mean (ppm)	Std. Dev. (ppm)	Coeff. of Var. (%)
		Core, Sample: CA-300, 150-160			
Co	3	7-145	81	69	85.19
Ni	3	44-2479	854	1407	164.75
Mn	3	1-8	4	4	100.00
Pb	3	45-175	108	65	60.19
Ti	3	6-31	17	13	76.47
Sn	3	58-176	97	68	70.10
Ag	3	25-125	63	54	85.71
		Core, Sample: CA-300, 30-40			
Co	5	21-240	115	86	74.78
Ni	4	16-39	27	10	37.04
Mn	5	1-6	3	2	66.67
Pb	4	20-104	63	37	58.73
Ti	5	2-19	9	7	77.78
Sn	5	35-123	92	41	44.57
Ag	5	12-74	39	25	64.10
		Core, Sample: CA-300, 10-20			
Co	3	7-97	47	46	97.87
Ni	3	16-662	292	333	114.04
Mn	3	1-12	8	6	75.00
Pb	3	91-567	238	285	119.75
Ti	3	5-61	26	31	119.23
Sn	3	47-166	90	66	73.33
Ag	3	91-805	372	380	102.15
		Core, Sample: CA-301, 0-10			
Co	3	36-66	49	20	40.82
Ni	3	2-207	78	113	144.87
Mn	3	4-8	6	2	33.33
Pb	3	29-69	44	22	50.00
Ti	3	5-29	14	13	92.86
Sn	3	58-101	83	23	27.71
Ag	3	17-72	36	31	86.11

Table H-2 (continued)

El	N	Range (ppm)	Mean (ppm)	Std. Dev. (ppm)	Coeff. of Var. (%)
		Core, Sample: CA-301, 80-90			
Co	3	7-51	31	22	70.97
Ni	3	7-29	22	13	59.09
Mn	3	1-2	1	1	100.00
Pb	3	15-22	18	4	22.22
Ti	3	1-3	2	1	50.00
Sn	3	24-112	68	44	64.71
Ag	3	39-102	61	36	59.02

Note: Samples are listed from the hanging wall to the footwall of the orebody.

Table H-3. Arithmetic Mean Data for Pyrite from the 469/470 Core in the Calloway Orebody.

El	N	Range (ppm)	Mean (ppm)	Std. Dev. (ppm)	Coeff. of Var. (%)
		Core, Sample: CA-469, 20-25			
Co	3	36-74	64	25	39.06
Ni	3	44-169	89	69	77.53
Mn	3	2-22	9	12	133.33
Pb	3	37-139	83	52	62.65
Ti	3	9-11	10	1	10.00
Sn	3	80-91	84	6	7.14
Ag	3	57-90	74	17	22.97
		Core, Sample: CA-469, 50-55			
Co	4	29-74	57	22	38.60
Ni	4	1-4	3	2	66.67
Mn	4	1-2	1	0	0.00
Pb	4	20-54	36	14	38.89
Ti	4	2-3	3	1	33.33
Sn	4	69-101	85	14	16.47
Ag	4	17-73	38	25	65.79
		Core, Sample: CA-469, 85-90			
Co	3	51-90	74	21	28.38
Ni	3	4-50	20	26	130.00
Mn	3	1-20	8	10	125.00
Pb	3	22-78	55	29	52.73
Ti	3	16-36	27	10	37.04
Sn	3	69-101	83	16	19.28
Ag	3	55-161	93	59	63.44

Note: Samples are listed from the hanging wall to the footwall of the orebody.

Table H-4. Arithmetic Mean Data for Pyrite from the 965/966 Core in the Calloway Orebody.

El	N	Range (ppm)	Mean (ppm)	Std. Dev. (ppm)	Coeff. of Var. (%)
		Core, Sample: CA-965, 80-85			
Co	6	113-232	157	41	26.11
Ni	6	2-16	11	6	54.55
Mn	6	2-25	10	8	80.00
Pb	6	15-135	71	49	69.01
Ti	6	5-29	14	9	64.29
Sn	6	58-155	96	38	39.58
Ag	6	15-124	73	48	65.75
		Core, Sample: CA-965, 70-75			
Co	4	82-146	116	26	22.41
Ni	4	7-134	63	59	93.65
Mn	3	8-27	16	10	62.50
Pb	4	32-128	64	48	75.00
Ti	3	19-158	71	76	107.04
Sn	3	91-363	189	151	79.89
Ag	4	69-259	163	78	47.85
		Core, Sample: CA-965, 65-70			
Co	3	36-82	56	23	41.07
Ni	3	9-118	55	56	101.82
Mn	3	4-25	13	11	84.62
Pb	3	60-494	232	231	99.57
Ti	3	34-111	60	44	73.33
Sn	3	24-155	79	68	86.08
Ag	3	43-101	73	29	39.73
		Core, Sample: CA-965, 35-40			
Co	9	224-461	311	92	29.58
Ni	9	1-61	18	21	116.67
Mn	9	1-11	5	4	80.00
Pb	9	22-45	35	9	25.71
Ti	9	9-29	16	8	50.00
Sn	9	69-208	104	41	39.42
Ag	9	4-13	7	3	42.86
		Core, Sample: CA-965, 15-20			
Co	3	57-97	70	23	32.86
Ni	3	25-46	34	11	32.35
Mn	3	5-5	5	0	00.00
Pb	3	87-142	116	28	24.14
Ti	3	23-222	91	114	125.27
Sn	3	69-516	222	255	114.86
Ag	3	82-73	80	7	8.75

Table H-4 (continued)

El	N	Range (ppm)	Mean (ppm)	Std. Dev. (ppm)	Coeff. of Var. (%)
		Core, Sample: CA-966, 10-15			
Co	3	82-137	103	30	29.13
Ni	3	1-16	6	9	150.00
Mn	3	2-33	14	17	121.43
Pb	3	13-32	22	10	45.45
Ti	3	8-48	21	23	109.52
Sn	3	47-80	62	17	27.42
Ag	3	42-117	84	38	45.24
		Core, Sample: CA-966, 45-50			
Co	3	14-51	36	20	55.56
Ni	3	4-7	5	2	40.00
Mn	3	1-15	7	7	100.00
Pb	3	4-29	13	14	107.69
Ti	3	9-43	21	9	42.86
Sn	3	47-58	54	6	11.11
Ag	3	11-44	22	19	86.36
		Core, Sample: CA-966, 70-75			
Co	6	36-66	49	12	24.49
Ni	6	2-16	8	5	62.50
Mn	6	1-13	4	5	125.00
Pb	6	7-24	17	7	41.18
Ti	6	3-34	12	12	100.00
Sn	6	47-91	60	18	30.00
Ag	6	11-67	36	20	55.56
		Core, Sample: CA-966, 95-100			
Co	2	105-121			
Ni	3	1-34	14	18	128.57
Mn	3	1-14	6	7	116.67
Pb	3	24-78	59	30	50.85
Ti	3	8-29	15	12	80.00
Sn	3	58-80	69	11	15.94
Ag	3	33-249	139	108	77.70

Note: Samples are listed from the hanging wall to the footwall of the orebody.

Table H-5. Arithmetic Mean Data for Pyrite from the 857/858 Core in the Cherokee Orebody.

El	N	Range (ppm)	Mean (ppm)	Std. Dev. (ppm)	Coeff. of Var. (%)
		Core, Sample: CH-857, 40-45			
Co	3	248-1042	578	413	71.45
Ni	3	4-24	117	12	10.26
Mn	3	1-4	2	2	100.00
Pb	3	22-37	27	9	33.33
Ti	3	2-23	9	12	133.33
Sn	3	80-187	130	54	41.54
Ag	3	35-212	96	101	105.21
		Core, Sample: CH-858, 20-25			
Co	3	36-105	77	36	46.75
Ni	3	2-13	6	6	100.00
Mn	3	1-15	6	8	133.33
Pb	3	27-45	34	10	29.41
Ti	3	1-71	24	40	166.67
Sn	3	101-373	195	154	78.97
Ag	3	20-56	32	21	65.63
		Core, Sample: CH-858, 25-30			
Co	4	113-224	160	47	29.38
Ni	4	2-16	9	7	77.78
Mn	4	1-2	2	1	50.00
Pb	4	32-45	40	6	15.00
Ti	4	1-5	3	2	66.67
Sn	4	58-101	85	19	22.35
Ag	4	24-55	38	13	34.21
		Core, Sample: CH-858, 30-35			
Co	4	121-216	174	49	28.16
Ni	3	4-9	6	3	50.00
Mn	4	2-7	4	2	50.00
Pb	4	20-75	41	25	60.98
Ti	4	11-19	14	4	28.57
Sn	4	80-112	99	13	13.13
Ag	4	42-66	50	12	24.00

Note: Samples are listed from the hanging wall to the footwall of the orebody.

Table H-6. Arithmetic Mean Data for Pyrrhotite from the 628/629 Core in the Calloway Orebody.

El	N	Range (ppm)	Mean (ppm)	Std. Dev. (ppm)	Coeff. of Var. (%)
		Core, Sample: CA-628, 210-215			
Co	3	44-66	59	13	22.03
Ni	3	16-134	84	61	72.62
Mn	3	15-67	39	26	66.67
Pb	3	191-300	254	56	22.05
Ti	3	55-207	118	79	66.95
Sn	3	112-176	144	32	22.22
Ag	3	129-193	164	32	19.51
		Core, Sample: CA-628, 130-135			
Co	3	7-105	49	50	102.04
Ni	3	20-134	64	61	95.31
Mn	3	12-139	79	64	81.01
Pb	3	111-157	136	23	16.91
Ti	3	14-83	40	38	95.00
Sn	3	112-166	134	29	21.64
Ag	3	53-137	83	47	56.63
		Core, Sample: CA-628, 100-105			
Co	3	14-44	34	17	50.00
Ni	3	13-55	28	23	82.14
Mn	3	15-49	30	17	56.67
Pb	3	51-94	68	23	33.82
Ti	3	25-80	53	28	52.83
Sn	3	69-134	98	33	33.67
Ag	3	56-93	74	19	25.68
		Core, Sample: CA-628, 15-20			
Co	3	28-249	109	122	111.93
Ni	3	12-63	30	28	93.33
Mn	3	1-4	2	2	100.00
Pb	3	34-107	79	40	50.63
Ti	3	9-21	16	6	37.50
Sn	3	69-176	123	54	43.90
Ag	3	19-55	38	18	47.37
		Core, Sample: CA-629, 75-80			
Co	4	14-90	52	40	76.92
Ni	3	7-34	22	14	63.64
Mn	3	3-14	10	6	60.00
Pb	4	104-300	215	87	40.47
Ti	3	31-98	56	37	66.07
Sn	4	91-291	189	102	53.97
Ag	3	91-214	143	64	44.76

Table H-6 (continued)

El	N	Range (ppm)	Mean (ppm)	Std. Dev. (ppm)	Coeff. of Var. (%)
		Core, Sample: CA-629, 140-145			
Co	3	36-97	66	31	46.97
Ni	3	39-178	109	70	64.22
Mn	3	2-14	6	7	116.67
Pb	3	69-246	135	96	71.11
Ti	3	38-86	50	31	62.00
Sn	3	80-144	112	32	28.57
Ag	3	109-289	210	92	43.81
		Core, Sample: CA-629, 210-215			
Co	6	21-97	45	29	64.44
Ni	6	7-61	30	19	63.33
Mn	6	3-14	7	5	71.43
Pb	6	60-131	85	26	30.59
Ti	6	17-77	43	26	60.47
Sn	6	69-144	107	32	29.91
Ag	6	36-102	65	24	36.92
		Core, Sample: CA-629, 270-275			
Co	6	7-144	67	53	79.10
Ni	6	4-50	22	17	77.27
Mn	6	1-7	3	2	66.67
Pb	6	11-72	37	23	62.16
Ti	6	5-48	26	15	57.69
Sn	6	58-187	101	48	47.52
Ag	6	15-102	61	34	55.74
		Core, Sample: CA-629, 330-335			
Co	4	21-66	42	21	50.00
Ni	3	13-20	16	4	25.00
Mn	4	1-24	12	12	100.00
Pb	4	32-146	86	48	55.81
Ti	4	14-66	36	24	66.67
Sn	4	35-155	93	61	65.59
Ag	3	29-94	54	35	64.81
		Core, Sample: CA-629, 370-375			
Co	3	7-144	78	69	88.46
Ni	3	24-68	40	24	60.00
Mn	3	31-108	68	39	57.35
Pb	3	27-81	59	28	47.46
Ti	3	9-74	35	34	97.14
Sn	3	80-229	130	86	66.15
Ag	3	46-161	105	58	55.24

Note: Samples are listed from the hanging wall to the footwall of the orebody.

Table H-7. Arithmetic Mean Data for Pyrrhotite from the 300/301 Core in the Calloway Orebody.

El	N	Range (ppm)	Mean (ppm)	Std. Dev. (ppm)	Coeff. of Var. (%)
		Core, Sample: CA-300, 150-160			
Co	5	21-113	49	37	75.51
Ni	5	29-1119	426	490	115.02
Mn	5	1-12	5	4	80.00
Pb	5	69-168	100	42	42.00
Ti	5	14-17	16	1	6.25
Sn	5	69-123	82	25	30.49
Ag	5	51-80	67	12	17.91
		Core, Sample: CA-300, 80-90			
Co	4	44-74	59	17	28.81
Ni	3	88-1119	439	589	134.17
Mn	4	5-34	17	14	82.35
Pb	3	124-146	135	11	8.15
Ti	4	38-111	116	112	96.55
Sn	4	69-187	142	51	35.92
Ag	3	60-358	200	150	75.00
		Core, Sample: CA-301, 80-90			
Co	3	44-97	69	27	39.13
Ni	3	44-373	164	182	110.98
Mn	3	1-11	11	10	90.91
Pb	3	13-37	29	14	48.28
Ti	3	3-50	22	25	113.64
Sn	3	69-270	147	108	73.47
Ag	3	55-119	79	35	44.30
		Core, Sample: CA-301, 100-110			
Co	4	21-105	67	38	56.72
Ni	3	118-373	243	128	52.67
Mn	4	25-88	55	33	60.00
Pb	4	20-118	61	46	75.41
Ti	4	8-114	57	44	77.19
Sn	4	24-301	161	120	74.53
Ag	3	24-148	80	63	78.75

Table H-7 (continued)

El	N	Range (ppm)	Mean (ppm)	Std. Dev. (ppm)	Coeff. of Var. (%)
		Core, Sample: CA-301, 130-140			
Co	5	14-66	35	26	74.29
Ni	4	13-227	130	109	83.85
Mn	5	1-29	12	12	100.00
Pb	5	75-361	180	133	73.89
Ti	5	5-141	61	60	98.36
Sn	5	91-144	116	26	22.41
Ag	5	53-293	161	120	74.53

Note: Samples are listed from the hanging wall to the footwall of the orebody.

Table H-8. Arithmetic Mean Data for Pyrrhotite from the 469/470 Core in the Calloway Orebody.

El	N	Range (ppm)	Mean (ppm)	Std. Dev. (ppm)	Coeff. of Var. (%)
		Core, Sample: CA-470, 135-140			
Co	3	36-97	59	33	55.93
Ni	3	151-475	262	185	70.61
Mn	3	25-73	48	24	50.00
Pb	3	146-300	247	88	35.63
Ti	3	45-127	99	47	47.47
Sn	3	69-91	84	13	15.48
Ag	3	265-311	284	24	8.45
		Core, Sample: CA-470, 55-60			
Co	4	14-44	23	14	60.87
Ni	4	50-61	55	5	9.09
Mn	4	2-22	8	10	125.00
Pb	4	54-238	138	76	55.07
Ti	4	14-55	32	20	62.50
Sn	4	35-155	93	52	55.91
Ag	4	39-115	75	32	42.67
		Core, Sample: CA-469, 20-25			
Co	3	7-44	24	19	79.17
Ni	3	13-95	41	47	114.63
Mn	3	3-72	33	35	106.06
Pb	3	48-72	57	13	22.81
Ti	3	9-11	10	1	10.00
Sn	3	58-112	87	27	31.03
Ag	3	35-157	78	68	87.18
		Core, Sample: CA-469, 50-66			
Co	4	14-29	20	7	35.00
Ni	3	20-95	65	40	61.54
Mn	3	2-2	2	0	0.00
Pb	4	40-114	75	30	40.00
Ti	4	3-11	6	4	66.67
Sn	4	47-101	69	23	33.33
Ag	3	36-59	49	12	24.49
		Core, Sample: CA-469, 85-90			
Co	3	36-59	49	12	24.49
Ni	3	13-34	27	12	44.44
Mn	3	2-8	5	3	60.00
Pb	3	29-72	46	23	50.00
Ti	3	3-12	7	5	71.43
Sn	3	80-155	105	43	40.95
Ag	3	41-115	68	41	60.29

Table H-8 (continued)

El	N	Range (ppm)	Mean (ppm)	Std. Dev. (ppm)	Coeff. of Var. (%)
		Core, Sample: CA-469, 110-115			
Co	3	7-36	24	15	62.50
Ni	3	74-2580	1043	1346	129.05
Mn	3	3-18	12	8	66.67
Pb	3	45-75	64	17	26.56
Ti	3	16-40	26	12	46.15
Sn	3	69-123	105	31	29.52
Ag	3	119-259	211	80	37.91

Note: Samples are listed from the hanging wall to the footwall of the orebody.

Table H-9. Arithmetic Mean Data for Pyrrhotite from the 965/966 Core in the Calloway Orebody.

El	N	Range (ppm)	Mean (ppm)	Std. Dev. (ppm)	Coeff. of Var. (%)
		Core, Sample: CA-965, 45-50			
Co	5	14-44	23	12	52.17
Ni	5	1-61	27	24	88.89
Mn	5	5-281	147	136	92.52
Pb	5	22-191	88	68	77.27
Ti	5	5-63	26	22	84.62
Sn	5	47-91	73	17	23.29
Ag	4	27-85	62	25	40.32
		Core, Sample: CA-965, 15-20			
Co	3	29-99	57	37	64.91
Ni	3	40-90	58	28	48.28
Mn	3	10-10	10	0	00.00
Pb	3	198-262	234	33	14.10
Ti	3	31-151	73	68	93.15
Sn	3	134-208	180	40	22.22
Ag	3	90-107	100	9	9.00
		Core, Sample: CA-966, 10-15			
Co	4	29-66	40	18	45.00
Ni	4	2-34	19	15	78.95
Mn	4	3-75	36	30	83.33
Pb	5	17-97	46	34	73.91
Ti	5	11-66	38	22	57.89
Sn	4	47-123	74	34	45.95
Ag	5	21-177	105	64	60.95
		Core, Sample: CA-966, 45-50			
Co	3	44-74	64	17	26.56
Ni	3	29-95	56	35	62.50
Mn	3	7-18	11	6	54.55
Pb	3	17-29	24	6	25.00
Ti	3	12-25	19	7	36.84
Sn	3	35-101	72	34	47.22
Ag	3	80-300	165	118	71.52
		Core, Sample: CA-966, 95-100			
Co	3	29-59	41	16	39.02
Ni	3	2-24	11	12	109.09
Mn	3	1-10	5	5	100.00
Pb	3	22-63	42	21	50.00
Ti	3	1-74	34	37	108.82
Sn	3	80-112	98	16	16.33
Ag	3	29-187	103	79	76.70

Table H-9 (continued)

El	N	Range (ppm)	Mean (ppm)	Std. Dev. (ppm)	Coeff. of Var. (%)
		Core, Sample: CA-966, 130-135			
Co	5	21-82	51	24	47.06
Ni	4	20-39	26	9	34.62
Mn	5	10-28	17	7	41.18
Pb	4	32-75	60	19	31.67
Ti	5	34-107	70	31	44.29
Sn	4	35-112	85	34	40.00
Ag	4	53-73	63	8	12.70
		Core, Sample: CA-966, 140-145			
Co	3	82-192	121	61	50.41
Ni	3	20-50	36	15	41.67
Mn	3	8-25	17	9	52.94
Pb	3	20-160	77	74	96.10
Ti	3	43-104	71	31	43.66
Sn	3	69-80	76	6	7.89
Ag	3	73-134	97	33	34.02
		Core, Sample: CA-966, 180-185			
Co	3	21-82	44	33	75.00
Ni	3	20-74	41	29	70.73
Mn	3	3-24	11	12	109.09
Pb	3	27-60	53	23	43.40
Ti	3	19-120	61	52	85.25
Sn	3	80-123	101	22	21.78
Ag	3	30-152	89	61	68.54

Note: Samples are listed from the hanging wall to the footwall of the orebody.

Table H-10. Arithmetic Mean Data for Pyrrhotite from the 857/858 Core in the Cherokee Orebody.

El	N	Range (ppm)	Mean (ppm)	Std. Dev. (ppm)	Coeff. of Var. (%)
		Core, Sample: CH-857, 40-45			
Co	3	2-36	17	17	100.00
Ni	4	2-24	12	9	75.00
Mn	4	4-257	99	128	129.29
Pb	4	9-51	38	20	52.63
Ti	4	2-36	18	15	83.33
Sn	4	24-101	63	34	53.97
Ag	4	15-102	55	40	72.73
		Core, Sample: CH-857, 5-10			
Co	3	21-90	44	40	90.91
Ni	3	2-50	22	25	113.64
Mn	3	3-117	44	64	145.45
Pb	3	9-27	17	9	52.94
Ti	3	5-21	12	8	66.67
Sn	3	47-895	499	427	85.57
Ag	3	25-51	42	14	33.33
		Core, Sample: CH-858, 0-5			
Co	4	21-59	46	18	39.13
Ni	4	1-29	15	14	93.33
Mn	4	1-8	3	4	133.33
Pb	3	11-37	21	14	66.67
Ti	4	5-11	8	3	37.50
Sn	4	58-123	83	28	33.73
Ag	4	16-70	35	24	68.57
		Core, Sample: CH-858, 10-15			
Co	4	29-74	48	19	39.58
Ni	4	2-34	22	16	72.73
Mn	5	3-10	7	3	42.86
Pb	4	24-63	48	18	37.50
Ti	5	5-43	31	24	77.42
Sn	5	24-91	67	27	40.30
Ag	4	55-107	74	24	32.43
		Core, Sample: CH-858, 25-30			
Co	4	121-313	217	79	36.41
Ni	4	2-9	7	3	42.86
Mn	4	1-3	2	1	50.00
Pb	4	32-94	59	26	44.07
Ti	4	2-8	4	3	75.00
Sn	4	58-112	88	24	27.27
Ag	4	29-46	38	8	21.05

Table H-10 (continued)

El	N	Range (ppm)	Mean (ppm)	Std. Dev. (ppm)	Coeff. of Var. (%)
		Core, Sample: CH-858, 30-35			
Co	3	7-14	12	4	33.33
Ni	3	2-13	8	6	75.00
Mn	3	4-6	5	1	20.00
Pb	3	13-48	30	18	60.00
Ti	4	5-25	16	8	50.00
Sn	4	24-69	47	21	44.68
Ag	3	24-53	36	15	41.67
		Core, Sample: CH-858, 40-45			
Co	5	7-36	16	13	81.25
Ni	4	4-29	13	11	84.62
Mn	5	2-32	16	12	75.00
Pb	4	27-48	71	10	24.39
Ti	5	4-27	11	10	90.91
Sn	5	58-123	68	45	66.18
Ag	5	48-109	74	28	37.84
		Core, Sample: CH-858, 70-75			
Co	4	29-44	35	7	20.00
Ni	4	29-397	178	157	88.20
Mn	3	2-9	6	4	66.67
Pb	3	48-128	85	40	47.06
Ti	4	16-58	30	19	63.33
Sn	3	35-58	50	13	26.00
Ag	3	80-162	120	41	34.17

Note: Samples are listed from the hanging wall to the footwall of the orebody.

APPENDIX I

REGRESSION LINE DATA

Table I-1. Regression Lines for Pyrite Trace Element Data.*

Core	Element	N	Slope	Y-Intercept	Correlation Coefficient
CA-628/629	Cobalt	4	0.0006	2.5948	0.5241
CA-300/301	Cobalt	5	-0.0019	2.0040	-0.6984
CA-469/470	Cobalt	3	0.0010	1.7777	0.5914
CA-965/966	Cobalt	9	-0.0019	2.1009	-0.4091
CH-857/858	Cobalt	4	-0.0093	2.7275	-0.8420
CA-628/629	Nickel	4	-0.0018	1.6397	-0.9831
CA-300/301	Nickel	5	-0.0065	2.8442	-0.7917
CA-469/470	Nickel	3	-0.0091	1.5291	-0.3991
CA-965/966	Nickel	9	-0.0040	1.5043	-0.6111
CH-857/858	Nickel	4	-0.0186	2.0538	-0.9833
CA-628/629	Manganese	4	0.0008	0.7550	0.8717
CA-300/301	Manganese	5	-0.0019	0.7986	-0.4574
CA-469/470	Manganese	3	-0.0001	0.6208	-0.0033
CA-965/966	Manganese	9	-0.0021	1.0528	-0.5825
CH-857/858	Manganese	4	0.0037	0.3174	0.5076
CA-628/629	Lead	4	-0.0020	2.2760	-0.9822
CA-300/301	Lead	5	-0.0030	2.2034	-0.5885
CA-469/470	Lead	3	-0.0025	1.8187	-0.4535
CA-965/966	Lead	9	-0.0039	1.9657	-0.5973
CH-857/858	Lead	4	0.0024	1.4270	0.9445
CA-628/629	Titanium	4	-0.0006	1.4022	-0.9701
CA-300/301	Titanium	5	-0.0034	1.4390	-0.6481
CA-469/470	Titanium	3	0.0072	0.7413	0.4905
CA-965/966	Titanium	9	-0.0026	1.6219	-0.4844
CH-857/858	Titanium	4	0.0003	0.9725	0.0296
CA-628/629	Tin	4	-0.0004	2.0753	-0.8385
CA-300/301	Tin	5	-0.0006	2.0125	-0.8712
CA-469/470	Tin	3	-0.0001	1.9270	-0.5408
CA-965/966	Tin	9	-0.0020	2.1119	-0.5733
CH-857/858	Tin	4	-0.0011	2.1357	-0.2272
CA-628/629	Silver	4	-0.0010	2.0727	-0.9894
CA-300/301	Silver	5	0.0002	1.8412	0.0303
CA-469/470	Silver	3	0.0018	1.7491	0.2885
CA-965/966	Silver	9	-0.0005	1.7793	-0.0786
CH-857/858	Silver	4	-0.0056	1.9631	-0.8704
CA-628/629	Co:Ni	4	0.0026	1.2091	0.9300
CA-300/301	Co:Ni	5	0.0013	0.1199	0.2499
CA-469/470	Co:Ni	3	0.0138	0.3453	0.6947
CA-965/966	Co:Ni	9	0.0031	0.8975	0.3242
CH-857/858	Co:Ni	4	-0.0088	2.0687	-0.8049

Note: 95 percent minimum statistically significant values are underlined.

*See Figure 24, p. 56.

Table I-2. Regression Lines for Pyrrhotite Trace Element Data.*

Core	Element	N	Slope	Y-Intercept	Correlation Coefficient
CA-628/629	Cobalt	10	0.0001	1.7263	0.1351
CA-300/301	Cobalt	5	-0.0001	1.7563	-0.1472
CA-469/470	Cobalt	6	-0.0011	1.6166	-0.4183
CA-965/966	Cobalt	8	0.0013	1.5688	0.4737
CH-857/858	Cobalt	8	0.0007	1.5093	0.0568
CA-628/629	Nickel	10	-0.0006	1.7594	-0.4445
CA-300/301	Nickel	5	-0.0013	2.6552	-0.8644
CA-469/470	Nickel	6	0.0003	1.9661	0.0402
CA-965/966	Nickel	8	-0.0001	1.4894	-0.0266
CH-857/858	Nickel	8	0.0066	0.8847	0.4964
CA-628/629	Manganese	10	-0.0008	1.3458	-0.2610
CA-300/301	Manganese	5	0.0014	0.8777	0.5913
CA-469/470	Manganese	6	-0.0040	1.5084	-0.5647
CA-965/966	Manganese	8	-0.0032	1.5567	-0.5319
CH-857/858	Manganese	8	-0.0102	1.5641	-0.5761
CA-628/629	Lead	10	-0.0008	2.2268	-0.6010
CA-300/301	Lead	5	-0.0002	1.9679	-0.1055
CA-469/470	Lead	6	-0.0034	2.3449	-0.8975
CA-965/966	Lead	8	-0.0010	1.8968	-0.2656
CH-857/858	Lead	8	0.0040	1.3486	0.5805
CA-628/629	Titanium	10	-0.0005	1.7737	-0.4495
CA-300/301	Titanium	5	0.0006	1.5094	0.2757
CA-469/470	Titanium	6	-0.0045	1.7919	-0.6942
CA-965/966	Titanium	8	0.0015	1.4929	0.5111
CH-857/858	Titanium	8	0.0011	1.0697	0.1230
CA-628/629	Tin	10	-0.0002	2.1324	-0.3673
CA-300/301	Tin	5	0.0004	2.0206	0.5496
CA-469/470	Tin	6	0.0004	1.9073	0.3975
CA-965/966	Tin	8	-0.0001	1.9656	-0.0524
CH-857/858	Tin	8	-0.0034	2.1175	-0.3481
CA-628/629	Silver	10	-0.0003	2.0177	-0.2164
CA-300/301	Silver	5	0.0001	2.0006	0.0993
CA-469/470	Silver	6	-0.0015	2.1863	-0.3501
CA-965/966	Silver	8	-0.0001	1.9841	-0.0661
CH-857/858	Silver	8	0.0029	1.5691	0.4989
CA-628/629	Co:Ni	10	0.0004	0.1694	0.3003
CA-300/301	Co:Ni	5	0.0003	-0.3609	0.2900
CA-469/470	Co:Ni	6	0.0001	-0.3489	0.0154
CA-965/966	Co:Ni	8	0.0005	0.3301	0.1133
CH-857/858	Co:Ni	8	-0.0077	0.9851	-0.4037

Note: 95 percent minimum statistically significant values are underlined.

*See Figure 24, p. 56.

APPENDIX J

STUDENT'S *t*-TEST, CORRELATION COEFFICIENTS, AND COEXISTING PHASE DATA

Table J-1. Student's t-Test Data.

El	Ocoee Gorge vs. Calloway Orebody			Ocoee Gorge vs. Cherokee Orebody			Calloway Orebody vs. Cherokee Orebody		
	D.F.*	95% Minimum Statistical Significance t-Value	Calc. t-Value	D.F.*	95% Minimum Statistical Significance t-Value	Calc. t-Value	D.F.*	95% Minimum Statistical Significance t-Value	Calc. t-Value
Pyrite									
Co	101	1.981	4.55	36	2.028	10.01	89	1.985	3.48
Ni	103	1.981	3.27	35	2.028	9.20	92	1.985	4.95
Mn	105	1.981	3.54	37	2.028	7.67	92	1.985	5.63
Pb	103	1.981	6.33	37	2.028	8.51	91	1.985	3.15
Ti	103	1.981	17.39	36	2.028	20.12	91	1.985	8.08
Sn	104	1.981	7.16	37	2.028	(1.21)	91	1.985	4.36
Ag	105	1.981	4.49	36	2.028	5.84	93	1.985	(0.82)
Pyrrhotite									
Co	131	1.980	4.57	54	2.004	6.26	135	1.980	4.36
Ni	130	1.980	4.31	55	2.004	13.27	135	1.980	10.80
Mn	128	1.980	3.42	54	2.004	5.89	134	1.980	3.77
Pb	131	1.980	9.70	56	2.004	13.65	135	1.980	8.38
Ti	131	1.980	9.37	55	2.004	17.22	136	1.980	12.16
Sn	130	1.980	(1.73)	55	2.004	7.73	135	1.980	9.60
Ag	131	1.980	9.84	55	2.004	14.84	136	1.980	8.49

* = Degrees of Freedom.

( ) = Not Significantly Different.

Table J-2. Correlation Coefficients for Trace Elements in Pyrite.

El	Co	Ni	Mn	Pb	Ti	Sn	Ag
			Ocoee Gorge				
Co	1						
Ni	.4509	1					
Mn	.0033	.0374	1				
Pb	.1437	.1619	-.0647	1			
Ti	.2247	-.1194	-.0297	.2270	1		
Sn	.1629	.2101	.2796	.3613	.1553	1	
Ag	.3595	.4511	.3596	.4387	.0672	.4289	1
			Calloway Orebody[b]				
Co	1						
Ni	-.0611	1					
Mn	-.0552	.0273	1				
Pb	.0096	.2965	.1887	1			
Ti	-.0900	.0704	.7931	.3220	1		
Sn	.0089	.1350	.7171	.2145	.9115	1	
Ag	-.1170	.2793	.2643	.6063	.3303	.2622	1
			Cherokee Orebody[c]				
Co	1						
Ni	-.2013	1					
Mn	-.0299	.0046	1				
Pb	-.3134	.2538	-.0157	1			
Ti	-.2059	.2180	.9200	.1918	1		
Sn	.1101	.0706	.8576	.0854	.8545	1	
Ag	.0027	.3942	.0611	.0901	.3081	.0708	1

[a] N = 27; 95 percent minimum statistical significance (r) = .3810.

[b] N = 83; 95 percent minimum statistical significance (r) = .2160.

[c] N = 14; 95 percent minimum statistical significance (r) = .5320.

Note: Statistically significant values are underlined.

Table J-3. Correlation Coefficients for Trace Elements in Pyrrhotite.

El	Co	Ni	Mn	Pb	Ti	Sn	Ag
			Ocoee Gorge				
Co	1						
Ni	-.0826	1					
Mn	.2053	.1938	1				
Pb	.0841	.2033	.3962	1			
Ti	-.1870	.6913	.2539	.2099	1		
Sn	.1228	.3536	.1272	.5236	.4753	1	
Ag	.1119	.5210	.4132	.6756	.4001	.3451	1
			Calloway Orebody[b]				
Co	1						
Ni	.0532	1					
Mn	-.0985	-.0040	1				
Pb	-.0276	.1102	.0152	1			
Ti	.1861	.4033	.1095	.5430	1		
Sn	.3415	.1684	.0712	.3305	.2337	1	
Ag	.0931	.3655	.0135	.4512	.4770	.3619	1
			Cherokee Orebody[c]				
Co	1						
Ni	.1571	1					
Mn	-.2902	-.1393	1				
Pb	.2478	.9045	-.2281	1			
Ti	.0613	.8295	-.2433	.7632	1		
Sn	.0642	-.0517	-.1738	-.1399	.0026	1	
Ag	.1180	.9409	-.1857	.9157	.8121	-.0844	1

[a] N = 28; 95 percent minimum statistical significance (r) = .3750.

[b] N = 110; 95 percent minimum statistical significance (r) = .1950.

[c] N = 33; 95 percent minimum statistical significance (r) = .3460.

Note: Statistically significant values are underlined.

Table J-4. Arithmetic Mean Values of Trace Element Concentrations for Coexisting Pyrite and Pyrrhotite.

Core Sample	Co	Ni	Mn	Pb	Ti	Sn	Ag	Co:Ni
CA-628,100-105								
Pyrite	812	27	8	147	25	94	107	45.89
Pyrrhotite	34	28	30	68	53	98	74	2.12
CA-629,270-275								
Pyrite	710	7	14	22	14	76	45	237.96
Pyrrhotite	67	22	3	37	26	101	61	5.95
CA-300,150-160								
Pyrite	81	854	4	108	17	97	63	.84
Pyrrhotite	49	426	5	100	16	82	67	.52
CA-301,80-90								
Pyrite	31	22	1	18	2	68	61	1.33
Pyrrhotite	69	164	11	29	22	147	79	.72
CA-469,20-25								
Pyrite	64	89	9	83	10	84	74	1.14
Pyrrhotite	24	41	33	57	10	87	78	.77
CA-469,50-55								
Pyrite	57	3	1	36	3	85	38	19.69
Pyrrhotite	20	65	2	75	6	69	49	1.05
CA-469,85-90								
Pyrite	74	20	8	55	27	83	93	9.86
Pyrrhotite	49	27	5	46	7	105	68	2.37
CA-965,15-20								
Pyrite	70	34	5	116	91	222	80	2.18
Pyrrhotite	57	58	10	234	73	180	100	1.21
CA-966,10-15								
Pyrite	103	6	14	22	21	62	84	74.88
Pyrrhotite	40	19	36	46	38	74	105	6.80
CA-966,45-50								
Pyrite	36	5	7	13	21	54	22	7.26
Pyrrhotite	64	56	11	24	19	72	165	1.44
CA-966,95-100								
Pyrite	110*	14	6	59	15	69	139	68.00
Pyrrhotite	41	11	5	42	34	98	103	8.14
CH-857,40-45								
Pyrite	578	117	2	27	9	130	96	127.36
Pyrrhotite	17	12	99	38	18	63	55	2.41
CH-858,25-30								
Pyrite	160	9	2	40	3	85	38	40.39
Pyrrhotite	217	7	2	59	4	88	38	45.24
CH-858,30-35								
Pyrite	174	6	4	41	14	99	50	41.33
Pyrrhotite	12	8	5	30	16	47	36	2.05

*Based on 2 values only.

VITA

Mike Allison was born in Durham, North Carolina, on November 9, 1955. He attended elementary schools in Stuart, Florida, and was graduated from Martin County High School in June 1973. In August 1973 he entered the University of Miami, Coral Gables, Florida, and received a Bachelor of Science degree in geology, in December 1976. In February 1977 Mike accepted employment with Exploration Logging, Inc., Houston, Texas, as a Logging Geologist. In the fall of 1977 he entered the University of Utah, Salt Lake City, and continued at this institution until March 1979. During this period Mike was employed by the Anaconda Company and later, by AAA Engineering and Drafting, Inc., until January 1980. He was also married to Mary Roderick in October 1979. In April 1980 he accepted employment with the Boeing Company, Seattle, Washington, as a Technical Aide, working on the Boeing 767 Flight Simulators. In September 1981 Mike entered The University of Tennessee, Knoxville, and began study towards a Master's degree in geology. In January 1982 he accepted a teaching assistantship and later became Vice-President of Sigma Gamma Epsilon (SGE). In March 1983 Mike accepted employment with Gulf Oil Company, New Orleans, Louisiana. He was awarded a Master of Science degree in geology in June 1984.



Plate 1. Generalized geologic cross section of the Calloway orebody.

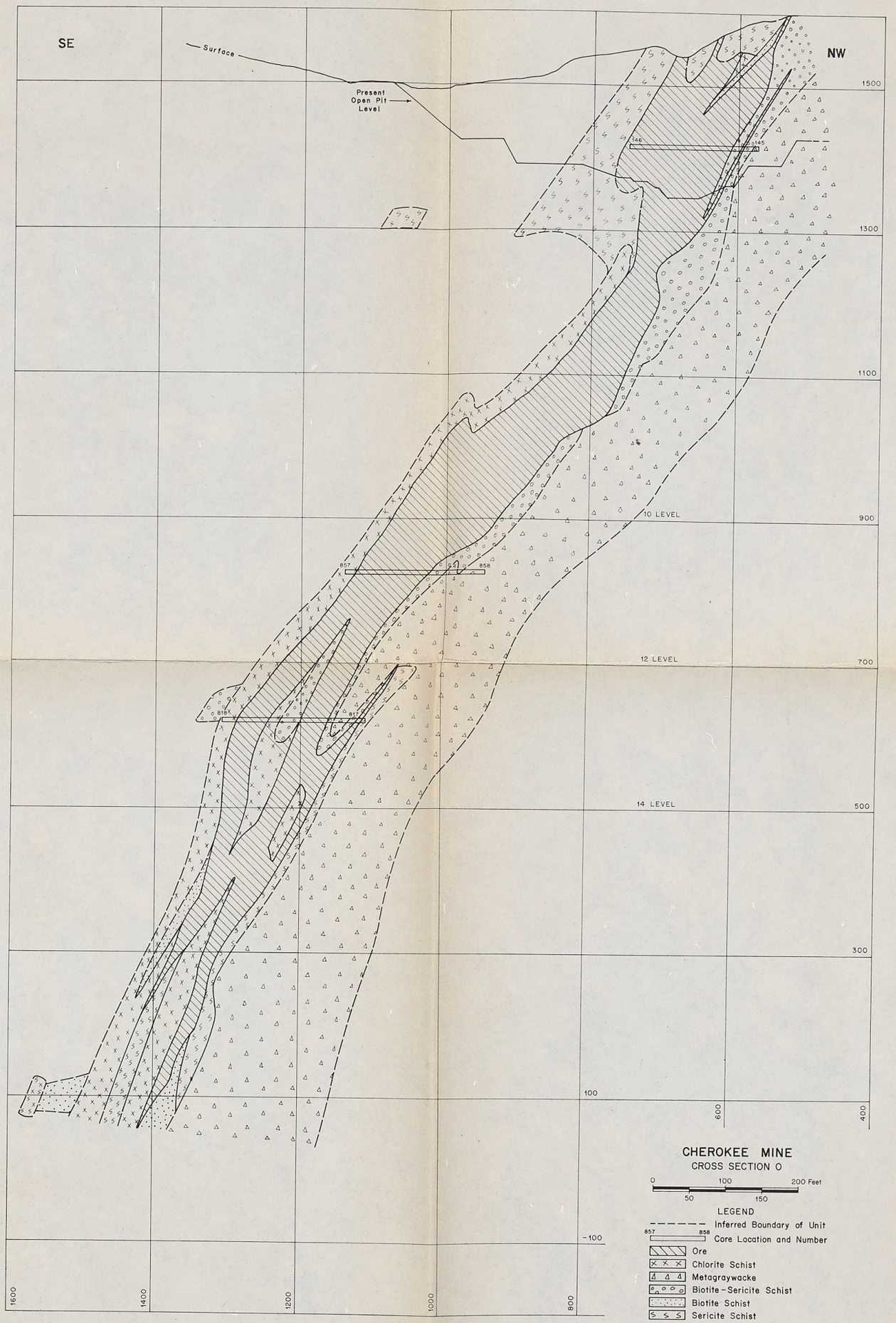


Plate 2. Generalized geologic cross section of the Cherokee orebody.